R-13-38

Quantification of rock matrix K_d data and uncertainties for SR-PSU

James Crawford, Kemakta AB

December 2013

Svensk Kärnbränslehantering AB
Swedish Nuclear Fuel
and Waste Management Co

Box 250, SE-101 24 Stockholm
Phone +46 8 459 84 00

ISSN 1402-3091
SKB R-13-38
ID 1398520

Quantification of rock matrix K_d data and uncertainties for SR-PSU

James Crawford, Kemakta AB

December 2013

Keywords: SFR, SR-PSU, Kd, Sorption coefficient, Rock matrix.

Abstract

The safety assessment SR-PSU forms an integral part of the licence application to extend and operate the existing SFR repository for short-lived low- and intermediate-level radioactive waste. This report contains a compilation of sorption partitioning (K_d) data recommended for use in the SR-PSU safety assessment for the purpose of making calculations of radionuclide transport in the geosphere. Since sorption partitioning data are obtained by laboratory experiments involving crushed and sieved rock samples in contact with synthetic groundwater, corrections typically need to be made to extrapolate the data to site-specific, in situ conditions. In this report, recommendations are provided that are cautiously chosen with regard to the particular transport scenarios being modelled to avoid underestimation of radiological risks. The use of these K_d values in safety assessment codes therefore does not provide a true representation of the transport mechanisms as they might actually occur.

Sammanfattning

Säkerhetsanalysen SR-PSU utgör en central del av licens applikationen att bygga ut och driver SFR slutförvaret för låg och medelaktivt radioaktivt avfall. Denna rapport innehåller en sammanställning av fördelningskoefficienter (K_d värden) rekommenderat för användning i säkerhetsanalysen SR-PSU för beräkningar av radionuklid transport i geosfären. Eftersom K_d data erhålls genom laboratorie-experiment med krossat och siktat berg då måste korrektionsfaktorer användas för att extrapolerar data till platsspecifika förhållanden. I denna rapport ges rekommendationer som är försiktigt valt med hänsyn till de specifika transportscenarier som modelleras för att undvika möjlig underskattning av radiologiska risker. Användandet av framtagna K_d värden i säkerhetsanalys är således inte en exakt representation av de verkliga transportprocesser som sker i geosfären.

Contents

1 Introduction

The Swedish Nuclear Fuel and Waste Management Co. (SKB) is currently preparing a licence application to extend and operate the existing SFR repository for short-lived low- and intermediate-level radioactive waste, which is located near the nuclear power plant in Forsmark. The safety assessment SR-PSU forms an integral part of this licence application. In the safety assessment, geosphere transport calculations are made to assess levels of radiological risk associated with different scenarios of repository evolution. Matrix diffusion coupled with sorption is the main retardation mechanism considered in the geosphere transport calculations.

This report contains a compilation of sorption partitioning (K_d) data recommended for use in the SR-PSU safety assessment for the purpose of making calculations of radionuclide transport in the geosphere. The K_d data are given as a central best estimate and an uncertainty range. These are intended to be used in deterministic and probabilistic simulations of radionuclide transport from the extended SFR repository. The dataset presented herein is based on a previous data compilation for the SR-Site safety assessment (Crawford 2010). Complementary analyses focusing on conditions relevant for SFR and SR-PSU have led to some revisions and additions compared to the SR-Site dataset.

The term sorption is a very broad concept that describes a number of processes by which dissolved solutes are sorbed (adsorbed or absorbed) on, or in another substance, which can also be taken to include processes such as surface precipitation and solid solution formation. In the context of radionuclide transport and the sense in which the term is used in this report, sorption is used strictly to refer to adsorptive interaction with mineral surfaces by way of electrostatic and covalent chemical bonding and specifically excludes other related processes. The representation of sorption phenomena using a K_d approach implies a number of assumptions that are not always fully defensible if the aim is to accurately represent the dynamics of radionuclide transport. In this report, recommendations are provided that are cautiously chosen with regard to the particular transport scenarios being modelled to avoid underestimation of radiological risks. The use of these K_d values in safety assessment codes therefore does not provide a true representation of the transport mechanisms as they might actually occur.

The Swedish concept for disposal of nuclear waste involves isolation of the waste in crystalline bedrock. For this reason, the focus of the present report is on sorption processes that may influence the transport of radionuclides within fractured granitic rock-types. In this definition we loosely include the entire family of intrusive (plutonic) igneous rocks common in Sweden. For the purposes of SR-PSU, K_d data are derived for sorption on site specific rock types in the Forsmark area. The underlying sorption data were obtained during the Forsmark and Laxemar site investigations that were performed in order to provide input data to SR-Site. No new site data on sorption in the geosphere have been produced for the SR-PSU safety assessment.

2 Methodology

Since sorption partitioning data are obtained by laboratory experiments involving crushed and sieved rock samples in contact with synthetic groundwater, corrections typically need to be made to extrapolate the data to site-specific, in situ conditions. This may include; corrections for the state of disaggregation of the laboratory samples relative to the in situ rock, corrections for differences in mineralogy, and corrections for deviations in the in situ groundwater composition. In this work, a transfer factor approach based on that described in Bradbury and Baeyens (2003), although in slightly modified form, is used to account for the various biases in the underlying measurement data derived from laboratory experiments. It is the same methodology as was applied previously in SR-Site (Crawford 2010). The various transfer factors are:

f_A A surface area normalisation transfer factor which accounts for the difference in sorptive surface area amongst different size fractions used in laboratory investigations. It is defined as the ratio of the sorptive surface area of a reference size fraction of crushed rock relative to the actual size fraction used in the experiment. This allows data obtained for different size fractions to be converted into a mutually compatible form that can then be pooled before extrapolation to in situ conditions.

f_m A mechanical damage transfer factor which accounts for differences between the sorptive surface area of the reference size fraction of crushed rock and undisturbed rock in situ.

f_{cec} A transfer factor which accounts for differences between the cation exchange capacity (CEC), of the site specific rock type and that used in laboratory experiments.

f_{chem} A transfer factor which accounts for differences between the groundwater chemistry under safety assessment conditions in situ and a reference groundwater composition used in laboratory investigations.

The f_A, f_m and f_{cec} transfer factors are defined as ratios, the latter two being associated with log-normally distributed uncertainty ranges. The first three transfer factors are multiplicative (additive in logarithmic space) since they are assumed to be approximately constant, average values for migration paths through the geosphere. The chemistry transfer factor, on the other hand, is deemed to be spatially and temporally variable to allow for variations in groundwater hydrochemical composition as predicted by the groundwater hydrochemical modelling detailed in Auqué et al. (2013). As such, except in the limiting case of a lognormally distributed f_{chem}, this transfer factor must be applied by convolution of the f_{chem} uncertainty distribution with the remaining terms:

$$\mathrm{K_d} = \left(\mathrm{R_d} \cdot f_A \cdot f_m \cdot f_{cec}\right) * f_{chem} = \mathrm{K_d^0} * f_{chem} \qquad (2\text{-}1)$$

Here, $\mathrm{K_d^0}$ is the probability density function for the site specific rock and a defined reference water chemical composition. The resulting probability density function (pdf) for the $\mathrm{K_d}$ obtained by convolution of the pdf's associated with $\mathrm{K_d^0}$ and f_{chem} may then be interpreted as the conditional probability of the partitioning coefficient marginalized over the phase space of the uncertain groundwater composition.

Since the SFR repository is hosted in rock which is geochemically similar to that for the deep waste repository which was the focus of SR-Site, the same basic data set is assumed to also be valid for SR-PSU. Given the similar geological setting and mineralogical characteristics of the host rock, the f_m and f_{cec} transfer factors are assumed to be identical to those calculated in Crawford (2010). The surface area normalisation factors, f_A are also the same since this is merely a device for internal harmonisation of experimental data obtained on different crushed size fractions. The $\mathrm{K_d}$ values recommended for SR-PSU are therefore largely the same as for SR-Site, although with some differences motivated by consideration of differing chemical environment of the SFR repository. The handling of the f_{chem} transfer factor is therefore the main difference between the previous work and that described in the following sections.

3 Key differences between SR-Site and SR-PSU groundwater compositions

In SR-Site, the most representative site-specific groundwater was chosen to be the composition characteristic of water sampled in borehole KFM03 in the borehole length interval 639–646 m (Byegård et al. 2008). This was designated as the Forsmark Saline reference composition in Crawford (2010). A comparison of this reference composition with the average type groundwater compositions defined by Auqué et al. (2013) is given in Table 3-1.

As can be noted in Table 3-1, the SR-PSU "type" groundwaters are less saline than the reference Saline groundwater assumed in SR-Site and are somewhat more meteoric in character with significantly lower Ca concentration levels, higher Na/Ca ratios, and higher carbonate content. For cation exchanging solutes that exhibit sensitivity to ionic strength, the SR-PSU groundwaters are predicted to give enhanced sorption relative to the SR-Site reference composition, mostly owing to reduced competition for electrostatic binding sites with the major groundwater cations. For solutes that sorb by surface complexation, on the other hand, the much higher dissolved carbonate concentrations imply increased binding competition from aqueous carbonate complexation reactions, which in some cases could imply a decrease in sorptivity relative to the SR-Site reference composition.

A further difference between the SR-PSU and SR-Site groundwaters is the possibility that the large amounts of concrete and ordinary Portland cement (OPC) structures and stray materials in the SFR repository lead to a significant and persistent plume of altered groundwater composition along migration paths leading from the repository. The leaching of alkali and alkaline metals from OPC is expected to give an altered composition of groundwater featuring significantly elevated pH, decreased carbonate concentration (by way of calcite equilibrium), and reduced redox potential (owing to the effect of pH on the $Fe^{2+}/Fe(OH)_3$ redox couple and possible influence of anoxic corrosion of Fe in the near field). The actual chemical characteristics of this leachate and its downstream dilution and consequent pH and redox buffering depend to a large extent on the degree of contact between groundwater and the cement structures as well as the characteristics of hydrodynamic mixing downstream along the migration paths leading to the surface. Dissolution and precipitation reactions involving rock matrix and fracture minerals may also play a significant role in the evolution of a high pH plume of altered groundwater composition.

Table 3-1. Composition of SR-Site reference saline groundwater (Crawford 2010) and representative compositions defined for different time domains in the SR-PSU safety assessment (Auqué et al. 2013).

	SR-Site	SR-PSU			
	Forsmark Saline reference composition	Temperate saline	Early Periglacial (20–40 ka)	Late Periglacial (extended global warming, > 40 ka)	Glacial-derived
pH	7.55	7.3	7.4	7.6	9.3
Eh (mV)	n/a*	–225	–210	–250	+400
Cl (mg/L)	5,150	3,500	190	90	0.5
SO_4^{2-} (mg/L)	195	350	50	40	0.5
HCO_3^- (mg/L)	21.9	90	300	200	22.7
Na (mg/L)	1,690	1,500	180	110	0.17
K (mg/L)	14.2	20	5	3	0.4
Ca (mg/L)	1,470	600	50	30	6.8
Mg (mg/L)	52.7	150	12	6	0.1
SiO_2 (mg/L)	6.28	11	12	10	12.8

* The redox potential of the SR-Site reference groundwater was not stipulated in the original type groundwater compositions defined by Byegård et al. (2008).

The temporal evolution and spatial extent of altered groundwater conditions depend in large part on the layout of the repository and the hydrogeological setting of individual migration paths and is therefore highly scenario-specific and difficult to model with precision. Although the detailed reactive transport modelling of such processes was beyond the scope of the present work, the consequences for sorptivity in groundwater affected by OPC leachate has been considered for some particular nuclides in a simplified and qualitative manner. However, although such modelling can give plausible insights into possible effects of OPC leachate on sorption, these must be considered as merely indicative since many of the mechanistic details and assumptions underlying sorption modelling at high pH $\geq$ 10 are either subject to considerable uncertainty or break down entirely. This is not least because silicate mineral surfaces become unstable at such high pH levels and dissolve at significantly accelerated rates relative to more normal groundwater pH conditions. Details of the qualitative modelling work are discussed in the following section.

4 Hydrogeochemical modelling in support of K_d recommendations

4.1 Previous modelling in SR-Site

As noted previously in Crawford (2010), a generalised thermodynamic model of sufficient reliability to predict the sorption of surface complexing solutes in granitic rock does not exist at the present time. In the majority of cases it was also not possible to observe clear and quantifiable differences related to groundwater composition in the measured sorptivity for most of the surface complexing solutes relevant to safety assessment examined in the data compilation. For the site specific measurement data obtained during the site investigations (Byegård et al. 2008, Selnert et al. 2009), there was also the problem of pH drift involving the contact water solutions used in the laboratory experiments which rendered any detailed mechanistic interpretation highly uncertain. In the SR-Site K_d data recommendation this was handled by pooling data for all relevant groundwater compositions in order to give an expanded range of K_d uncertainty that was implicitly assumed to account for all groundwater compositional variability likely to be encountered along geosphere migration paths associated with the repository system. While this was not an optimal solution, it was nevertheless deemed to be the only reasonable way in which to handle this uncertainty at the time.

For the cation exchanging solutes Cs, Sr, Ba, and Ra on the other hand, a simplified single site cation exchange model for some Swedish granitic rock types was available. Although this model was conditioned on laboratory sorption data for Äspö diorite and fine-grained granite (Byegård et al. 1998) as well as Finnsjön granite (Byegård et al. 1995), the geochemical similarity of these rock types was considered sufficiently close to the site-specific, Forsmark metagranite reference rock type that the model could be used to make approximate estimates of likely chemical correction factors, f_{chem} for site specific groundwater compositions relative to the compositions used in the Site investigation laboratory experiments.

In SR-Site, groundwater compositional changes were not modelled on the level of individual migration paths and only large-scale changes in bulk groundwater chemistry were modelled in the hydrochemical simulations described in Salas et al. (2010). The available hydrochemical input data for different time domains thereby consisted of statistics of groundwater compositional variability within a large control volume surrounding the repository. Since the changes in groundwater composition were not modelled for individual migration paths, extrapolation to the groundwater situations existing at different times required consideration of the statistical distribution of spatially variable groundwater compositions throughout the entire repository volume.

Although this approach captured the average statistics of compositional variation and its likely impact on sorption K_d, the approach was not entirely satisfactory and gave only small shifts in the central estimates of the K_d uncertainty distributions. This is a particularly problematic deficiency when it is considered that flowpaths featuring high advective flows and low F-factors (i.e. hydrodynamic transport resistance) will exhibit profound changes in chemical composition over time, whereas flowpaths with very low advective flowrates and high F-factors may hardly change at all over the modelled timescale of the safety assessment. On average, there were only very small changes in chemical composition over time, although very significant changes within high flow regions of the repository control volume.

4.2 Modelling in SR-PSU

In SR-PSU, the hydrochemical modelling approach was slightly different in that detailed statistics of compositional variability were not computed for a control volume surrounding the repository in the same fashion as was done for SR-Site. Instead, the modelling approach was centred on interpretation of existing groundwater chemistry profiles at the site including adjacent inland areas deemed representative of the hydrochemical situation likely to exist at future times featuring different shoreline displacement locations relative to the repository. The hydrochemical modelling work described in Auqué et al. (2013) therefore has resulted in the prediction of a series of representative groundwater compositional ranges for the different time domains in the reference glacial cycle of the safety assessment.

In the modelling work performed in support of the present data compilation, these type groundwater compositions were considered separately to give K_d recommendations for each specific groundwater type where deemed feasible to do so. The impact of a high pH plume was also considered as a variant for each of these groundwater compositions where pH buffering was simulated as a simple hydrodynamic mixing process involving OPC leachate and the initial, unaffected groundwater composition as defined by Auqué et al. (2013).

4.2.1 Simplified modelling of groundwater compositional trends

The chemical evolution of OPC leachate was not considered in detail and a very simplified composition was obtained by simply assuming Portlandite, $Ca(OH)_2$ in equilibrium with the respective type groundwater for each time domain under consideration. This representation was considered sufficiently accurate for the purposes of the SR-PSU data recommendation. All chemical calculations in this report were performed using PhreeqC (Parkhurst and Appelo 1999) in conjunction with the official SKB Thermodynamic database (SKB-TDB, SKBdoc 1261302 ver 3.0) as described by Duro et al. (2006). The in situ groundwater temperature was assumed to be 15°C for all time domains. In the PhreeqC calculations, the Portlandite equilibrated OPC water and the unaffected type groundwater are the assumed end-members for a batch mixing model which is intended to simulate changes in chemical composition along a flowpath arising due to hydrodynamic mixing.

The simulations only consider changes in composition as they can be related to an equivalent mixing fraction downstream from the repository and no attempt has been made to model detailed reactive transport processes along migration paths. The generation of an OPC affected groundwater plume and its spatial and temporal persistence along a flowpath is therefore not directly considered in the simulations. This affords the SR-PSU modelling team flexibility to define scenarios of pH plume development independently of the work performed in support of the K_d data recommendation presented in these chapters. Although the possibility of kinetic dissolution reactions of aquifer minerals with OPC leachate has not been considered, the net effect on pH buffering and its concomitant effect on groundwater carbonate concentrations by way of calcite equilibrium should be qualitatively similar to the case of a pure mixing model of pH buffering, although with subtly altered concentration versus distance profiles for various key groundwater components along a migration path. For the present purposes the neglection of these additional kinetic processes is not considered to be a large uncertainty for the qualitative calculations performed in support of the K_d recommendation.

Figure 4-1 shows the trends of groundwater chemical composition for mixing of the simplified OPC leachate (Portlandite equilibrated groundwater), with un-affected groundwater as might occur along a migration path due to hydrodynamic mixing. Since the groundwater compositions typically drift in response to equilibration when not completely specified and charge-balanced, it was necessary to force the pH and Eh of the initial unaffected groundwaters to stabilize at the specified levels by titration with HCl in the case of pH and Fe^{2+} for the redox system while simultaneously fixing the Fe^{3+} activity by imposing forced equilibrium with a ferric hydroxide phase.

Owing to the very low Cl^- level in the glacial-derived groundwater, titration with Ca^{2+} was used to fix the initially specified pH for this type groundwater. At the same time, the equilibrium phases quartz, calcite, brucite, and pyrite were allowed to precipitate if oversaturated. The ferric hydroxide phase assumed the calibrated equilibrium constant described by Banwart (1999). This assumption was made on the basis of the descriptions in the Hydrochemistry Site Descriptive Modelling report (Nilsson et al. 2011) where it was speculated that this calibrated value was found to give the most accurate match to actual groundwater measurement data at the site. Apatite equilibrium was also imposed on the system in order to simulate the phosphate levels in the groundwater which in certain situations can be an important ligand for nuclide complexation.

The redox potential, Eh (mV) is plotted in Figure 4-2 together with pH as a function of mixing fraction for the four different groundwater types. The calculations assume $Fe^{2+}/Fe(OH)_3$ redox control based on the Banwart (1999) calibration for the Temperate saline and both Periglacial groundwater types. The dilute composition of the Glacial derived groundwater, however, is poorly poised and it is very difficult to obtain reliable numerical convergence in mixing calculations using the $Fe^{2+}/Fe(OH)_3$ redox system. In this case, an $O_{2(g)}$ partial pressure of $\approx 1.6\times10^{-19}$ atm. was specified instead to give the initial Eh of roughly +400 mV as specified for the Glacial derived groundwater in Table 3-1.

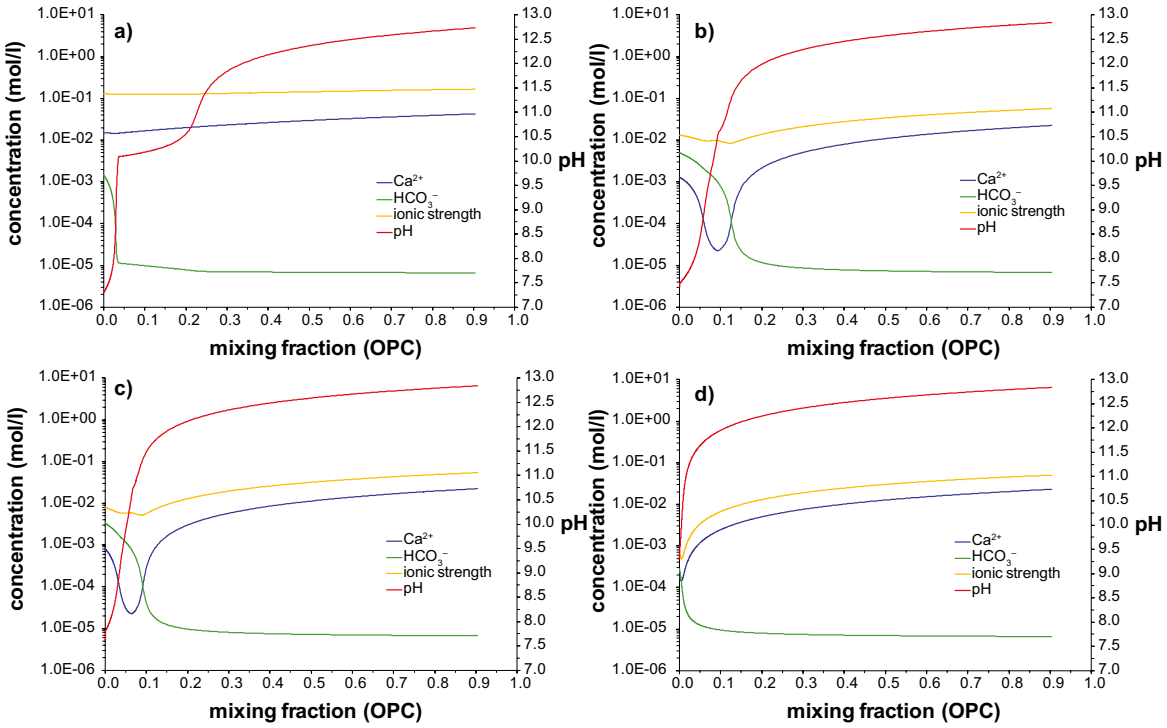

Figure 4-1. *Trends in groundwater composition (total concentrations, ionic strength, and pH) as a function of mixing fraction for mixing of Portlandite equilibrated groundwater with un-affected groundwater. Plots are shown for a) Temperate saline, b) Early Periglacial, c) Late Periglacial, and d) Glacial derived groundwater.*

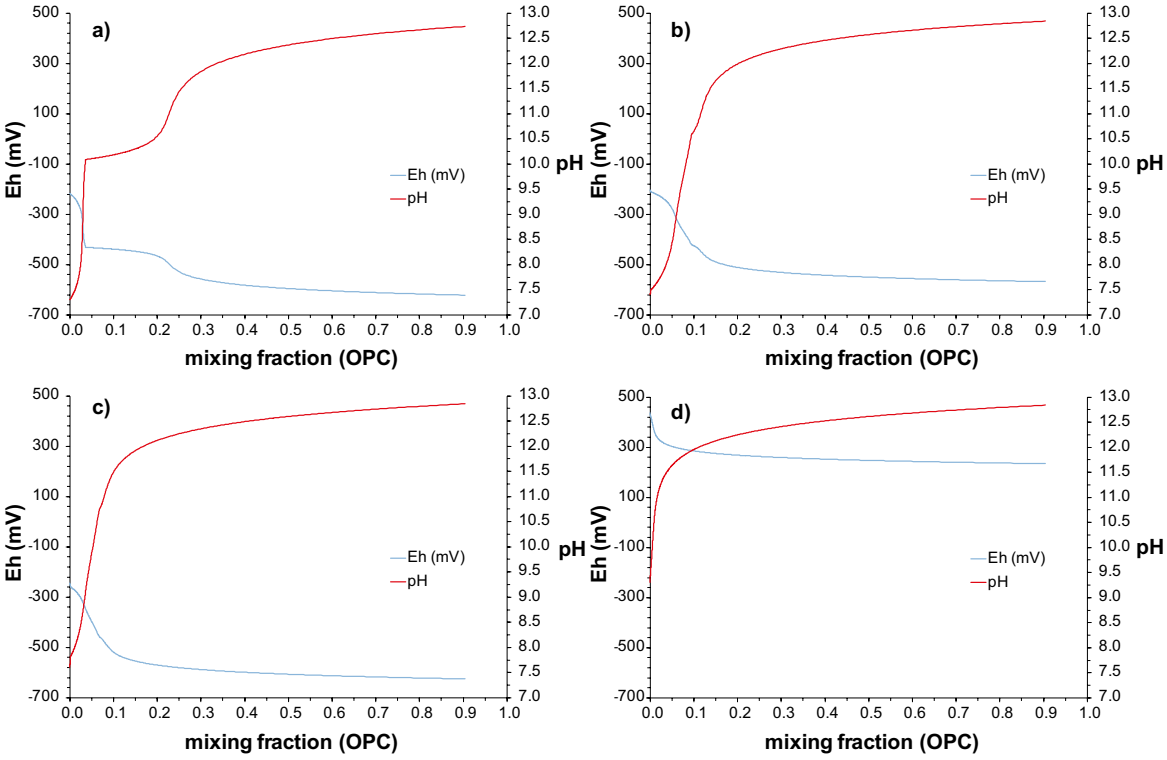

Figure 4-2. *Trends in groundwater composition (Eh and pH) as a function of mixing fraction for mixing of Portlandite equilibrated groundwater with un-affected groundwater. Plots are shown for a) Temperate saline, b) Early Periglacial, c) Late Periglacial, and d) Glacial derived groundwater.*

4.2.2 Overview of qualitative modelling used to identify possible radionuclide sorptive trends

As noted in the Geosphere Process Report, the free concentration of a solute makes up a variable part of, what is referred to as, the *total dissolved concentration* of that solute and its distribution amongst various aqueous complexed forms (*species*), whether it is a nuclide or a major groundwater component, is referred to as the *speciation* of that solute. Speciation also can refer to the particular redox state of an element amongst various reduced or oxidised states in which it can reside (i.e. *redox speciation*). Surface complexation is analogous to aqueous phase complexation with the exception that one of the ligands takes the form of a reactive functional group on a mineral surface in the case of surface complexation and the resulting complex is therefore immobile (unless the surface itself is mobile such as in the case of carrier colloid particles). The formation of aqueous complexes may greatly affect the distribution of a radionuclide between the aqueous and solid phases both directly and indirectly. Knowledge of the speciation of a nuclide is therefore very useful for understanding the impact that altered physicochemical conditions such as a change in pH, temperature, or gas partial pressure might have upon the mobility of that nuclide in flowing groundwater.

Speciation can affect the mobility of a nuclide by binding it in a relatively stable, less reactive form. There are, however, many direct and indirect competitive effects of speciation on sorption that can only really be understood through simultaneous modelling of sorption and aqueous phase speciation and the idea of binding of a nuclide in a less reactive form is really only strictly true for an irreversible reaction mechanism (this can sometimes be reasonably assumed for exceptionally strong complexing agents). While chemical speciation calculations by themselves can inform discussions about relative importance of different aqueous phase complexation reactions for the competitive binding of nuclides in solution, it is very difficult to directly extrapolate this to sorptivity since the aqueous phase speciation continuously adjusts to accommodate mass transfer changes related to the surface binding reactions.

As an example of this, one might consider the behaviour of a radioelement in trace concentrations such as Am(III). When making speciation calculations, one typically finds that the free concentration of Am^{3+} is some orders of magnitude less than the concentration of hydroxyl and carbonate complexed forms in solution. If it is the free cation that is deemed to react with surface groups, one might suspect on the basis of speciation calculations that the K_d of Am in the presence of dissolved carbonate might be reduced in proportion to the ratio of free Am^{3+} concentrations when modelled in the presence and absence of carbonate. When the reactive processes involving both the surface and solution are modelled simultaneously there is indeed a difference in K_d, although nowhere near as great as what pure speciation modelling might lead one to believe. This is due to the mutual interaction between the different processes which cannot properly be understood by consideration of either process in isolation.

In order to enliven a discussion on the impact of variable groundwater chemistry on sorption processes it is therefore necessary to examine some simplified mechanistic models of sorption in combination with speciation calculations of radionuclides to gain a proper understanding of the importance of various direct and indirect interactions. Since a satisfactory surface complexation model for sorption in granitic type rock does not currently exist, a simplified approach was adopted whereby a single mineral was used as a proxy to describe the sorption in granite.

In many studies (for a discussion see Crawford (2010) and references therein) biotite has been identified as a particularly important sorbing phase relative to the relatively less-reactive surfaces of the quartz, plagioclase, orthoclase, and feldspar minerals that comprise the bulk of most granitic rocks. Although a suitable sorption model for biotite is not available either, it shares many crystallographic features with the clay mineral illite which could potentially serve as a geochemical analogue. A relatively detailed non-electrostatic surface complexation model exists for illite as described by Bradbury and Baeyens (2009a, b) and has been adopted as an analogue for sorption in granite (henceforth referred to as the BB09 model). It can be noted that all sorption calculations described in this report assume picomole radionuclide concentrations together with a much larger concentration of binding or exchange sites to ensure sorption linearity and so that the presence of the nuclide itself does not introduce a bias by exerting an influence on the bulk composition of the contacting solution.

In the approach to K_d data recommendation adopted in SR-Site, the chemistry transfer factor, f_{chem} is defined simply as the ratio of the K_d value *expected* under application conditions and the corresponding value *expected* for the reference groundwater composition:

$$f_{chem} = K_{d(calc)} \Big/ K^0_{d(calc)} \qquad (4\text{-}1)$$

In the method description given in Crawford (2010), it is proposed that chemistry transfer factors should be calculated theoretically if sufficiently robust empirical or thermodynamic models of sorption are available. The main reason for the use of chemistry transfer factors rather than calculation of K_d values directly from mechanistic models is that it is usually not possible to specify key parameters of mechanistic models to the degree of accuracy necessary to give a reliable estimate of the K_d value in an ***absolute*** sense, although such models still might provide a mechanistically plausible account of ***relative*** sorptive variation. Here, the core assumption is that uncertain parameters are normalizable (i.e. the unknown quantity proportionally affects both the numerator and denominator of Equation 4-1 and therefore cancels out when calculating the ratio). Such parameters would typically include sorptive surface area, binding site density, and cation exchange capacity, although in certain situations might also encompass intrinsic surface reactive properties of particular mineral phases in the site specific rock.

In addition to this, it can be argued that an empirically measured data point for a given set of conditions will always be a better estimator of true behaviour *for those exact conditions* than a theoretical model which is, by necessity, always a simplified representation of the system in question. The use of a chemistry transfer factor that *adequately* captures the main features of relative sorptive variation together with an accurate central estimate of K_d for a known and well-defined groundwater chemical composition should then always outperform direct theoretical estimates of K_d made using a model with highly uncertain parameterization.

It must be remembered that such simulations can only be considered to give very rough indications of possible trends since the contact water compositions and the pre-conditioned state of the illite upon which the literature model is calibrated are quite different from the physicochemical conditions under present consideration. Furthermore, at pH levels above about 10 the instability of silicate mineral surfaces makes predictions of sorptive chemistry quite uncertain. Nevertheless, and in spite of being a very simplified approach, it was deemed that since sorption reactions often exhibit similar relative pH dependent characteristics for different mineral surfaces (e.g. Bertetti et al. 1998, Pabalan et al. 1998), this should still give useful insights into the impact of severe geochemical gradients in the form of a high pH plume, at least in a qualitative sense.

Since the simulations are only used to give qualitative indications of sorptive trends as a function of the simulated groundwater chemistry shown in Figure 4-1, full details are not given for all nuclides which have been modelled beyond that which is necessary for a brief discussion of the reasonableness of recommended data in the following sections. In this section, however, the underlying ideas are illustrated using Am (as a relatively "well-behaved" example) to show the interplay between various aqueous and surface complexation reaction mechanisms and why aqueous speciation cannot be considered in isolation of surface reaction mechanisms to predict sorptive trends. In the calculations, the cation-exchange part of the BB09 model is neglected since it is mostly important at low pH levels and may not be fully consistent with the known cation exchange behaviour of granite for the groundwater compositions under consideration.

In the BB09 model, a systematic dependency referred to as a linear free-energy relation (LFER) is developed which can be used to relate binding constants for specific surface reactions with corresponding analogous reactions in the aqueous phase. LFER relations are used frequently in aquatic chemistry (e.g. Stumm and Morgan 1996) since they facilitate the empirical correlation of related sets of phenomena in a chemically consistent manner. In the BB09 framework, the sorption tends to follow a pattern whereby surface reactions corresponding to successive hydrolysis steps in the aqueous phase reach an optimum level and then decline at increasing pH. It is the net sum of all the relevant surface reactions, however, that gives the overall K_d for the sorption of that solute. In the case of Am(III) sorption, the pH dependent trend (sorption edge) shown in Figure 4-3 illustrates this principle.

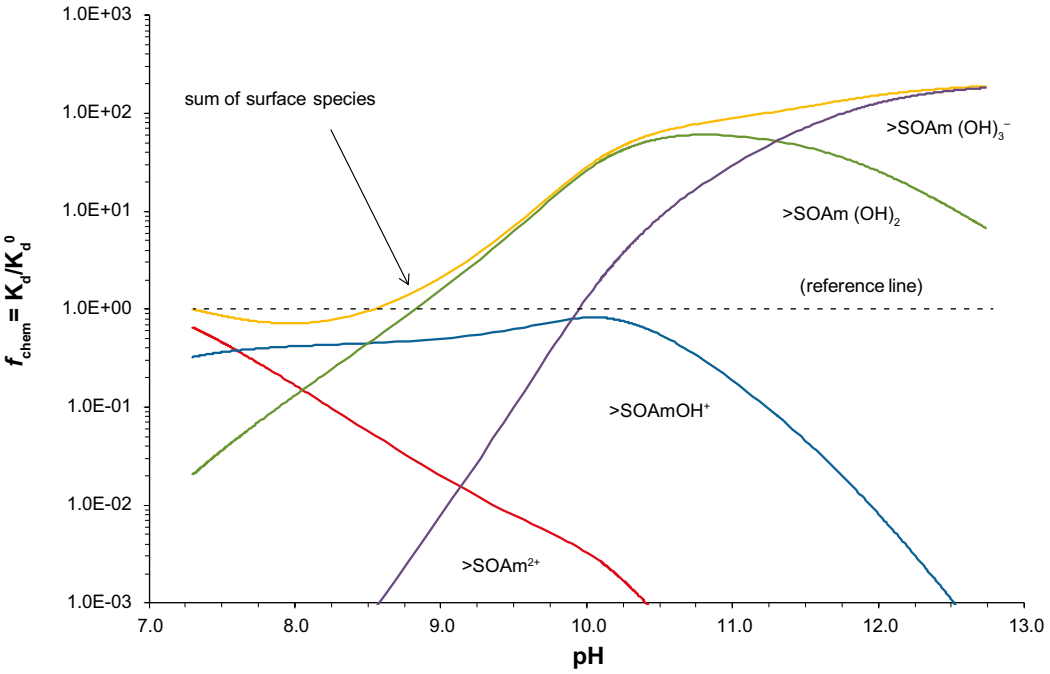

Figure 4-3. *The sorption edge for Am(III) sorption versus pH on illite modelled using the BB09 model and the groundwater compositional trend implied by mixing of OPC leachate and the groundwater characteristic of the Temperate saline time domain (Figure 4-1a). Predominance of individual surface species is shown as well as the theoretical overall K_d value (sum of surface species) plotted relative to the reference level of the unaffected groundwater.*

The surface reactions shown in Figure 4-3 correspond to the following reaction stoichiometries:

$$Am^{3+} + > SOH \rightleftharpoons \; > SOAm^{2+} + H^+ \qquad (4\text{-}2)$$

$$Am^{3+} + > SOH + H_2O \rightleftharpoons \; > SOAmOH^+ + 2H^+ \qquad (4\text{-}3)$$

$$Am^{3+} + > SOH + 2H_2O \rightleftharpoons \; > SOAm(OH)_2 + 3H^+ \qquad (4\text{-}4)$$

$$Am^{3+} + > SOH + 3H_2O \rightleftharpoons \; > SOAm(OH)_3^- + 4H^+ \qquad (4\text{-}5)$$

Based on the LFER methodology, the first three of these surface reactions correspond to the following analogous aqueous phase reactions:

$$Am^{3+} + H_2O \rightleftharpoons \; AmOH^{2+} + H^+ \qquad (4\text{-}6)$$

$$Am^{3+} + 2H_2O \rightleftharpoons \; Am(OH)_2^+ + 2H^+ \qquad (4\text{-}7)$$

$$Am^{3+} + 3H_2O \rightleftharpoons \; Am(OH)_3 + 3H^+ \qquad (4\text{-}8)$$

In this particular example, an additional surface reaction was required to fit the empirical sorption edge for Am(III) in Bradbury and Baeyens (2009b), although this reaction does not have a recognised aqueous phase counterpart (i.e. $Am(OH)_4^-$) with a quantifiable hydrolysis constant. In the case of the analogous $Am(OH)_4^-$ aqueous complex, the existence of such an anionic species should cause an increase in Am(III) solubility at high pH which is not observed experimentally (Hummel et al. 2002), and therefore it is not included in the thermodynamic database. In this respect, the BB09 model must be considered to be semi-empirical in the sense that it is at least partially based on fitting considerations to a presumed reaction mechanism which, although of the correct form to fit the macroscopic measurement data, may not necessarily conform to the actual reaction mechanisms, or underlying assumption of systematic correlation through the LFER (unless, of course, the surface species can be directly confirmed by spectroscopic measurement).

The interplay between aqueous phase complexation reactions and surface reactions is important since they compete with each other to bind Am(III) in various mobile and immobile forms which is key to understanding the variation in K_d with groundwater composition. In the case of the aqueous phase complexation reactions, the different complexation reactions follow similar although subtly different trends to the surface reactions, with different hydroxyl complexes dominating the speciation at different pH levels as shown in Figure 4-4.

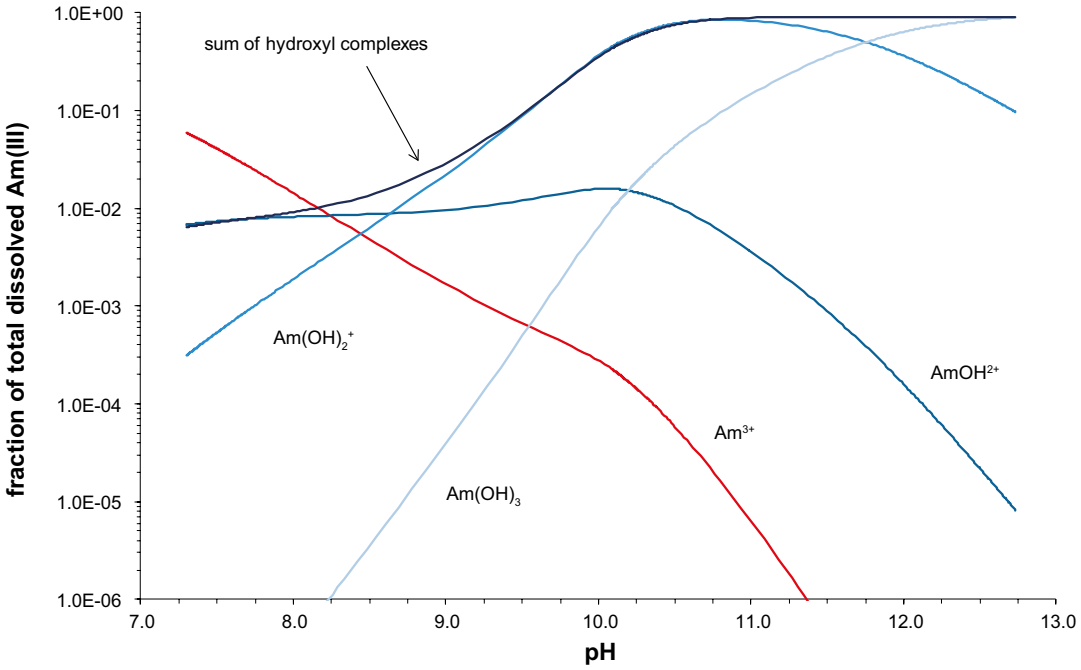

Figure 4-4. *Relative predominance of the free Am^{3+} aqua ion and other hydroxyl complexes in the aqueous phase as a function of pH for the groundwater compositional trend implied by mixing of OPC leachate and the groundwater characteristic of the Temperate saline time domain (Figure 4-1a).*

This, however, is only part of the picture since one must also consider the multitude of other speciation reactions involving Am^{3+}. A plot of the relative predominance of different complexed forms of dissolved Am(III) is shown in Figure 4-5 as a function of pH for the Temperate saline type groundwater. As can be seen from the figure, the dominant complexed form at the low pH end of the scale is silicate complexation, specifically the $AmOSi(OH)_3^{2+}$ complex. The inclusion or neglection of this reaction is of considerable significance for the relative predicted sorption trend for the Temperate saline groundwater composition as it is defined. If the role of silicate complexation is neglected, then the reference level for the Temperate saline type groundwater would be higher by up to 1–2 orders of magnitude relative to the high pH end of the sorption edge. This is significant because it not only affects the predicted K_d in groundwater where silicate might be an important ligand, but also the perceived difference in sorptivity relative to situations where it is clearly not an important ligand.

This presents a particular modelling uncertainty in the case of Am(III) and other trivalent nuclides since dissolved silicate is not usually considered to be an important complexing ligand for these elements in natural groundwaters. The speciation calculations here, however, suggest it cannot be entirely neglected. In the SKB-TDB (Duro et al. 2006) a 1:1 Am(III)-silicate complexation reaction is included as well as 1:1 and 1:2 Eu(III)-silicate complexes. These reactions are the same as those found in the Nagra-PSI TDB (Hummel et al. 2002). Thermodynamic constants for the silicate complexation reactions in the TDB are based on interpretation of solvent extraction measurement data by Jensen and Choppin (1996) for Eu(III) and by Wadsak et al. (2000) for Am(III).

At the time the Nagra-PSI TDB was published, the existence of the Am/Eu-silicate species was considered speculative on account of the fact that they had not been confirmed independently by spectroscopic studies. Since then, further studies of Cm(III) and Eu(III) silicate complexation have been reported by Panak et al. (2005) and Wang et al. (2005) whereby the existence of analogous postulated silicate complexes has been confirmed using time-resolved laser fluorescence spectroscopy (TRLFS).

The sorption calculations here indicate that this complexation reaction decreases in importance at the high pH levels characteristic of a strong OPC component in the groundwater and under such conditions it is the competition between hydrolysis reactions in the aqueous phase (hydroxyl complexes) and the corresponding surface reactions that determines the partitioning between the aqueous phase and surface bound fraction and thus the overall K_d value.

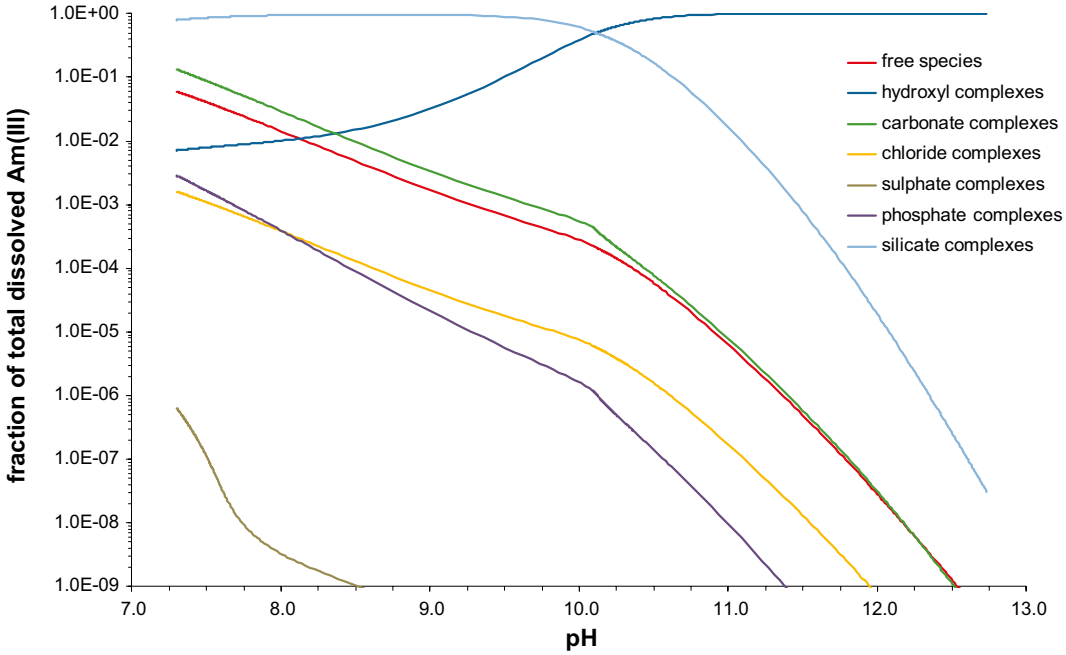

Figure 4-5. *Relative predominance of the free Am^{3+} aqua ion and different complexed forms in the aqueous phase as a function of pH for the groundwater compositional trend implied by mixing of OPC leachate and the groundwater characteristic of the Temperate saline time domain (Figure 4-1a).*

Redoing the sorption calculations for the Early Periglacial type groundwater, which is more meteoric in character, one finds a very different impact of speciation initially dominated by carbonate complexation as illustrated in Figure 4-6. The net impact of all considered aqueous phase complexation processes and surface reactions on the relative sorptive behaviour is shown in Figure 4-7 which gives a comparison for each groundwater type represented in Figure 4-1. The slightly reduced K_d for Am(III) in the non-OPC affected Periglacial groundwater in Figure 4-7 is largely due to the impact of aqueous carbonate complexation as can be seen from Figure 4-6, although the effect is nowhere near as great as what would be predicted purely on the basis of speciation considerations (as discussed previously).

In the literature, ternary carbonato- and hydroxo-carbonato surface complexes of trivalent actinides have been inferred from spectroscopic measurements in sorption experiments involving phyllosilicates (Marques Fernandes et al. 2008, 2010, Stumpf et al. 2002). Since the illite sorption model used in the present calculations only considers reactions of the free aqua ion, Am^{3+} with surface hydroxyl groups, it is therefore possible the model under predicts sorption in the presence of carbonate. Whether this actually happens at the carbonate concentrations characteristic of the groundwater system under present consideration, however, is unclear.

While this discussion is limited to Am(III), it should illustrate the importance of the interplay between speciation and surface complexation reactions as well as the underlying assumptions inherent in the modelling such as specific reaction mechanisms included or neglected as well as the accuracy and completeness of thermodynamic data used in such calculations. Although the example calculations described here appear complicated, the sorptive properties of the non-redox sensitive trivalent elements such as Am are relatively straight-forward to describe in comparison to some of the redox sensitive elements such as U, Np, and Pu where the impact of redox speciation must be additionally considered.

It may also be added that not all nuclides exhibit increases in relative sorptivity in response to elevated pH conditions. In some cases, the K_d at the high pH end of the mixing curve is predicted to be significantly less than that for normal groundwater pH levels unaffected by OPC leachate. While the enhancement of sorptivity in the presence of an OPC leachate plume might be neglected for some nuclides where this can be shown to be a conservative assumption (i.e. if it can't be accurately quantified), the same cannot be said for nuclides where sorption decreases significantly at high pH levels. Since the calculations are only qualitative, this presents a problem since a quantitative measure of sorptivity is required for transport calculations. The recommendation for how this should be handled in SR-PSU is discussed on a case by case basis in the following sections.

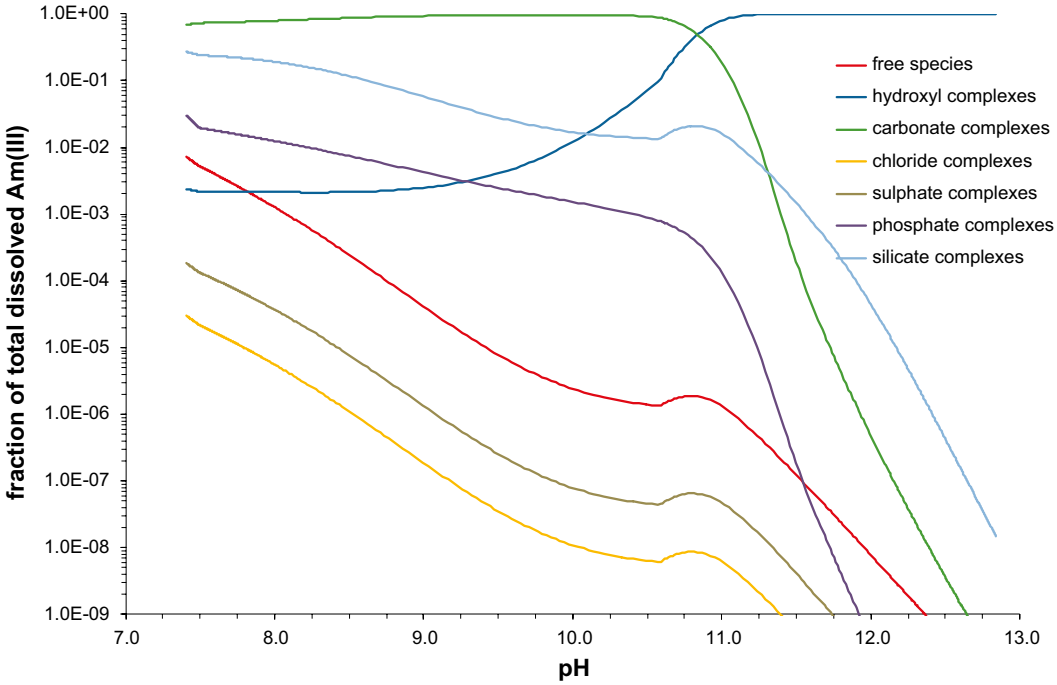

Figure 4-6. *Relative predominance of the free Am^{3+} aqua ion and different complexed forms in the aqueous phase as a function of pH for the groundwater compositional trend implied by mixing of OPC leachate and the groundwater characteristic of the Periglacial time domain (Figure 4-1b).*

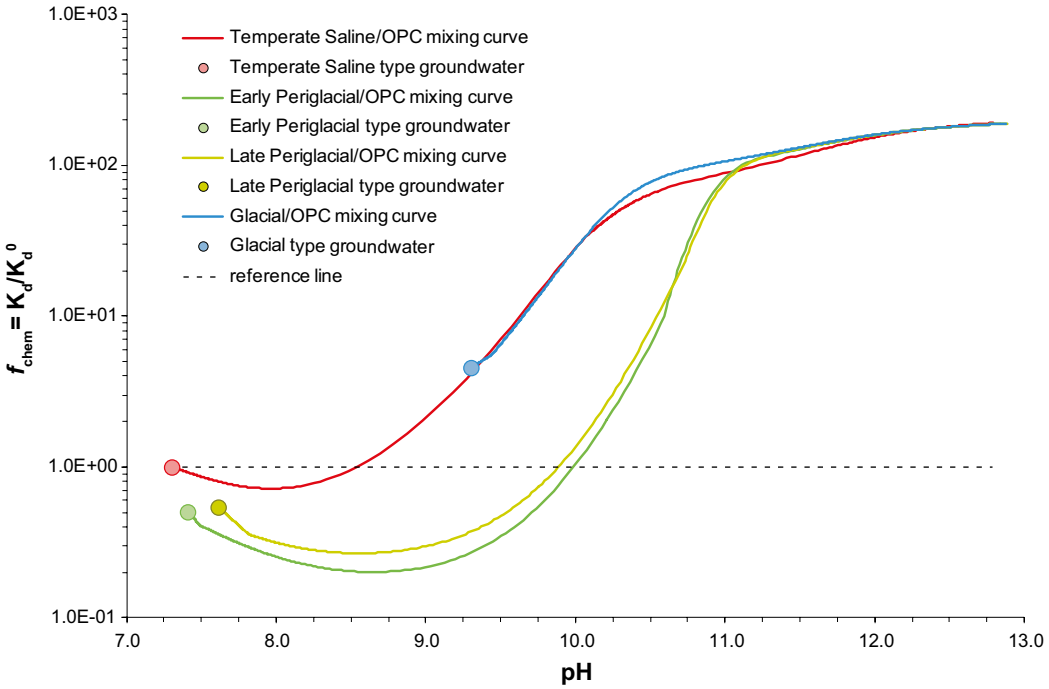

Figure 4-7. *The sorption edge for Am(III) sorption versus pH on illite modelled using the BB09 model and the groundwater compositional trend implied by mixing of OPC leachate and each of the groundwater types considered in Figure 4-1. The theoretical K_d value (sum surface species) is plotted relative to the reference level of the unaffected Temperate Saline type groundwater.*

5 Sorption data for specific radionuclides of interest

This section contains a brief overview of the main features of each radionuclide, or analogue group, designated as being of importance in the SR-PSU safety assessment as defined in the inventory list (SKB 2013). This includes a basic description of the chemical reactive characteristics of each nuclide as well as specific details relevant to the selection of K_d data to be used in transport calculations. This is based in part on the corresponding descriptions given in Crawford (2010), although expanded to include discussion of groundwater compositions deemed to be representative of expected conditions in and around the SFR repository. Sorption and speciation calculations are based on the type groundwater compositions reported by Auqué et al. (2013) for the different time domains with additional consideration given to the impact of high pH leachate from cement and concrete materials comprising the repository in cases where this was deemed particularly relevant.

5.1 Americium (Am)

The principal Am isotopes deemed of interest in the SFR waste materials are the ^{241}Am (432.2 y half-life), ^{242m}Am (141 y half-life), and ^{243}Am (7,370 y) decay chain products. The trivalent Am(III) form is the only relevant redox state for this radioelement and its importance also relates to the fact that, together with Eu(III), it is considered a geochemical analogue for the other trivalent actinides and lanthanides. The sorption of Am(III) and its analogue Eu(III) on site specific rock materials and in association with site specific groundwater compositions was studied as part of the Forsmark site descriptive modelling work (Byegård et al. 2008). It has also been discussed extensively in connection with the K_d data recommendation for the SR-Site safety assessment (Crawford 2010). Am(III) is expected to bind strongly to geological materials by way of a surface complexation sorption mechanism.

Am^{3+} is strongly hydrolysed in groundwater and readily forms complexes with dissolved carbonate reducing the availability of the free aqua ion. In the fresh groundwater type associated with the Early Periglacial and Late Periglacial (extended global warming) climate domains, carbonate complexation is thought to dominate the speciation of Am(III) and its analogue elements. At the higher pH levels characteristic of groundwater influenced by cement (OPC) leachate, however, hydrolysis plays an increasingly important role and carbonate complexation typically decreases steeply at pH > 11. This, however, is at least partly related to the reduced availability of carbonate at higher pH levels as regulated by calcite equilibrium.

For the Temperate saline type groundwater, on the other hand, silicate complexation is expected to dominate the aqueous phase speciation up to at least pH ≈ 10 for a total Si concentration on the order of 10 mg/l, the predominant species being $AmOSi(OH)_3^{2+}$. Previously, dissolved silicate has not been considered to be an important complexing ligand for Am(III). This is partly due to its lesser importance in groundwater with carbonate concentrations exceeding ~200 mg/l, but also due to the uncertain status of reported stability constants in the literature for complexation with dissolved silicate (e.g., Reiller et al. 2012).

As noted in Crawford (2010), the data for Am(III) in contact with Forsmark and Laxemar site specific rocks suggest a slightly reduced K_d value for fresh groundwater relative to saline conditions, most likely due to the impact of carbonate complexation. In the SR-Site K_d data recommendation, however, the effect was deemed to be weak relative to the overall data variability/uncertainty and also difficult to quantify due to additional uncertainty concerning the actual contact groundwater compositions achieved in the laboratory sorption experiments. In the SR-Site K_d recommendation, data for Am(III) and its analogue Eu(III), were therefore pooled over all contact solution compositions and assumed to represent an overall uncertainty distribution arising due to groundwater compositional uncertainty.

In the laboratory studies carried out as a part of the site investigation SDM-Site (Byegård et al. 2008, Selnert et al. 2009), a drift of up to 1.5 pH units was observed during the course of the sorption experiments for all groundwater compositions used. This was interpreted to be due to degassing of carbonate to a lower CO_2 partial pressure in the headspace of the glovebox where experiments were conducted since the same drift was observed in control samples without geological materials added.

It is noted that the elevated pH and reduced carbonate concentrations resulting from this process are similar to that which would be expected due to mixing of groundwater with OPC leachate in the geosphere surrounding SFR. For this reason, the SDM-Site laboratory data are arguably more appropriate for groundwater conditions in the SR-PSU safety assessment than for SR-Site. The previous K_d data recommendation for Am(III) may therefore be considered conservative for application within SR-PSU. A best estimate K_d value of 1.48×10^{-2} m^3/kg is thus recommended where the uncertainty distribution is assumed to be lognormally distributed ($\log_{10} K_d = -1.83 \pm 0.72$). For stochastic simulations, it is recommended that the uncertainty distribution be sampled in log space between the 2.5% (5.74×10^{-4} m^3/kg) and 97.5% percentiles (3.83×10^{-1} m^3/kg).

The qualitative sorption and speciation calculations made using the BB09 illite sorption analogue (see Section 4.2), suggest that the K_d will be significantly enhanced at high pH by as much as a factor of 10–100 relative to the non-OPC affected reference groundwaters depending on underlying assumptions. Sensitivity analyses may therefore need to be made to assess the impact of enhanced sorptivity at high pH levels since the ^{241}Am and ^{242m}Am radioisotopes are members of the Neptunium ($4n+1$) and Radium ($4n+2$) decay chains, respectively (this is discussed in more detail in Section 6). The strongly enhanced sorptivity of Am(III) at high pH may therefore have dose consequences for the less strongly sorbing daughter nuclides in these decay chains.

5.2 Barium (Ba)

The principal isotope of Barium present in the SFR waste materials is ^{133}Ba with a half-life of 10.51 y. It is formed principally as an activation product of naturally occurring ^{130}Ba in concrete reactor structural materials and is not considered to be an important nuclide for radiological risk except in cases involving very fast release. The divalent Ba(II) form is the only relevant redox state for this radioelement and it is geochemically analogous with Ra(II).

Calculations made using the single site cation-exchange model for Äspö diorite described in Byegård et al. (1998), suggest a lower K_d value for the Temperate saline type groundwater than for the Periglacial or Glacial type groundwaters. It is also found that the magnitude of the K_d value varies approximately in inverse proportion to the background Ca^{2+} concentration. This is the same model used previously to estimate f_{chem} correction factors for cation-exchanging solutes in Crawford (2010). Since reactions for the aqueous phase complexes $BaOH^+$, $BaCO_3$, $BaHCO_3^-$, and $BaSO_4$ are not included in the SKB-TDB (Duro et al. 2006), data for these reactions were imported from the Nagra-PSI database (Hummel et al. 2002). Although this might represent an internal inconsistency with regard to the careful selection of thermodynamic data in the SKB-TDB, this is deemed to have only a minor impact on the overall groundwater composition in the present calculations and thus can be reasonably neglected.

For the temperate saline groundwater, the Ca^{2+} concentration and ionic strength vary only very slightly in response to mixing with OPC leachate as can be seen from Figure 4-1. Very little change in K_d is therefore predicted for this groundwater type as a function of OPC mixing fraction, although it does decline slightly with increasing OPC mixing fractions. The K_d at high OPC mixing fractions is only about half that of the unaffected groundwater, which given the uncertainties of the underlying cation-exchange model, can probably be neglected.

Both of the Periglacial groundwater sub-types, on the other hand, are associated with a non-monotonic variation in Ca^{2+} concentration with a minimum at an OPC mixing fraction of roughly 5–10%. The minimum Ca^{2+} concentration is roughly 1.5 orders of magnitude less that in the non-OPC affected groundwater. This is related to the chemical buffering effect of the calcite/bicarbonate system in response to mixing with OPC leachate. A relative K_d increase of slightly greater magnitude is predicted for the sorption of Ba^{2+} which mirrors the envelope of Ca^{2+} variation. This implies an optimum K_d at 5–10% OPC mixing fraction roughly ≈ 1,000 greater than the corresponding K_d value for the non-OPC affected groundwater followed by a decline towards higher OPC mixing fractions converging to the same value as the Temperate saline groundwater. For the glacial-derived groundwater, the minimum concentration of Ca^{2+} is shifted to a very low mixing fraction ≤ 0.5% on account of the low buffering capacity of the unaffected groundwater which is very dilute. For the Glacial derived groundwater, the K_d follows a largely monotonic decreasing trend in response to increasing mixing fractions of OPC leachate also eventually converging to the same value as for the Temperate saline groundwater.

For Temperate saline groundwater conditions, a best estimate K_d value of 10^{-3} m^3/kg is recommended where the uncertainty distribution is assumed to be lognormally distributed ($\log_{10} K_d = -3.00 \pm 0.46$). For stochastic simulations, it is recommended that the uncertainty distribution be sampled in log space between the 2.5% (1.3×10^{-4} m^3/kg) and 97.5% percentiles (8.0×10^{-3} m^3/kg). Corresponding K_d values for other type groundwater compositions are given in Table 6-1.

Since ^{133}Ba is not part of a nuclide decay chain and because the estimated K_d for Temperate saline groundwater barely changes in response to mixing with OPC leachate, it is reasonable to assume the K_d value for Saline groundwater as being conservative even in the presence of a high pH plume. If consideration is otherwise given to the different prevailing groundwater compositions in different time domains, the appropriate K_d values for non-OPC affected groundwater are somewhat higher than for the Temperate saline case. In such situations it is reasonable to assume the value for Temperate saline groundwater as a lower limit for the K_d value in parts of the geosphere that are strongly OPC-affected (i.e. pH > 10).

5.3 Cadmium (Cd)

The principal isotope of Cadmium present in the SFR waste materials is ^{113m}Cd with a half-life of 14.1 y. It is formed principally as an activation product of stable Cd in reactor structural materials and is not considered to be an important nuclide for radiological risk except in cases involving very fast release. The divalent Cd(II) form is the only relevant redox state for this radioelement. Cd(II) does share certain geochemical similarities to Ni(II), although the analogy is weak owing to the considerably larger ionic radius and weaker hydrolysis of the Cd^{2+} cation. A more detailed account of Cd chemistry can be found in Crawford (2010). In the absence of more reliable data for Cd sorption, and owing to its minor importance for geosphere transport calculations, it is recommended that the corresponding K_d range for Ni(II) sorption be used for this nuclide.

5.4 Calcium (Ca)

The principal isotope of Calcium present in the SFR waste materials is ^{41}Ca with a half-life of 1.02×10^5 y. It is formed as an activation product of stable ^{40}Ca present in concrete reactor structural materials. The divalent Ca(II) form is the only relevant redox state for this radioelement. Ca(II) is one of the most abundant major cations present in groundwater and its availability is usually governed by calcite equilibrium although it also participates in cation-exchange reactions.

Isotope fractionation and dilution of ^{41}Ca can occur by reaction with calcite present both within fracture coatings and within the small amounts which are ubiquitous in the rock matrix. The effective K_d for the isotope dilution process involving calcite can be derived by analogy with that for ^{14}C labelled bicarbonate ion (see Appendix A) and can therefore be expected to exhibit a theoretical inverse proportionality to the total background concentration of non-active Ca^{2+}. Unlike ^{14}C, however, the effective K_d attributable to the calcite isotope dilution reaction is expected to be less than that for non-OPC affected groundwater since the OPC leachate is characterised by elevated Ca^{2+} concentrations (although less so for Temperate saline groundwater). Based on the high background concentrations of non-active Ca^{2+} present in the groundwater, the ^{41}Ca radioisotope can be reasonably assumed to be effectively non-sorbing for all conceivable groundwater compositions in the surroundings of SFR, both for the rock matrix proper and for isotope exchange on fracture calcites.

5.5 Carbon-14 (^{14}C)

The Carbon 14 (^{14}C) radioisotope with a half-life of 5,730 y is a very important nuclide in the SFR inventory and was found to dominate radiological risk in a previous safety assessment (Thomson et al. 2008). ^{14}C is expected to migrate from the SFR repository in the form of methane or organic acids resulting from anaerobic fermentation processes and also in inorganic form either as gaseous $CO_{2\,(g)}$ or dissolved carbonate, HCO_3^-. Migration of ^{14}C labelled methane in gaseous form or dissolved in groundwater is not expected to be associated with significant retardation and therefore

may be assumed to be effectively non-sorbing for the purposes of SR-PSU transport calculations. The same is likely to be true for organic acids. It is implicitly assumed in this work that the inorganic ^{14}C fraction will dissolve in groundwater and be transported in the form of the bicarbonate ligand HCO_3^- and its various speciated forms.

In Crawford (2010) a K_d of zero was recommended for ^{14}C on account of its minor importance as a nuclide for the SR-Site transport calculations and owing to the lack of unambiguous data indicating non-zero sorptivity on granitic rock. In the previous safety assessment for SFL 3–5 the recommended K_d data range (Skagius et al. 1999) for inorganic ^{14}C sorption was based on the recommendation by Carbol and Engkvist (1997) used in the SR-97 safety assessment (SKB 1999). The earlier, non-zero K_d recommendation was derived from a scoping calculation described previously by Albinsson (1991) using a literature K_d value for ^{14}C sorption on calcite scaled by an order of magnitude guesstimate of the mass fraction of calcite thought to be present in generic Swedish granitic rocks as an accessory mineral.

Recommended K_d ranges for sorption of $H^{14}CO_3^-$ in calcite fracture coatings are given in Appendix A. The recommended data are based on thermodynamic calculations of isotope exchange in calcite scaled by the effective fraction of exchangeable carbonate (derived from the measured BET surface area of fracture calcites and an assumed accessible penetration depth for the isotope exchange process). If quantitative data were available for the abundance of the trace calcite amounts in Forsmark site-specific rocks (i.e. as secondary precipitates in the rock matrix), then these could be used in principle to estimate non-zero K_d values for sorption of inorganic ^{14}C in the rock matrix. Since such data are not currently available, the recommendation of non-sorbing status for the rock matrix is deemed cautious for SR-PSU transport calculations.

5.6 Cesium (Cs)

The principal Cesium isotopes of interest in SFR waste materials are the ^{135}Cs (2.3×10^6 y half-life) and ^{137}Cs (30.2 y half-life) fission products. The monovalent Cs(I) form is the only relevant redox state for this radioelement. The sorption of Cs on site specific rock materials and representative groundwater compositions is discussed in some detail in connection with the data recommendation for the SR-Site safety assessment. The Cs^+ cation is only very weakly hydrolysed and does not form any aqueous complexes with other ligands that are likely to influence K_d values in groundwater.

Cs^+ sorbs by way of an ion-exchange mechanism and the K_d value is therefore dependent on ionic strength and not considered to be particularly pH sensitive (i.e. no direct impact of pH on sorptivity). Indirect effects of pH on speciation may occur, for example, by formation of CsOH at very high pH levels, although the effect is deemed to be small relative to other uncertainties and can be neglected. In Crawford (2010) the effect of ionic strength was quantified by introducing a chemistry correction factor to account for ion-exchange competition. For the previous data recommendation the most cautious assumption was deemed to be the selection of data based on the most saline conditions expected given that spatial and temporal changes in groundwater chemistry were not resolved on the level of individual migration paths.

Calculations made using the single site cation-exchange model for Äspö diorite described in Byegård et al. (1998) for SR-PSU specific groundwater compositions suggest qualitatively similar behaviour for Cs^+ as that already described for Ba^{2+} sorption. The predicted overall relative variation in K_d as a function of OPC mixing fraction is, however, less than that for Ba^{2+}. Nonetheless, the calculations imply a lower K_d value for the Temperate saline type groundwater than for the Periglacial or Glacial type groundwaters. For Temperate saline groundwater conditions, a best estimate K_d value of 8.8×10^{-4} m^3/kg is recommended where the uncertainty distribution is assumed to be lognormally distributed ($\log_{10} K_d = -3.05 \pm 0.58$). For stochastic simulations, it is recommended that the uncertainty distribution be sampled in log space between the 2.5% (6.6×10^{-5} m^3/kg) and 97.5% percentiles (1.2×10^{-2} m^3/kg). Corresponding K_d values for the other type groundwater compositions are given in Table 6-1.

Since the radioisotopes of Cs are not part of nuclide decay chains and because the estimated K_d for Temperate saline groundwater barely changes in response to mixing with OPC leachate, it is reasonable to assume the K_d value for Saline groundwater as being conservative even in the presence of a high pH plume. If consideration is otherwise given to the different prevailing groundwater compositions in different time domains, the appropriate K_d values for non-OPC affected groundwater are somewhat

higher than for the Temperate saline case. In such situations it is reasonable to assume the value for Temperate saline groundwater as a lower limit for the K_d value in parts of the geosphere that are strongly OPC-affected (i.e. pH > 10).

5.7 Chloride (Cl)

The principal isotope of Chlorine is the ^{36}Cl fission product with a half-life of 3.01×10^5 y. The chloride anion, Cl^- is the only relevant redox state for this radioelement and it may be reasonably assumed to be non-sorbing.

5.8 Cobalt (Co)

The principal isotopes of Co are the ^{58}Co and ^{60}Co activation products with half-lives of 70.9 y and 5.27 y, respectively. They are formed principally as activation products of stable Co in cladding materials and are not considered to be important nuclides for radiological risk except in cases involving very fast release. The divalent Co(II) form is the only relevant redox state for this radioelement. Co(II) is a close geochemical analogue of Ni(II) and it is therefore recommended that the corresponding K_d range for Ni(II) sorption be used for these nuclides.

5.9 Curium (Cm)

The principal isotopes of Curium present in the SFR waste materials are ^{242}Cm (0.45 y half-life), ^{243}Cm (29.1 y half-life), and ^{244}Cm (18.1 y half-life). They are formed by neutron capture reactions involving Pu and U in nuclear fuel. On account of their very short half-lives they are not considered to be important nuclides for radiological risk except in cases involving very fast release. The trivalent Cm(III) form is the only relevant redox state for this radioelement and it may be assumed to be geochemical analogous to Am(III). The recommended K_d range for Cm(III) sorption is therefore the same as the corresponding recommendation for Am(III). Since the ^{243}Cm and ^{244}Cm radioisotopes are members, respectively, of the actinium ($4n$+3) and thorium ($4n$) decay chains, sensitivity analyses may need to be made to assess the impact of enhanced sorptivity at high pH levels (this is discussed in more detail in Section 6).

5.10 Europium (Eu)

The principal Europium isotope of interest in the SFR waste materials is the ^{152}Eu fission product with a half-life of 13.54 y. On account of its very short half-life it is not considered to be an important nuclide for radiological risk except in cases involving very fast release. The trivalent Eu(III) form is the only relevant redox state for this radioelement and it may be assumed to be geochemical analogous to Am(III). As noted previously, the site specific K_d recommendation for Am(III) is actually based on a mixture of sorption data for Am(III) and Eu(III) which are combined under the assumption of a close geochemical analogy between these solutes. The recommended K_d range for Eu(III) sorption is therefore the same as the corresponding recommendation for Am(III). The enhancement of sorptivity at high pH may be conservatively neglected since ^{152}Eu is not part of a decay chain.

5.11 Holmium (Ho)

The principal isotope of Holmium present in the SFR waste materials is the ^{166m}Ho fission product with a half-life of 1,200 y. The trivalent Ho(III) form is the only relevant redox state for this radioelement and it may be assumed to be geochemically analogous to Am(III). The recommended K_d range for Ho(III) sorption is therefore the same as the corresponding recommendation for Am(III). The enhancement of sorptivity at high pH may be conservatively neglected since ^{166m}Ho is not part of a decay chain.

5.12 Iodine (I)

The principal Iodine isotope of interest in the SFR waste materials is the long-lived ^{129}I fission product with a half-life of 1.57×10^7 y. The iodide anion, I^- is the only relevant redox state for this radioelement and it may be reasonably assumed to be non-sorbing.

5.13 Molybdenum (Mo)

The principal Molybdenum isotope present in the SFR waste materials is the ^{93}Mo activation product with a half-life of 4,000 y. It is formed by neutron capture from the stable ^{92}Mo present in fuel alloy cladding. The hexavalent Mo(VI) form is the only relevant redox state for this radioelement which is found in groundwater as the molybdate, MoO_4^{2-} oxyanion species. Although measurement data has not been reported for sorption on granitic rocks, a large body of literature exists describing the sorption of MoO_4^{2-} on oxides, clay minerals, and soils (e.g. Goldberg et al. 1996, 2007).

Being negatively charged, MoO_4^{2-} is not expected to sorb very strongly on matrix minerals which exhibit predominantly negative charge at normal groundwater pH levels and even less so under alkaline conditions. Any sorption of MoO_4^{2-} that does occur is most likely associated with minerals that have point of zero charge around normal groundwater pH levels, such as ferric oxide accessory minerals (including goethite, hematite, or magnetite) in the rock matrix. Owing to its very weak sorption the MoO_4^{2-} oxyanion can be reasonably assumed to be effectively non-sorbing for the purposes of SR-PSU transport calculations. Since ^{93}Mo is not part of a decay chain, this may be regarded as a conservative assumption.

5.14 Neptunium (Np)

The principal isotope of Neptunium present in the SFR waste materials is the ^{237}Np decay chain product with a half-life of 2.14×10^6 y. Np is redox sensitive and can exist in a number of oxidation states from Np(III) to Np(VII), although only the Np(IV) and Np(V) redox states are relevant for normal groundwater compositions and Eh ranges. If the groundwater is sufficiently reducing, the strongly sorbing Np(IV) state is predominant, whereas the weakly sorbing Np(V) state occurs under oxidic conditions. The sorption of Np was studied in contact with site specific rock materials and groundwater compositions as part of the Forsmark and Laxemar site descriptive modelling work, SDM-Site (Byegård et al. 2008, Selnert et al. 2009). It has also been discussed extensively in connection with the K_d recommendation for the SR-Site safety assessment (Crawford 2010). Both Np(IV) and Np(V) are expected to sorb primarily by way of a surface complexation sorption mechanism.

In the previous data recommendation it was noted that redox conditions in the SDM-Site laboratory experiments were probably not sufficiently reducing to give rise to unambiguous sorption in the tetravalent state. The weak sorptivity measured for this radioelement was therefore assumed to represent a predominantly pentavalent redox speciation, or possibly a mixed redox state. The K_d recommendation given in Crawford (2010) for Np(V) was based on the SDM-Site data, whereas that for Np(IV) was based on an assumed geochemical analogy with Pu(IV) for which qualified data were available (i.e. qualified with regard to SKB's data qualification policy document).

The qualitative sorption and speciation calculations made using the BB09 illite sorption analogue (see Section 4.2) suggest that Np should be speciated in the tetravalent form for the Temperate saline and Periglacial type groundwaters. The calculations also suggest that the K_d will exhibit a decreasing trend with increasing pH (i.e. for an increasing mixing fraction of OPC leachate). The calculations indicate that the K_d in groundwater strongly influenced by OPC leachate could be reduced by a factor of as much as 10^4–10^5 relative to the K_d associated with unaffected groundwater, although with Np(IV) surface species still dominating the redox speciation.

For the comparison between Np(IV) and Np(V) sorption, a theoretical difference of at least four orders of magnitude is also found between the K_d values predicted for Temperate saline (reducing) and the Glacial (oxidizing) type groundwaters. This seems to present a data consistency problem, however, since the empirically derived K_d values previously cited in SR-Site (Crawford 2010) sug-

gest a factor ≈ 130 difference between Np(IV) and Np(V) sorptivity for non-OPC affected groundwaters. It is therefore not clear whether the difference between empirically measured K_d values for Np(IV) and Np(V) can be squared with the simplified model predictions of relative sorptivity in an internally consistent manner.

To avoid this apparent inconsistency (and given that the calculations of pH dependent trends in relative K_d are at best, a guesstimate), it was deemed cautious to assume that the K_d value for sorption of Np(IV) in strongly OPC-affected groundwater should be scaled to roughly the same level as that empirically established for Np(V) sorption rather than adopting the much larger reduction in K_d implied by the BB09 model. On the other hand, for the reducing saline Temperate and Periglacial groundwater types at pH < 10 the K_d value from SR-Site for Np(IV) sorption is recommended for use in migration calculations. This implies a best estimate K_d value of 5.3×10^{-2} m^3/kg where the uncertainty distribution is assumed to be lognormally distributed ($\log_{10} K_d = -1.28 \pm 0.65$). For stochastic simulations, it is recommended that the uncertainty distribution be sampled in log space between the 2.5% (2.8×10^{-3} m^3/kg) and 97.5% percentiles (9.8×10^{-1} m^3/kg).

For the oxidising, Glacial type groundwater a best estimate K_d value of 4.1×10^{-4} m^3/kg is recommended for Np(V) sorption where the uncertainty distribution is assumed to be lognormally distributed ($\log_{10} K_d = -3.38 \pm 0.74$). For stochastic simulations, it is recommended that the uncertainty distribution be sampled in log space between the 2.5% (1.5×10^{-5} m^3/kg) and 97.5% percentiles (1.2×10^{-2} m^3/kg). The K_d range for Glacial groundwater is thus the same as that for the Temperate saline and Periglacial groundwaters at high pH in OPC-affected groundwater (pH > 10).

5.15 Nickel (Ni)

The principal Nickel isotopes present in the SFR waste materials are the ^{59}Ni (1.01×10^5 y half-life) and ^{63}Ni (100 y half-life) activation products resulting from irradiation of the metallic cladding of fuel elements. The divalent Ni(II) form is the only relevant redox state under normal groundwater conditions. Although Ni is not considered to be redox sensitive it may in certain situations exhibit an indirect sensitivity to redox conditions owing to competitive sorption with Fe(II) which may be present in elevated concentrations under reducing conditions (see, e.g. Bradbury and Baeyens 2005).

The geochemistry of Ni has been discussed in some detail previously in relation to the K_d data recommendation for SR-Site. Ni was also one of the elements chosen for study in the site descriptive modelling laboratory programme for SDM-Site (Byegård et al. 2008, Selnert et al. 2009). Ni is expected to sorb by way of a surface complexation mechanism, although it may also be influenced by ion exchange at lower pH levels. A non-trivial K_d trend related to ionic strength was identified in the SDM-Site sorption experiments which could be indicative of an ion-exchange process. Although the empirically identified trend was taken into consideration for the K_d recommendation in Crawford (2010) it was also noted that the pH of the contact groundwater compositions used in the experiments were correlated with ionic strength, implying the possibility that the observations might also be related to hydrolysis of the free aqua ion (ionic strength therefore being a confounding factor).

Speciation calculations made using PhreeqC indicate that the free cation, Ni^{2+} should be the dominant species in both the Temperate saline and Periglacial groundwater (Auqué et al. 2013). The calculations suggest that free Ni^{2+} should be dominant up to pH ≈ 9.5 after which hydrolysis starts to play an increasingly important role with increasing mixing fraction of OPC leachate. The main hydrolysed forms of Ni(II) are calculated to be $NiOH^+$, $Ni(OH)_2$, $Ni(OH)_3^-$, and $Ni(OH)_4^{2-}$ although their relative proportion varies as a function of pH. Chloride complexation in the form of $NiCl^+$ and $NiCl_2$ is relatively important for the Temperate saline groundwater accounting for up to ~30% of the dissolved concentration of Ni in non-OPC affected groundwater. For the Periglacial type groundwaters, chloride complexation plays a subordinate role and the carbonate complexed forms, $NiCO_3$ and $NiHCO_3^+$ are found to be more important with a peak around pH 9.0–9.5. For the Glacial type groundwater, the free Ni^{2+} aqua ion and hydroxyl complexes are of roughly equal importance with increasing predominance of hydrolysed species at higher pH levels characteristic of OPC affected groundwater.

Qualitative sorption calculations were also made for Ni(II) sorption using the BB09 illite analogue model, although it is difficult to draw proper conclusions since the cation-exchange part of the model was neglected (for reasons outlined previously in Section 4.2). While this is of limited significance for the Temperate saline groundwater where competition with Ca^{2+} appears to give very little additional sorption by way of the cation exchange mechanism, it may have a much larger impact on trends calculated for the Periglacial and Glacial type groundwaters.

On balance, however, the calculations which have been made suggest that the K_d value for non-OPC affected, saline groundwater should be conservative for application in SR-PSU at all groundwater pH levels. The surface complexation reactions appear to give an increasing K_d up to an optimum at roughly pH 10–11, followed by a decrease in K_d at higher pH levels, although at all times greater than that characteristic of non-OPC affected groundwater. The surface complexation calculations also suggest negligible competition for sorption sites with Fe^{2+} at the concentration levels implied by the mixing calculations and the assumed redox controls.

Even though the SDM-Site data indicated that the sorptivity of Ni can be empirically related to groundwater salinity, the selection of the K_d range for the Saline contact water used in the laboratory experiments in Byegård et al. (2008) and Selnert et al. (2009) may be considered a cautious assumption for the purposes of SR-PSU transport calculations even if actual conditions in and around the SFR repository are less saline. This implies a best estimate K_d value of 7.4×10^{-4} m^3/kg where the uncertainty distribution is assumed to be lognormally distributed ($\log_{10} K_d = -3.13 \pm 0.79$). For stochastic simulations, it is recommended that the uncertainty distribution be sampled in log space between the 2.5% (2.1×10^{-5} m^3/kg) and 97.5% percentiles (2.7×10^{-2} m^3/kg). Any enhancement of sorptivity at high pH may be conservatively neglected since the radioisotopes of Ni do not occur in a decay chain.

5.16 Niobium (Nb)

The principal Niobium isotopes present in the SFR waste materials are the ^{93m}Nb (16.1 y half-life) and ^{94}Nb (2.03×10^4 y half-life) activation products of the stable ^{93}Nb present in fuel alloy cladding. The pentavalent Nb(V) form is the only relevant redox state for this radioelement. Only ^{94}Nb is considered an important nuclide for SR-PSU transport calculations although the metastable ^{93m}Nb isotope may have some significance in cases involving very fast release. The SR-Site K_d recommendation for Nb(V) was based on data reported by Kulmala and Hakanen (1993) for samples of Olkiluoto tonalite and Rapakivi granite in contact with native groundwaters of fresh and saline characters, respectively. In the cited Finnish study, sorption measurements were also made using cement equilibrated groundwater (pH 12.7–12.9) and significant increases in measured K_d values were noted relative to the non-affected groundwater samples.

Calculations indicate that under normal groundwater conditions, Nb(V) is speciated as the NbO_3^- oxyanion and $Nb(OH)_5$ hydroxo-complex in roughly equal proportion, with the balance shifting towards a predominance of the oxyanion at increasing pH. Even though the speciation as an oxyanion might imply lower sorptivity, the measurement data described above suggest this appears to be outweighed by the increased surface complexation at higher pH levels. Sorption calculations have not been made for Nb(V).

Given the uncertainties concerning the underlying data set and the unknown extent of high pH conditions surrounding the SFR repository, it is deemed cautious that the same data recommendation given for SR-Site also be used for transport calculations involving this radioelement in SR-PSU. This implies a best estimate K_d value of 2.0×10^{-2} m^3/kg where the uncertainty distribution is assumed to be lognormally distributed ($\log_{10} K_d = -1.70 \pm 0.64$). For stochastic simulations, it is recommended that the uncertainty distribution be sampled in log space between the 2.5% (1.1×10^{-3} m^3/kg) and 97.5% percentiles (3.5×10^{-1} m^3/kg). Although the experimental data suggest an increase in K_d at high pH this is difficult to quantify for the site specific materials and groundwater. For pH > 10 it is therefore recommended that the K_d values remain unchanged. Since the radioisotopes of Nb are not part of a decay chain this may be considered a conservative assumption.

5.17 Plutonium (Pu)

The isotopes of Plutonium present in SFR waste materials are the same as those normally present in spent nuclear fuel deriving from the thorium ($4n$), neptunium ($4n+1$), radium ($4n+2$), and actinium ($4n+3$) series. The relevant nuclides and their half-lives are ^{238}Pu (87.7 years), ^{239}Pu (2.41×10^4 years), ^{240}Pu (6.56×10^3 years), ^{241}Pu (14.4 years), and ^{242}Pu (3.75×10^5 years). The chemistry of Pu is discussed in considerable detail in Crawford (2010) and is not repeated here except to note that the interplay between aqueous phase speciation and surface sorption including redox transitions gives rise to very complicated sorption behaviour for Pu.

Qualitative sorption and speciation calculations made using the BB09 illite sorption analogue (see Section 4.2) suggest that Pu(III) should be the dominant redox species in the aqueous phase for the Temperate saline groundwater up until roughly pH 8.75, after which Pu(IV) becomes more abundant. For the Temperate saline groundwater, the free Pu^{3+} aqua ion and carbonate complexes dominate the aqueous speciation, although with an increasing proportion of hydroxyl complexation up to about pH 8.5. Although Pu(IV) becomes the prominent dissolved redox species at pH ≥ 8.75, surface complexation reactions involving Pu(III) still dominate over the entire range of OPC mixing fractions for this groundwater type. The apparent K_d rises slightly to an optimum level at roughly pH 8.5 after which it decreases at higher pH levels. The minimum K_d value at pH 12 is predicted to be roughly an order of magnitude less than that for the non-OPC affected groundwater. It is important to note here that the dominant redox species are often predicted to be (simultaneously) different in the aqueous phase and the sorbed phase, which although counterintuitive, is fully in agreement with the mass action relations describing the redox equilibria in combination with those describing surface species partitioning.

A similar redox transition from Pu(III) to Pu(IV) predominance in the aqueous phase is seen for both Periglacial groundwater subtypes, although at the slightly higher pH of 10. For these groundwater types, Pu(III)-carbonate complexed forms dominate the aqueous speciation in the Pu(III) region, while Pu(IV)-hydroxyl complexes dominate in the Pu(IV) region. Surface complexation reactions involving Pu(III) dominate the sorption of Pu except for an interval between roughly pH 8.5–11.5 where surface complexation reactions involving Pu(IV) are dominant. The K_d value decreases with increasing pH reaching a minimum value at pH > 12, predicted to be roughly 2 orders of magnitude less than that for the non-OPC affected groundwater.

For the oxidizing Glacial-derived groundwater, Pu(IV) is the dominant redox species at all modeled pH levels. In this case, Pu(IV)-hydroxyl complexes overwhelmingly dominate the aqueous phase speciation. Similarly to the Periglacial groundwater, the K_d value decreases with increasing pH reaching a minimum value at pH > 12, at least 2 orders of magnitude less than that for the non-OPC affected groundwater.

Owing to the complex pH dependent behaviour of the aqueous Pu redox chemistry and associated sorption reactions it is difficult to assign unequivocal K_d values for a definite redox state in SR-PSU transport calculations and a mixed Pu(III/IV) redox state must generally be assumed. This is particularly the case where there is the likelihood of even a small OPC leachate influence on groundwater composition along a migration path. For this reason the K_d value recommended for Am(III), based on geochemical analogy with Pu(III), is recommended to be used for all groundwater types considered in SR-PSU (oxidizing and reducing conditions). This implies a best estimate K_d value of 1.5×10^{-2} m^3/kg where the uncertainty distribution is assumed to be lognormally distributed ($\log_{10}K_d = -1.83 \pm 0.72$). For stochastic simulations, it is recommended that the uncertainty distribution be sampled in log space between the 2.5% (5.7×10^{-4} m^3/kg) and 97.5% percentiles (3.8×10^{-1} m^3/kg).

Since the qualitative sorption calculations indicate a significantly reduced K_d at high pH levels, a K_d value reduced by about a factor of 1,000 is suggested as a reasonable K_d value for pH > 10. Although this is a greater K_d reduction than what is simulated using the BB09 illite analogue model, this is proposed as a limiting case for high pH conditions since the K_d associated with the non-OPC affected region of the migration path will still largely dominate the transport retardation of Pu itself. The neglection of a pH plume altogether (or K_d otherwise assumed unchanged relative to the case of non-OPC affected groundwater), on the other hand, might be considered to give the opposite limiting case for the relevant decay chains where the relatively less mobile Pu may have dose consequences for daughter nuclides. If there is any uncertainty as to which assumption has the greatest impact on dose rates involving daughter nuclides, sensitivity analyses may need to be made to identify the most conservative case in SR-PSU.

5.18 Polonium (Po)

The only safety relevant nuclide of polonium is ^{210}Po which is part of the ^{238}U decay chain/radium series ($4n$+2) where it is the last radioactive daughter preceding stable ^{206}Pb. It is not often considered directly in radionuclide transport calculations on account of its short half-life (138.4 days) and since its decay can be readily incorporated in the dose factor for its parent nuclide ^{210}Pb (e.g. Avila et al. 2010). This, however, is based on the assumption of secular equilibrium with ^{210}Pb, which may not always be a good assumption, particularly if migration of ^{210}Po is less strongly retarded. In a study by Seiler (2011), for example, ^{210}Po activities were found to significantly exceed the ^{210}Pb parent nuclide in Nevada groundwater wells with naturally high background uranium levels. This could be interpreted as indicating low sorptivity of the daughter nuclide relative to the parent during aquifer migration thus giving transported ^{210}Po/^{210}Pb activity ratios greater than that predicted by secular equilibrium. In a review of Finnish groundwater data by the same author (Seiler et al. 2011), on the other hand, ^{210}Po activities were found to be roughly equal to, or less than ^{210}Pb. In cases where ^{210}Po/^{210}Pb activity ratios are equal or less than unity, the assumption of secular equilibrium could be considered conservative for risk assessment calculations.

Recommendation of a K_d value for ^{210}Po migration is clearly problematic, partly due to its uncertain redox chemistry, but also due to the fact that the transport retardation of ^{210}Po arriving at the biosphere is most probably associated with no more than the first few tenths of a mm of the rock matrix adjacent to flow bearing fracture surfaces. This very low effective depth of penetration is due to its short half-life allowing little opportunity for more intimate contact with deeper parts of the rock matrix. Additionally, the very short half-life of ^{210}Po also means that only the last few metres (to perhaps some tens of meters under high flow situations) are relevant for the K_d data selection. If the groundwater redox conditions in these parts of the migration flowpath are less strongly reducing than the specified SR-PSU type groundwaters, sorption of Po(IV) would probably occur.

In the tetravalent state, dissolved Po(IV) is mostly expected to be found as the oxyanion, PoO_3^{2-} and will only sorb on mineral surfaces that have non negligible amounts of positive surface charge at normal groundwater pH levels (e.g. ferric oxides including hematite, goethite, etc). The lower abundance of positive charge above the pH_{PPZC} (pristine point of zero charge) implies significantly reduced sorption at elevated pH levels. The sorption chemistry of ^{210}Po has been considered in some detail in Appendix C where a geochemical analogy with Se is invoked. As a conservative lower bound for the sorption of Po(IV), the K_d value of 3×10^{-4} m^3/kg given by Crawford (2010) for Se(IV) in the undisturbed rock matrix can be used. As discussed in Appendix C, any redox state other than tetravalent can be considered to be effectively non-sorbing ($K_d \approx 0$).

However, since ^{210}Po is expected to only interact with a very thin layer of rock immediately adjacent to fracture surfaces, best estimate K_d values for Po(IV) in the present author's judgement are unlikely to be less than about 10^{-3} m^3/kg and probably higher if there are significant amounts of ferric oxide minerals (or MnO_2) present. It is also noted in Appendix C that the more metallic character of Po relative to Se and its well-documented tendency to form intrinsic colloids (e.g. Ansoborlo et al. 2012 and references therein) means that use of sorption data for the possibly more weakly sorbing Se species may be over-conservative.

The relevant redox state of Po is unclear owing to highly uncertain thermodynamic data. From the available data, however, and comparison with its nearest geochemical analogues (Se and Te) it appears not possible to rule out Po(–II) redox speciation for the specified Eh ranges of Saline, Early- and Late-Periglacial groundwaters and most likely Po(VI) for glacial-derived groundwater. In OPC-affected groundwater (pH > 10), the K_d can be reasonably assumed to be zero for all Po redox states.

5.19 Samarium (Sm)

The principal isotope of Samarium present in the SFR waste materials is the ^{151}Sm fission product with a half-life of 90 y. The trivalent Sm(III) form is the only relevant redox state for this radio-element and it may be assumed to be geochemically analogous to Am(III). The recommended K_d range for Sm(III) sorption is therefore the same as the corresponding recommendation for Am(III). The enhancement of sorptivity at high pH may be conservatively neglected since ^{151}Sm is not part of a decay chain.

5.20 Selenium (Se)

The principal isotope of Selenium present in the SFR waste materials is the ^{79}Se fission product with a half-life currently estimated to be 3.77×10^5 y (this has been subject to some uncertainty in historic safety assessments owing to the difficulty of measuring ^{79}Se decay in impure samples in an unambiguous fashion). Se is redox sensitive and can exist in Se(-II), Se(0), Se(IV), and Se(VI) states. In the –II redox state it exists primarily as the HSe^- anion whereas in the tetravalent and hexavalent redox state, Se is predominantly speciated in oxyanion form as $HSeO_3^-$ and SeO_4^{2-}, respectively. The elemental form of Se(0) is not expected to exist as an aqueous species although may precipitate by heterogeneous reduction of surface sorbed Se(IV) or Se(VI).

The sorption chemistry of Se is discussed in some detail in Appendix C on account of it being a geochemical analogue for Po. The sorption of Se is generally weak and is expected to follow a similar pattern as that for Mo. A non-zero K_d for Se sorption was assigned in the SR-Site data recommendation based upon data for generic granitic materials as reported by Papelis (2001) and Ticknor et al. (1996), although owing to large data uncertainties it was noted that the case of non-sorbing status could also be defended by appealing to arguments of caution. In order to maintain consistency with the recommendation of zero sorptivity for the MoO_4^{2-} oxyanion, it is recommended that Se also be assigned non-sorbing status for the purposes of SFR-PSU transport calculations. It can also be noted that on the basis of thermodynamic calculations it is not possible to rule out predominance of Se(-II) for the specified Temperate saline and Periglacial groundwater Eh ranges, or Se(VI) for the glacial groundwater type. Both Se(-II) and Se(VI) are considered to be effectively non-sorbing. Since ^{79}Se is not part of a decay chain, the assumption of non-sorbing status may therefore be regarded as a conservative assumption.

5.21 Silver (Ag)

The principal isotope of Silver present in the SFR waste materials is the ^{108m}Ag fission product with a half-life of 418 y. The monovalent Ag(I) form is the only relevant redox state for this radioelement. As outlined previously in Crawford (2010), silver is problematic in that its sorption is not well characterised in granitic rock and the only candidate analogue element for which data exists, Cs(I) is considered to be a relatively poor match for the geochemical behaviour of this element. Although this analogy has been invoked in previous investigations (e.g. Carbol and Engkvist 1997), essentially the only commonality between these two elements is their monovalent charge. Ag^+ is a B-type soft cation in the classification introduced by Pearson (1963) which renders it much closer in behaviour to Cu^+ or Hg^+ than Cs^+ (possibly also closer to Ni^{2+} than Cs^+, although this is uncertain). The Ag^+ cation has an effective radius of hydration that is somewhere between K^+ and Na^+ and greater than Cs^+ which should imply lower ion-exchange sorptivity than Cs^+, all other things being equal. Unpublished data cited by Carbol and Engkvist (1997), on the other hand, suggests stronger sorptivity for Ag^+ in contact with sand (mostly quartz) than Cs^+ at low ionic strength and pH 6.

Cation exchange modelling described by Bradbury and Baeyens (2003) suggested vanishingly low K_d values for montmorillonite which led to the proposal of non-sorbing status for sorption on MX-80 bentonite in their data recommendation. In the SR-Can data report dealing with migration parameters for bentonite clay (Ochs and Talerico 2004) it was suggested that the low sorptivity estimated by Bradbury and Baeyens (2003) may be the result of the neglection of surface complexation sorption. This appears to be a reasonable notion given the chemical similarity of Ag^+ to the other heavy transition metal cations Cu^+, Hg^+, or Ni^{2+} mentioned above. Ag^+ can undergo hydrolysis to form AgOH and $Ag(OH)_2^-$.

An additional issue concerning the selection of a cautious K_d value for Ag(I) sorption is the fact that Ag^+ is strongly complexed by to form AgCl and $AgCl_2^-$, the free Ag^+ aqua ion typically comprising only a small fraction of the total Ag(I) concentration. Since it is presumably only the free aqua ion that undergoes sorption, this would imply a large uncertainty if K_d values for Cs(I) sorption were to be used for Ag(I) since Cs^+ does not readily form stable chloride complexes. Given the various uncertainties associated with this element and its greater importance in SR-PSU relative to SR-Site, it is not possible to recommend anything other than non-sorbing status for this particular radionuclide. Since ^{108m}Ag is not part of a decay chain, this may be regarded as a conservative assumption.

5.22 Strontium (Sr)

The principal Strontium isotope of interest in SFR waste materials is the ^{90}Sr fission product with a half-life of 28.7 years. The divalent Sr(II) form is the only relevant redox state for this radioelement. The sorption of Sr on site specific rock materials and representative groundwater compositions is discussed in some detail in connection with the data recommendation for the SR-Site safety assessment. Sr^{2+} is weakly hydrolysed and can form simple complexes with dissolved carbonate and sulphate although the free Sr^{2+} aqua ion is usually the predominant species. Sr sorbs by way of an ion-exchange mechanism and the K_d value is therefore dependent on ionic strength and not particularly pH sensitive.

In Crawford (2010) the effect of ionic strength was quantified by introducing a chemistry correction factor to account for cation-exchange competition. Since groundwater chemistry was not resolved on the scale of individual migration paths, the most cautious assumption was deemed to recommend data based on the most saline conditions expected in a similar fashion to that already described for Cs(I). Groundwater compositions surrounding the SFR repository are expected to exhibit trends towards decreasing salinity during the site evolution as outlined in Auqué et al. (2013).

Calculations made using the single site cation-exchange model for Äspö diorite described in Byegård et al. (1998) for SR-PSU specific groundwater compositions suggest qualitatively similar behaviour for Sr^{2+} as that already described for Ba^{2+} sorption. This implies a lower K_d value for the Temperate saline type groundwater than for the Periglacial or Glacial type groundwaters. For Temperate saline groundwater conditions, a best estimate K_d value of 1.5×10^{-5} m^3/kg is recommended where the uncertainty distribution is assumed to be lognormally distributed ($\log_{10} K_d = -4.83 \pm 0.60$). For stochastic simulations, it is recommended that the uncertainty distribution be sampled in log space between the 2.5% (9.7×10^{-7} m^3/kg) and 97.5% percentiles (2.2×10^{-4} m^3/kg). It can be noted that the K_d value for the lower limit may be assumed to be effectively zero since the storage porosity will dominate the bulk matrix retention. K_d values for the other type groundwater compositions are given in Table 6-1.

Since the relevant radioisotopes of Sr are not part of a nuclide decay chain and because the estimated K_d for the Temperate saline groundwater barely changes in response to mixing with OPC leachate, it is reasonable to assume the K_d value for Saline groundwater as being conservative even in the presence of a high pH plume. If consideration is given to the different prevailing groundwater compositions in different time domains, it is also reasonable to assume the K_d value for Temperate saline groundwater for high pH regions along the migration path. This is the same handling procedure as proposed previously in the case of Ba and Cs.

5.23 Technetium (Tc)

The principal radioisotope of Tc present in SFR waste materials is the ^{99}Tc fission product which has a half-life of 2.11×10^5 years. Tc is redox sensitive and can exist as Tc(IV) or Tc(VII) in groundwater. In the tetravalent state, the $TcO(OH)_2$ complex is the predominant specie, although $TcO(OH)_3^-$ and $Tc(OH)_3CO_3^-$ play a minor role depending on pH and carbonate concentration. In the oxidised Tc(VII) state, the pertechnate oxyanion, TcO_4^- is the overwhelmingly dominant aqueous specie for all reasonable groundwater compositions.

Owing to a lack of a suitable analogue sorption model for Tc(IV), the K_d value recommended for use in SR-Site (Crawford 2010) is also recommended for SR-PSU transport calculations for all non-Glacial groundwater types. This implies a best estimate K_d value of 5.3×10^{-2} m^3/kg where the uncertainty distribution is assumed to be lognormally distributed ($\log_{10} K_d = -1.28 \pm 0.65$). For stochastic simulations, it is recommended that the uncertainty distribution be sampled in log space between the 2.5% (2.8×10^{-3} m^3/kg) and 97.5% percentiles (9.8×10^{-1} m^3/kg). The redox potential of the Glacial-derived groundwater, on the other hand, is sufficiently high that Tc(VII) redox speciation can be safely assumed. The pertechnate oxyanion, TcO_4^- existing under oxidising conditions may be considered to be, for all practical purposes, non-sorbing. Since ^{99}Tc is not part of a decay chain, any potential increase in the K_d value for Tc(IV) in response to the influence of OPC leachate may be conservatively neglected, while the opposite case of very low K_d at high pH levels may be handled by assuming zero sorptivity in the OPC affected region of the migration path.

5.24 Tin (Sn)

The principal Tin isotope of interest in SFR waste materials is the ^{126}Sn fission product with a half-life of 2.3×10^5 y. Sn is redox sensitive and can exist as Sn(II) and Sn(IV) although for the groundwater compositions of interest in SFR-PSU only the tetravalent state is considered likely. As noted previously in Crawford (2010), Sn(IV) is strongly hydrolysed and the hydroxo-complexes $Sn(OH)_4$, $Sn(OH)_5^-$, and $Sn(OH)_6^{2-}$ are typically found to overwhelmingly dominate the aqueous speciation. Sn(IV) is expected to sorb by way of a surface complexation mechanism and may therefore be assumed to exhibit sensitivity to groundwater pH.

Based on modelling described by Bradbury and Baeyens (2009a) it is possible to surmise that the sorptivity of Sn(IV) should exhibit an optimum around normal groundwater pH levels (7–9) although is likely to decrease at higher pH levels owing to increasing binding competition from hydroxyl ligands in solution. Sorption calculations for site specific groundwaters have not been made for Sn(IV) owing to its simple speciation and because the results from Bradbury and Baeyens (2009a) emphatically suggest a large decrease in K_d at high pH.

Sorption data for Sn(IV) are sparse in the literature on account of its very strong sorption and since it is not normally considered to be a safety critical nuclide. The data recommendation given in Crawford (2010) for SR-Site was based on generic data reported by Ticknor et al. (1996) although is associated with some uncertainty. In the absence of any information suggesting otherwise, the previously recommended K_d values may be considered also applicable for SR-PSU transport calculations. This implies a best estimate K_d value of 1.6×10^{-1} m^3/kg where the uncertainty distribution is assumed to be lognormally distributed ($\log_{10} K_d = -0.80 \pm 0.28$).

For stochastic simulations, it is recommended that the uncertainty distribution be sampled in log space between the 2.5% (4.5×10^{-2} m^3/kg) and 97.5% percentiles (5.6×10^{-1} m^3/kg). Sorption calculations have not been made for Sn(IV) although based on the corresponding results in Bradbury and Baeyens (2009a), a K_d reduced by several orders of magnitude is considered possible for groundwater affected by OPC leachate. For pH > 10 it is therefore recommended that the best estimate K_d value be reduced by a factor of 1,000. Since ^{126}Sn is not part of a decay chain, this may be regarded as a conservative assumption.

5.25 Tritium (^3H)

Tritium (^3H) with a half-life of 12.3 years is produced as both a fission and activation product. Owing to its short half-life it is not considered to be an important nuclide for radiological risk except in cases involving very fast release. Tritium may be reasonably assumed to be non-sorbing for the purposes of SR-PSU transport calculations.

5.26 Uranium (U)

The isotopes of Uranium present in SFR waste materials are the same as those normally present in spent nuclear fuel. The isotopes of uranium and their half-lives are; ^{232}U (68.9 years), ^{233}U (1.592×10^5 years), ^{234}U (2.455×10^5 years), ^{235}U (7.04×10^8 years), ^{236}U (2.342×10^7 years), ^{237}U (6.75 days), and ^{238}U (4.468×10^9 years). The ^{232}U, ^{234}U, ^{235}U, ^{236}U and ^{238}U radioisotopes are all considered important nuclides for geosphere transport calculations in SR-PSU. The environmental chemistry of U is discussed in considerable detail in Crawford (2010) and is not repeated here, although specific details relevant to SR-PSU specific conditions are discussed in the following paragraphs.

Qualitative sorption and speciation calculations made using the BB09 illite sorption analogue (see Section 4.2) give indications of extremely complex redox interactions that cannot be understood by consideration of speciation effects in isolation. In the calculations, surface complexation reactions were defined for both U(IV) and U(VI) species based on the LFER for the corresponding aqueous phase reactions as discussed in Bradbury and Baeyens (2009a, b). The coupling of the surface reactions with aqueous phase speciation and the redox control imposed by the $Fe^{2+}/Fe(OH)_3$ system allows U to be proportionated in different dominant redox states between the aqueous and solid phases in

a thermodynamically consistent manner. The calculations assume equilibrium transitions between U(IV) and U(VI) which may not always be a good assumption, although on the timescales of safety assessment this is considered appropriate. Although not included in the SKB-TDB (Duro et al. 2006), an additional reaction for the $Ca_2UO_2(CO_3)_3$ complex was included in the calculations, since there is now considerable evidence for its existence (Bernhard et al. 2001, Bradbury and Baeyens 2011).

U(VI) is calculated to be the dominant aqueous redox state for the Temperate saline and both Periglacial type groundwaters (i.e. non-OPC affected), while the U(IV) form is found to dominate the sorbed redox speciation. Although the existence of different redox speciation in the aqueous and surface sorbed phases seems counterintuitive, it is fully consistent with the underlying thermodynamic description as it is mathematically formulated. The dissolved U(VI) speciation is overwhelmingly dominated by $Ca_2UO_2(CO_3)_3$ with U(VI) hydroxyl complexes comprising a smaller fraction. U(VI) carbonate complexes appear to be of some importance for the Periglacial groundwater types, although of only minor significance for the Temperate saline groundwater.

Based on the BB09 model, the theoretical K_d value for Temperate saline groundwater is expected to increase to an optimum at pH ≈ 7.6 and thereafter decline steadily with increasing pH. For pH ≥ 7.5, U(VI) ceases to be the dominant aqueous redox state and U(IV) becomes predominant in the aqueous phase. In the pH interval 8.5–10.5, U(IV) is predominant in both the aqueous and surface sorbed phases, while at pH ≥ 12 U(VI) becomes the predominant surface sorbed redox state. Hydroxyl complexes dominate the aqueous phase speciation when U(IV) is the dominant redox form. The BB09 model calculations suggest that the K_d at pH ≈ 12 is at least 3 orders of magnitude less than that predicted for non-OPC affected groundwater.

Qualitatively similar behaviour is seen for both Periglacial groundwater subtypes, although with a more prominent role for U(VI) carbonate complexes in the pH interval 8.5–9.75. The transition from U(VI) to U(IV) predominance in the aqueous and surface sorbed phases also occurs at slightly different pH levels for the Early and Late Periglacial groundwater sub-types. There is also no identifiable pH interval where the redox speciation is the same in the aqueous phase and surface sorbed phases (unlike the Temperate saline groundwater). The K_d at high pH exhibits a decrease of similar magnitude as that predicted for Temperate saline groundwater with U(VI) surface complexes becoming the dominant sorbed redox state at pH 11.0–11.5.

The Glacial-derived groundwater, on the other hand, is sufficiently oxidizing that U(VI) is always predominant across the entire pH range simulated in both the aqueous and surface sorbed phases. The sorption edge for U(VI) sorption in the Glacial type groundwater rises rapidly to an optimum at pH ≈ 10.5 and thereafter decreases, although nowhere near to the same extent as that predicted for the U(IV) surface complexes relevant for the other groundwater types. The theoretical K_d predicted for U(VI) at pH ≥ 12 is slightly higher than that for the non-OPC affected groundwater. This suggests that the switchover from U(IV) to U(VI) dominated surface speciation predicted for the Temperate saline and Periglacial groundwaters is related to a strong decrease in the sorptivity of U(IV) at high pH levels rather than an increase in the sorptivity of U(VI).

In a similar fashion to what has already been described for Pu (Section 5.17), the extremely complex redox behaviour of U makes it difficult to assign unequivocal K_d values for a definite redox state in SR-PSU transport calculations. Furthermore, a comparison of the theoretical K_d values estimated for the sorptivity of U in Temperate saline and Glacial groundwater suggest a maximum factor of ≈ 40 theoretical difference between the sorptivity of U(IV) and U(VI) surface complexes. In the SR-Site data compilation, however, the K_d values for U(IV) and Np(IV) are based on a geochemical analogy with Pu(IV) owing to a lack of unambiguous empirical data for U(IV) or Np(IV) sorption on granite. The SR-Site recommended data implies a ratio of U(IV) to U(VI) sorptivity on the order of about 500 which is obviously not consistent with the predictions made by the BB09 illite analogue model.

To avoid inconsistency in the data recommendation for U sorption and how this extrapolates to high pH conditions characteristic of an OPC plume, it is proposed that the K_d for U sorption in the non-OPC affected Temperate saline and Periglacial groundwaters be given the same value as that specified for U(IV) in SR-Site. This implies a best estimate K_d value of 5.3×10^{-2} m^3/kg where the uncertainty distribution is assumed to be lognormally distributed ($\log_{10} K_d = -1.28 \pm 0.65$). For stochastic simulations, it is recommended that the uncertainty distribution be sampled in log space between the 2.5% (2.8×10^{-3} m^3/kg) and 97.5% percentiles (9.8×10^{-1} m^3/kg).

The K_d range given for U(VI) sorption in the SR-Site data compilation is recommended for the oxidising conditions associated with the Glacial type groundwater. This implies a best estimate K_d value of 1.1×10^{-4} m^3/kg where the uncertainty distribution is assumed to be lognormally distributed ($\log_{10} K_d = -3.97 \pm 0.66$). For stochastic simulations, it is recommended that the uncertainty distribution be sampled in log space between the 2.5% (5.5×10^{-6} m^3/kg) and 97.5% percentiles (2.1×10^{-3} m^3/kg). It can be noted that the K_d value for the lower limit may be assumed to be effectively zero since the matrix storage porosity will dominate the bulk matrix retention.

Given the uncertainty of the qualitative calculations and the small relative variation in the theoretically calculated K_d for U(VI) in response to mixing with OPC leachate it is also reasonable to assume an unchanged K_d for high pH regions along the migration path. For OPC affected (pH > 10), although still reducing Temperate saline and Periglacial groundwater types, a K_d range for U corresponding to that estimated for U(VI) is proposed.

5.27 Zirconium (Zr)

The principal Zirconium isotope of interest in SFR waste materials is the ^{93}Zr activation product with a half-life of 1.53×10^6 y. Zr is not considered to be redox sensitive and the tetravalent form, Zr(IV) is the only relevant redox state for this radioelement under normal groundwater conditions. As noted previously in Crawford (2010), Zr(IV) is strongly hydrolysed and the $Zr(OH)_4$ hydroxo-complex is expected to dominate the aqueous speciation for all groundwater compositions likely to be found in the geosphere surround the SFR repository. Zr(IV) is expected to sorb by way of a surface complexation mechanism and may therefore be assumed to exhibit sensitivity to groundwater pH.

The SR-Site K_d recommendation for Zr(IV) was based on data reported by Kulmala and Hakanen (1993) for samples of Olkiluoto tonalite and Rapakivi granite in contact with native groundwaters of fresh and saline characters, respectively. In the cited Finnish study, sorption measurements were also made using cement equilibrated groundwater (pH 12.7–12.9) and significant increases in measured K_d values were noted relative to the non-affected groundwater samples. Given the uncertainties concerning the underlying data set and the unknown extent of the region of alkaline influence surrounding the SFR repository, it is deemed cautious that the same data recommendation given for SR-Site also be used for transport calculations involving this radioelement in SR-PSU. This implies a best estimate K_d value of 2.1×10^{-2} m^3/kg where the uncertainty distribution is assumed to be lognormally distributed ($\log_{10} K_d = -1.67 \pm 0.35$). For stochastic simulations, it is recommended that the uncertainty distribution be sampled in log space between the 2.5% (4.5×10^{-3} m^3/kg) and 97.5% percentiles (1.0×10^{-1} m^3/kg).

Sorption calculations have not been made for Zr(IV), although since it is considered to be a very close geochemical analogue of Sn(IV), one would expect similar behaviour. The experimental data described by Kulmala and Hakanen (1993), however, suggest that the reduction in K_d expected for Sn(IV) does not occur in the case of Zr(IV). Although the experimental data suggest an increase in K_d at high pH this is difficult to quantify for the site specific materials and groundwater. For pH > 10 it is therefore recommended that the K_d values remain unchanged. Since ^{93}Zr is not part of a decay chain this may be considered a conservative assumption.

6 Summary of recommended data for use in SR-PSU

The decision whether to consider the presence or absence of a high pH plume in transport calculations is left up to the SR-PSU modelling team in accordance with specific scenarios of repository evolution to be subsequently defined. If a high pH plume is considered, the impact on sorptivity should be quantified for radionuclide migration calculations. For a plume in a steady-state configuration it is possible, in principle, to integrate the calculated value of f_{chem} along a flowpath to estimate an average correction factor to derive an appropriate K_d value to be used in transport calculations. This, however, presupposes the validity of the underlying sorption model used to predict the relative variation in the expected K_d value. In certain cases, such flowpath averaging might also need to take into account the sorptive properties of daughter nuclides in decay chains which may be more or less sorbing than their parent nuclides. Here, the assumption of strongly enhanced sorptivity of the parent at high pH might be conservative if the daughter nuclide is known to be weakly sorbing. This is because increased retention of the parent nuclide would also imply increased in-growth of the daughter along a migration path and thus potentially higher dose rates to the biosphere.

Since the sorption and speciation calculations used here to inform the predictions of K_d variation can only be considered to be qualitative, rigorous flowpath averaging calculations are not feasible at the present time. In order to simplify the handling of such situations, a short-cut procedure is proposed based on the fraction of the flowpath featuring pH conditions below and above pH 10, respectively. The choice of pH 10 as a relevant threshold for such a calculation is arbitrary, although based on consideration of the mixing calculations shown in Figure 4-1.

From the simulated pH buffering characteristics of each of the type groundwaters, it can be seen that the pH tends to make a rapid transition to high levels over a short mixing fraction interval, typically 5%–20% OPC leachate. If there is a relatively linear variation in the equivalent mixing fraction along a migration path (which is not unreasonable for a dilution/mixing), one would therefore expect a relatively sharp transition between high pH and normal groundwater pH conditions as a function of distance. Based on this assumption, one could approximately define the flowpath average as:

$$\overline{K}_d \approx K_d^A \left(1 - \frac{x}{L}\right) + K_d^B \frac{x}{L} \qquad (6\text{-}1)$$

Where, K_d^A is the average K_d value for the part of the geosphere unaffected by OPC leachate (i.e. the "reference groundwater"), K_d^B is the average K_d value for the high pH region, and x/L is the fraction of the flowpath length featuring high pH conditions (here defined as pH ≥ 10). If K_d^B is much less than K_d^A, then this can be simplified even further to:

$$\overline{K}_d \approx K_d^A \left(1 - \frac{x}{L}\right) \qquad (K_d^B << K_d^A) \qquad (6\text{-}2)$$

Put simply, if the OPC plume affects say half the length of a migration path and the K_d at high pH is known to be significantly reduced, then the flowpath average K_d should be roughly half the reference K_d value. In this case, provided the OPC plume spans a non-trivial distance and the difference between the limiting K_d values is sufficiently large, the actual value of reduced K_d at high pH does not have a large impact on the estimated flowpath average. In the opposite situation, however, where the K_d might be greatly increased at high pH (e.g. Am, Eu, Cm, Ho, Th), a significant uncertainty remains concerning the correct flowpath average to use in transport calculations.

In situations where the nuclide is part of a decay chain with possibly less strongly sorbing daughters, sensitivity analyses in the transport calculations might be used to assess the likely impact of the uncertainty (say, assuming a K_d in the high pH region 10–100 times larger than that of the reference groundwater). This is because the more strongly sorbing parent nuclide, being far less mobile, then becomes a large source for ingrowth of daughter nuclide activity along the flowpath. Here, although the biosphere dose rate attributable to the parent nuclide decreases, it may be offset by a large increase

in dose rate due to daughter nuclides. Based on cursory examination of the relevant decay chains, this might be an issue for the nuclides ^{241}Am, ^{242m}Am, ^{243}Cm, ^{244}Cm which are considered important in the radionuclide data request list for SR-PSU.

It can be noted that Equation 6-1 and 6-2 assume a constant proportionality between flowpath length and total flowpath hydrodynamic transport resistance (F-factor). Although this is sufficient for a simplified discussion of alkaline plume impact on radionuclide transport, it would be strictly more accurate to discuss flowpath averaging of K_d values in terms of the proportioning of hydrodynamic transport resistance along the flowpath instead of physical length. For the purpose of the present discussion, however, this distinction may be neglected.

Although the K_d for Pu is qualitatively expected to decrease at high pH, it is not clear exactly how great this decrease should be since the scoping calculations are only very approximate and are complicated by redox transitions. There is additional uncertainty given that this prediction is based solely on the basis of sorption model calculations involving the illite geochemical analogue (Bradbury and Baeyens 2009b) and an assumed surface complexation mechanism. In the K_d data recommendation (see Section 5.17), a K_d reduction on the order of 1,000 is given as a limiting case for Pu(III/IV) sorption at high pH, although it is acknowledged this may be a more severe reduction than physically motivated. Given that Pu isotopes are present in all of the relevant decay chains, it may be necessary to test this assumption by sensitivity analysis for its effect on dose rates involving less strongly sorbing daughter nuclides. This, however, should only be an issue in situations where the OPC leachate is deemed to affect the groundwater composition along much of the migration path and can probably be neglected in most cases.

Geosphere K_d values recommended for use in SR-PSU radionuclide transport calculations are given in Table 6-1 for the rock matrix. Values are given for the different groundwater types associated with specific time domains corresponding to those described in Auqué et al. (2013). K_d values applicable for high pH conditions (pH > 10) are also given in those cases where it is deemed feasible to do so. Recommended values are only given where the sorptivity is predicted to decrease at high pH. The situation in which high pH conditions give rise to increased sorptivity is not quantified in the table owing to data uncertainty and since the neglection of this is deemed conservative for its direct impact on transport retardation in most cases. As outlined above, propagated uncertainty involving this assumption for decay chains may require additional sensitivity analysis in transport calculations.

K_d values for sorption on minerals comprising fracture coatings were not requested, although scoping calculations are made for inorganic ^{14}C (HCO_3^-) owing to its importance as a safety relevant nuclide and its otherwise poor sorption in the rock matrix. This radioelement is treated in a separate Appendix A. Retardation factors for instantaneous sorption in gravel comprising the hydraulic cage surrounding the repository can be derived using the methodology outlined in Appendix B. This, however, requires knowledge of advective travel times for individual pathlines through the gravel bed, which together with gravel particle sizes and the gravel bed void fraction, can be used to estimate effective equilibration fractions for the gravel based on diffusion penetration theory.

Table 6-1. Recommended sorption partitioning coefficient, K_d values for prioritised nuclides in SR-PSU transport calculations. Values are given for the best estimate (median), parameters for the lognormal distribution (μ and σ), as well as lower and upper limits corresponding to the 2.5% and 97.5% percentiles, respectively. Groundwater types are Temperate saline (T-sal), Periglacial (Per), Late Periglacial (L-Per), and Glacial (Glac). Separate values are given for high pH conditions where deemed feasible to do so. Lower limit Kd values less than the storage porosity of the rock matrix are effectively zero and specified as such in the table. Non-zero numerical values were provided to the SR-PSU modelling team, however, for the purpose of probabilistic calculations.

Radionuclide (Redox State)	GW Type	Best estimate K_d (m^3/kg)	μ	σ	Lower K_d (m^3/kg)	Upper K_d (m^3/kg)
H(I)	all	0.0	–	–	0.0	0.0
C, HCO_3^-	all	0.0	–	–	0.0	0.0
C, CH_4	all	0.0	–	–	0.0	0.0
C, -CO_2H	all	0.0	–	–	0.0	0.0
Cl(-I)	all	0.0	–	–	0.0	0.0
Ca(II)	all	0.0	–	–	0.0	0.0
Co(II)	all	$7.4\cdot10^{-4}$	–3.13	0.79	$2.1\cdot10^{-5}$	$2.7\cdot10^{-2}$
Ni(II)	all	$7.4\cdot10^{-4}$	–3.13	0.79	$2.1\cdot10^{-5}$	$2.7\cdot10^{-2}$
Se(-II, IV, VI)	all	0.0	–	–	0.0	0.0
Sr(II)	T-Sal	$1.5\cdot10^{-5}$	–4.83	0.6	0.0	$2.2\cdot10^{-4}$
	Per	$2.0\cdot10^{-4}$	–3.69	0.6	$1.3\cdot10^{-5}$	$3.1\cdot10^{-3}$
	L-Per	$3.5\cdot10^{-4}$	–3.46	0.6	$2.3\cdot10^{-5}$	$5.3\cdot10^{-3}$
	Glac	$1.6\cdot10^{-3}$	–2.79	0.6	$1.1\cdot10^{-4}$	$2.5\cdot10^{-2}$
	all, pH > 10	$1.5\cdot10^{-5}$	–4.83	0.6	0.0	$2.2\cdot10^{-4}$
Mo(VI)	all	0.0	–	–	0.0	0.0
Nb(V)	all	$2.0\cdot10^{-2}$	–1.70	0.64	$1.1\cdot10^{-3}$	$3.5\cdot10^{-1}$
Zr(IV)	all	$2.1\cdot10^{-2}$	–1.67	0.35	$4.5\cdot10^{-3}$	$1.0\cdot10^{-1}$
Tc(IV)	non-Glac	$5.3\cdot10^{-2}$	–1.28	0.65	$2.8\cdot10^{-3}$	$9.8\cdot10^{-1}$
Tc(VII)	Glac	0.0	–	–	0.0	0.0
Ag(I)	all	0.0	–	–	0.0	0.0
Cd(II)	all	$7.4\cdot10^{-4}$	–3.13	0.79	$2.1\cdot10^{-5}$	$2.7\cdot10^{-2}$
Sn(IV)	all, pH < 10	$1.6\cdot10^{-1}$	–0.80	0.28	$4.5\cdot10^{-2}$	$5.6\cdot10^{-1}$
	all, pH > 10	$1.6\cdot10^{-4}$	–3.80	0.28	$4.5\cdot10^{-5}$	$5.6\cdot10^{-4}$
I(-I)	all	0.0	–	–	0.0	0.0
Ba(II)	T-Sal	$1.0\cdot10^{-3}$	–3.00	0.46	$1.3\cdot10^{-4}$	$8.0\cdot10^{-3}$
	Per	$1.4\cdot10^{-2}$	–1.86	0.46	$1.7\cdot10^{-3}$	$1.1\cdot10^{-1}$
	L-Per	$2.4\cdot10^{-2}$	–1.62	0.46	$3.0\cdot10^{-3}$	$1.9\cdot10^{-1}$
	Glac	$1.1\cdot10^{-1}$	–0.96	0.46	$1.4\cdot10^{-2}$	$8.9\cdot10^{-1}$
	all, pH > 10	$1.0\cdot10^{-3}$	–3.00	0.46	$1.3\cdot10^{-4}$	$8.0\cdot10^{-3}$
Cs(I)	T-Sal	$8.8\cdot10^{-4}$	–3.05	0.58	$6.6\cdot10^{-5}$	$1.2\cdot10^{-2}$
	Per	$3.0\cdot10^{-3}$	–2.52	0.58	$2.2\cdot10^{-4}$	$4.0\cdot10^{-2}$
	L-Per	$3.8\cdot10^{-3}$	–2.42	0.58	$2.8\cdot10^{-4}$	$5.1\cdot10^{-2}$
	Glac	$7.7\cdot10^{-3}$	–2.12	0.58	$5.7\cdot10^{-4}$	$1.0\cdot10^{-1}$
	all, pH > 10	$8.8\cdot10^{-4}$	–3.05	0.58	$6.6\cdot10^{-5}$	$1.2\cdot10^{-2}$
Sm(III)	all	$1.5\cdot10^{-2}$	–1.83	0.72	$5.7\cdot10^{-4}$	$3.8\cdot10^{-1}$
Eu(III)	all	$1.5\cdot10^{-2}$	–1.83	0.72	$5.7\cdot10^{-4}$	$3.8\cdot10^{-1}$
Ho(III)	all	$1.5\cdot10^{-2}$	–1.83	0.72	$5.7\cdot10^{-4}$	$3.8\cdot10^{-1}$
U(IV)	non-Glac, pH < 10	$5.3\cdot10^{-2}$	–1.28	0.65	$2.8\cdot10^{-3}$	$9.8\cdot10^{-1}$
	non-Glac, pH > 10	$1.1\cdot10^{-4}$	–3.97	0.66	0.0	$2.1\cdot10^{-3}$
U(VI)	Glac	$1.1\cdot10^{-4}$	–3.97	0.66	0.0	$2.1\cdot10^{-3}$
Np(IV)	non-Glac, pH < 10	$5.3\cdot10^{-2}$	–1.28	0.65	$2.8\cdot10^{-3}$	$9.8\cdot10^{-1}$
	non-Glac, pH > 10	$4.1\cdot10^{-4}$	–3.38	0.74	$1.5\cdot10^{-5}$	$1.2\cdot10^{-2}$
Np(V)	Glac	$4.1\cdot10^{-4}$	–3.38	0.74	$1.5\cdot10^{-5}$	$1.2\cdot10^{-2}$
Pu(III/IV)	all, pH < 10	$1.5\cdot10^{-2}$	–1.83	0.72	$5.7\cdot10^{-4}$	$3.8\cdot10^{-1}$
	all, pH > 10	$1.5\cdot10^{-5}$	–4.83	0.72	0.0	$3.8\cdot10^{-4}$
Am(III)	all	$1.5\cdot10^{-2}$	–1.83	0.72	$5.7\cdot10^{-4}$	$3.8\cdot10^{-1}$
Cm(III)	all	$1.5\cdot10^{-2}$	–1.83	0.72	$5.7\cdot10^{-4}$	$3.8\cdot10^{-1}$

Although not part of the official data request, a number of additional nuclides belonging to the ^{238}U decay chain plus ^{227}Ac were additionally requested informally by the SR-PSU modelling team. Although sorption data for these nuclides has not been examined in the same detail as for the prioritised nuclides in Table 6-1 (with the notable exception of Po), recommended values for modelling in SR-PSU are given in Table 6-2. These data are taken mainly from the corresponding recommendations given in SR-Site (Crawford 2010), with the exception of Ra which is based on site specific data corrected for groundwater composition (as done previously for Ba), and Po which is examined in detail in Appendix C.

Table 6-2. Recommended sorption partitioning coefficient, K_d values for non-prioritised nuclides belonging to the ^{238}U decay chain plus ^{227}Ac. Values are given for the best estimate (median), parameters for the lognormal distribution (μ and σ), as well as lower and upper limits corresponding to the 2.5% and 97.5% percentiles, respectively. Groundwater types are Temperate saline (T-sal), Periglacial (Per), Late Periglacial (L-Per), and Glacial (Glac). Separate values are given for high pH conditions were deemed feasible to do so.

Radionuclide (Redox State)	GW Type	Best estimate K_d (m^3/kg)	μ	σ	Lower K_d (m^3/kg)	Upper K_d (m^3/kg)
Ac(III)	all	$1.5\cdot10^{-2}$	–1.83	0.72	$5.7\cdot10^{-4}$	$3.8\cdot10^{-1}$
Pa(V)	all	$5.9\cdot10^{-2}$	–1.23	0.48	$6.8\cdot10^{-3}$	$5.1\cdot10^{-1}$
Th(IV)	all	$5.3\cdot10^{-2}$	–1.28	0.65	$2.8\cdot10^{-3}$	$9.8\cdot10^{-1}$
Ra(II)	T-Sal	$1.0\cdot10^{-3}$	–3.00	0.46	$1.3\cdot10^{-4}$	$8.0\cdot10^{-3}$
	Per	$1.4\cdot10^{-2}$	–1.86	0.46	$1.7\cdot10^{-3}$	$1.1\cdot10^{-1}$
	L-Per	$2.4\cdot10^{-2}$	–1.62	0.46	$3.0\cdot10^{-3}$	$1.9\cdot10^{-1}$
	Glac	$1.1\cdot10^{-1}$	–0.96	0.46	$1.4\cdot10^{-2}$	$8.9\cdot10^{-1}$
	all, pH > 10	$1.0\cdot10^{-3}$	–3.00	0.46	$1.3\cdot10^{-4}$	$8.0\cdot10^{-3}$
Pb(II)	all	$2.5\cdot10^{-2}$	–1.60	0.56	$2.0\cdot10^{-3}$	$3.1\cdot10^{-1}$
Po(IV)/PoO_3^{2-}	all	~$1.0\cdot10^{-3}$	–	–	$3.0\cdot10^{-4}$	$1.0\cdot10^{-2}$
	all, pH > 10	0	–	–	0	0
Po(-II, II, VI)	all	0	–	–	0	0

References

SKB's (Svensk Kärnbränslehantering AB) publications can be found at www.skb.se/publications. References to SKB's unpublished documents are listed separately at the end of the reference list. Unpublished documents will be submitted upon request to document@skb.se.

Albinsson Y, 1991. Sorption of radionuclides in grantic rock. SKB AR 91-07, Svensk Kärnbränslehantering AB.

Andersson K, Torstenfelt B, Allard B, 1983. Sorption of radionculides in geologic systems. SKBF/KBS Technical Report 83-63, Svensk Kärnbränsleförsörjning AB.

Ansoborlo E, Berard P, Den Auwer C, Leggett R, Menetrier F, Younes A, Montavon G, Moisy P, 2012. Review of chemical and radiotoxicological properties of polonium for internal contamination purposes. Chemical Research in Toxicology 25, 1551–1564.

Auqué L F, Gimeno M, Acero P, Gómez J, 2013. Compositions of groundwater for SFR and its extention, during different climatic cases, SR-PSU. SKB R-13-16, Svensk Kärnbränslehantering AB.

Avila R, Ekström P-A, Åstrand P-G, 2010. Landscape dose conversion factors used in the safety assessment SR-Site. SKB TR-10-06, Svensk Kärnbränslehantering AB.

Bagnall K W, 1962. The chemistry of polonium. In Emeléus H J, Sharpe A G (eds). Advances in Inorganic Chemistry and Radiochemistry. Vol 4. New York: Academic Press, 197–230.

Balistrieri L S, Murray J W, Paul B, 1995. The geochemical cycling of stable Pb, ^{210}Pb, and ^{210}Po in seasonally anoxic Lake Sammamish, Washington, USA. Geochimica et Cosmochimica Acta 59, 4845–4861.

Banwart S A, 1999. Reduction of iron(III) minerals by natural organic matter in groundwater. Geochimica et Cosmochimica Acta 63, 2919–2928.

Baston G M N, Berry J A, Brownsword M, Heath T G, Ilett D J, McCrohon R, Tweed C J, Yui M, 1998. The sorption of polonium, actinium and protactinium onto geological materials. In Wronkiewicz D J, Lee J H (eds). Scientific basis for nuclear waste management XXII: symposium held in Boston, Massachusetts, 30 November – 4 December 1998. Warrendale, PA: Materials Research Society. (Materials Research Society Symposium Proceedings 556), 1107–1114.

Beauwens T, De Cannière P, Moors H, Wang L, Maes N, 2005. Studying the migration behaviour of selenate in Boom Clay by electromigration. Engineering Geology 77, 285–293.

Benoit G, Hemond H F, 1990. Polonium-210 and lead-210 remobilization from lake sediments in relation to iron and manganese cycling. Environmental Science & Technology 24, 1224–1234.

Bernhard G, Geipel G, Reich T, Brendler V, Amayri S, Nitsche H, 2001. Uranyl(VI) carbonate complex formation: validation of the $Ca_2UO_2(CO_3)_3$(aq.) species. Radiochimica Acta 89, 511–518.

Bertetti F P, Pabalan R T, Almendarez M G, 1998. Studies of neptunium(V) sorption on quartz, clinoptilolite, montmorillonite, and α-alumina. In Jenne E A (ed). Adsorption of metals by geomedia: variables, mechanisms, and model applications. San Diego, CA: Academic Press, 131–148.

Bonotto D M, Bueno T O, 2008. The natural radioactivity in Guarani aquifer groundwater, Brazil. Applied Radiation and Isotopes 66, 1507–1522.

Bradbury M, Baeyens B, 2003. Near-field sorption data bases for compacted MX-80 bentonite for performance assessment of a high-level radioactive waste repository in Opalinus clay host rock. Nagra Technical Report NTB 02-18, Nagra, Switzerland.

Bradbury M H, Baeyens B, 2005. Experimental measurements and modeling of sorption competition on montmorillonite. Geochimica et Cosmochimica Acta 69, 4187–4197.

Bradbury M H, Baeyens B, 2009a. Sorption modelling on illite Part I: Titration measurements and the sorption of Ni, Co, Eu and Sn. Geochimica et Cosmochimica Acta 73, 990–1003.

Bradbury M H, Baeyens B, 2009b. Sorption modelling on illite. Part II: Actinide sorption and linear free energy relationships. Geochimica et Cosmochimica Acta 73, 1004–1013.

Bradbury M H, Baeyens B, 2011. Predictive sorption modelling of Ni(II), Co(II), Eu(IIII), Th(IV) and U(VI) on MX-80 bentonite and Opalinus clay: a "bottom-up" approach. Applied Clay Science 52, 27–33.

Bradbury M H, Baeyens B, Thoenen T, 2010. Sorption data bases for generic Swiss argillaceous rock systems. Nagra Technical Report NTB 09-03, Nagra, Switzerland.

Breynaert E, Scheinost A C, Dom D, Rossberg A, Vancluysen J, Gobechiya E, Kirschhock C E A, Maes A, 2010. Reduction of Se(IV) in Boom Clay: XAS solid phase speciation. Environmental Science & Technology 44, 6649–6655.

Byegård J, Skarnemark G, Skålberg M, 1995. The use of some ion-exchange sorbing tracer cations in in situ experiments in high saline groundwaters. In Murakami T, Ewing R C (eds). Scientific basis for nuclear waste management XVIII: symposium held in Kyoto, Japan, 23–27 October 1994. Pittsburgh, PA: Materials Research Society. (Materials Research Society Symposium Proceedings 353), 1077–1084.

Byegård J, Johansson H, Skålberg M, Tullborg E-L, 1998. The interaction of sorbing and non-sorbing tracers with different Äspö rock types. Sorption and diffusion experiments in the laboratory scale. SKB TR-98-18, Svensk Kärnbränslehantering AB.

Byegård J, Selnert E, Tullborg E-L, 2008. Bedrock transport properties. Data evaluation and retardation model. Site descriptive modelling, SDM-Site Forsmark. SKB R-08-98, Svensk Kärnbränslehantering AB.

Carbol P, Engkvist I, 1997. Compilation of radionuclide sorption coefficients for performance assessment. SKB R-97-13, Svensk Kärnbränslehantering AB.

Cherniak D J, 2010. Diffusion in carbonates, fluorite, sulfide minerals, and diamond. Reviews in Mineralogy & Geochemistry 72, 871–897.

Colle R, Lin Z C, Hutchinson J M R, Schima F J, Hodge P A, Thomas J W L, 1995. Preparation and calibration of carrier-free Po-209 solution standards. Journal of Research of the National Institute of Standards and Technology 100, 1–36.

Coulson J, Richardson J, Backhurst J, Harker J, 1991. Chemical engineering. Vol. 2, Particle technology and separation processes. 4th ed. Oxford: Pergamon.

Crank J, 1975. The mathematics of diffusion. 2nd ed. Oxford: Clarendon.

Crawford J, 2006. Modelling in support of bedrock transport property assessment. Preliminary site description. Laxemar subarea – version 1.2. SKB R-06-28, Svensk Kärnbränslehantering AB.

Crawford J, 2010. Bedrock K_d data and uncertainty assessment for application in SR-Site geosphere transport calculations. SKB R-10-48, Svensk Kärnbränslehantering AB.

Duro L, Grivé M, Cera E, Domènech C, Bruno J, 2006. Update of a thermodynamic database for radionuclides to assist solubility limits calculation for performance assessment. SKB TR-06-17, Svensk Kärnbränslehantering AB.

Figgins P E, 1961. The radiochemistry of polonium. NAS-NS 3037, National Academy of Sciences – National Research Council.

Finck N, Dardenne K, Bosbach D, Geckeis H, 2012. Selenide retention by mackinawite. Environmental Science & Technology 46, 10004–10011.

Fisler D K, Cygan R T, 1999. Diffusion of Ca and Mg in calcite. American Mineralogist 84, 1392–1399.

Focazio M J, Szabo Z, Kraemer T F, Mullin A H, Barringer T H, 1998. Occurrence of selected radionuclides in ground water used for drinking water in the United States: a targeted reconnaissance survey. Water-Resources Investigations Report 00-4273, U.S. Geological Survey, Reston, Virginia.

Goldberg S, Forster H S, Godfrey C L, 1996. Molybdenum adsorption on oxides, clay minerals, and soils. Soil Science Society of America Journal 60, 425–432.

Goldberg S, Johnston C T, Suarez D L, Lesch S M, 2007. Mechanism of molybdenum adsorption on soils and soil minerals evaluated using vibrational spectroscopy and surface complexation modeling. In Barnett M O, Kent D B (eds). Adsorption of metals by geomedia II: variables, mechanisms, and model applications. Amsterdam: Elsevier. (Developments in earth & environmental sciences), 235–266.

Hershey R L, Howcroft W, Reimus P W, 2003. Laboratory experiments to evaluate diffusion of ^{14}C into Nevada test site carbonate aquifer matrix. Las Vegas, NV: Desert Research Institute.

Hummel W, Berner U, Curti E, Pearson F J, Thoenen T, 2002. Nagra/PSI chemical thermodynamic data base 01/01. Boca Raton, FL: Universal Publishers.

Isam Salih M M, Pettersson H B, Lund E, 2002. Uranium and thorium series radionuclides in drinking water from drilled bedrock wells: correlation to geology and bedrock radioactivity and dose estimation. Radiation Protection Dosimetry 102, 249–258.

Jan Y-L, Wang T-H, Li M-H, Tsai S-C, Wei Y-Y, Hsu C-N, Teng S-P, 2007. Evaluating adsorption ability of granite to radioselenium by chemical sequential extraction. Journal of Radioanalytical and Nuclear Chemistry 273, 299–306.

Jan Y-L, Wang T-H, Li M-H, Tsai S-C, Wei Y-Y, Teng S-P, 2008. Adsorption of Se species on crushed granite: a direct linkage with its internal iron-related minerals. Applied Radiation and Isotopes 66, 14–23.

Jensen M P, Choppin G R, 1996. Complexation of Europium(III) by aqueous orthosilicate acid. Radiochimica Acta 72, 143–150.

Kang M, Ma B, Bardelli F, Chen F, Liu C, Zheng Z, Wu S, Charlet L, 2013. Interaction of aqueous Se(IV)/Se(VI) with FeSe/$FeSe_2$: implication to Se redox process. Journal of Hazardous Materials 248–249, 20–28.

Kim G, Kim S-J, Harada K, Schultz M K, Burnett W C, 2005. Enrichment of excess ^{210}Po in anoxic ponds. Environmental Science & Technology 39, 4894–4899.

Kinniburgh D, Cooper D, 2011. PhreePlot: Creating graphical output with PHREEQC. Available at: http://nora.nerc.ac.uk/19744/1/PhreePlot.pdf

Kulmala S, Hakanen M, 1993. The solubility of Zr, Nb and Ni in groundwater and concrete water, and sorption on crushed rock and cement. Report YJT-93-21, Nuclear Waste Commission of Finnish Power Companies.

Lahav N, Bolt G H, 1964. Self-diffusion of Ca45 into certain carbonates. Soil Science 97, 293–299.

Löfgren M, Sidborn M, 2010. Statistical analysis of results from the quantitative mapping of fracture minerals in Forsmark. Site descriptive modelling – complementary studies. SKB R-09-30, Svensk Kärnbränslehantering AB.

Löfgren M, Crawford J, Elert M, 2007. Tracer tests – possibilities and limitations. Experience from SKB fieldwork: 1977–2007. SKB R-07-39, Svensk Kärnbränslehantering AB.

Marques Fernandes M, Baeyens B, Bradbury M H, 2008. The influence of carbonate complexation on lanthanide/actinide sorption on montmorillonite. Radiochimica Acta 96, 691–697.

Marques Fernandes M, Stumpf T, Baeyens B, Walther C, Bradbury M H, 2010. Spectroscopic identification of ternary Cm−carbonate surface complexes. Environmental Science & Technology 44, 921–927.

McPhail D C, 1995. Thermodynamic properties of aqueous tellurium species between 25 and 350°. Geochimica et Cosmochimica Acta 59, 851–866.

Missana T, 2013. CIEMAT activity in the project (WP2). In Proceedings of the Final Workshop of the Collaborative Project "Crystalline ROCK Retention Processes" (7th EC FP CP CROCK), Karlsruhe, Germany, 14–16 May 2013.

Moreno L, Crawford J, 2009. Can we use tracer tests to obtain data for performance assessment of repositories for nuclear waste? Hydrogeology Journal 17, 1067–1080.

Neretnieks I, 1980. Diffusion in the rock matrix: An important factor in radionuclide migration? Journal of Geophysical Research 85, 4379–4397.

Neuhausen J, Köster U, Eichler B, 2004. Investigation of evaporation characteristics of polonium and its lighter homologues selenium and tellurium from liquid Pb-Bi-eutecticum. Radiochimica Acta 92, 917–923.

Nilsson A-C, Tullborg E-L, Smellie J, Gimeno M J, Gómez J B, Auqué L F, Sandström B, Pedersen K, 2011. SFR site investigation. Bedrock hydrogeochemistry. SKB R-11-06, Svensk Kärnbränslehantering AB.

Ochs M, Talerico C, 2004. SR-Can. Data and uncertainty asessment. Migration parameters for the bentonite buffer in the KBS-3 concept. SKB TR-04-18, Svensk Kärnbränslehantering AB.

Pabalan R T, Turner D R, Bertetti F P, Prikryl J D, 1998. Uranium(VI) sorption onto selected mineral surfaces. In Jenne E A (ed). Adsorption of metals by geomedia: variables, mechanisms, and model applications. San Diego, CA: Academic Press, 99–130.

Panak P J, Kim M A, Klenze R, Kim J-I, Fanghänel T, 2005. Complexation of Cm(III) with aqueous silicic acid. Radiochimica Acta 93, 133–139.

Papelis C, 2001. Cation and anion sorption on granite from the Project Shoal Test Area, near Fallon, Nevada, USA. Advances in Environmental Research 5, 151–166.

Parkhurst D L, Appelo C A J, 1999. User's guide to PHREEQC (version 2): a computer program for speciation, batch-reaction, one-dimensional transport, and inverse geochemical calculations. Water-Resources Investigations Report 99-4259, U.S. Geological Survey, Denver, Colorado.

Pearson R G, 1963. Hard and soft acids and bases. Journal of the American Chemical Society 85, 3533–3539.

Pourbaix M, 1974. Atlas of electrochemical equilibria in aqueous solutions. 2nd ed. Houston, TX: National Association of Corrosion Engineers.

Reiller P E, Vercouter T, Duro L, Ekberg C, 2012. Thermodynamic data provided through the FUNMIG project: analyses and prospective. Applied Geochemistry 27, 414–426.

Ruberu S R, Liu Y-G, Perera S K, 2007. Occurrence and distribution of ^{210}Pb and ^{210}Po in selected California groundwater wells. Health Physics 92, 432–441.

Salas J, Gimeno M J, Auqué L, Molinero J, Gómez J, Juárez I, 2010. SR-Site – hydrogeochemical evolution of the Forsmark site. SKB TR-10-58, Svensk Kärnbränslehantering AB.

Sandström B, Tullborg E-L, Smellie J, MacKenzie A, Suksi J, 2008. Fracture mineralogy of the Forsmark site. SDM Site Forsmark. SKB R-08-102, Svensk Kärnbränslehantering AB.

Seiler R L, 2011. ^{210}Po in Nevada groundwater and its relation to gross alpha radioactivity. Ground Water 49, 160–171.

Seiler R L, Stillings L L, Cutler N, Salonen L, Outola I, 2011. Biogeochemical factors affecting the presence of ^{210}Po in groundwater. Applied Geochemistry 26, 526–539.

Selnert E, Byegård J, Widestrand H, Carlsten S, Döse C, Tullborg E-L, 2009. Bedrock transport properties. Data evaluation and retardation model. Site descriptive modelling, SDM-Site Laxemar. SKB R-08-100, Svensk Kärnbränslehantering AB.

Sheppard S C, Ticknor K V, Evenden W G, 1998. Sorption of inorganic ^{14}C on to calcite, montmorillonite and soil. Applied Geochemistry 13, 43–47.

Skagius K, Pettersson M, Wiborgh M, Albinsson Y, Holgersson S, 1999. Compilation of data for the analysis of radionuclide migration from SFL 3-5. SKB R-99-13, Svensk Kärnbränslehantering AB.

SKB, 1999. Deep repository for spent nuclear fuel. SR 97 – Post-closure safety. Main report – Vol. I, Vol. II and Summary. SKB TR-99-06, Svensk Kärnbränslehantering AB.

SKB, 2010. Radionuclide transport report for the safety assessment SR-Site. SKB TR-10-50, Svensk Kärnbränslehantering AB.

SKB, 2013. Låg- och medelaktivt avfall i SFR – Referensinventarium för avfall 2013. SKB R-13-37, Svensk Kärnbränslehantering AB.

Stipp S L S, Eggleston C M, Nielsen B S, 1994. Calcite surface structure observed at microtopographic and molecular scales with atomic force microscopy (AFM). Geochimica et Cosmochimica Acta 58, 3023–3033.

Stipp S L S, Gutmannsbauer W, Lehmann T, 1996. The dynamic nature of calcite surfaces in air. American Mineralogist 81, 1–8.

Stumm W, Morgan J J, 1996. Aquatic chemistry: chemical equilibria and rates in natural waters. 3rd ed. New York: Wiley.

Stumpf T, Bauer A, Coppin F, Fanghänel T Kim J-I, 2002. Inner-sphere, outer-sphere and ternary surface complexes: a TRLFS study of the sorption process of Eu(III) onto smectite and kaolinite. Radiochimica Acta 90, 345–349.

Thomson G, Miller A, Smith G, Jackson D, 2008. Radionuclide release calculations for SAR-08. SKB R-08-14, Svensk Kärnbränslehantering AB.

Ticknor K V, Vandergraaf T T, McMurry J, Boisvenue L, Wilkin D, 1996. Parametric studies of factors affecting Se and Sn sorption. AECL TR-723, COG-95-554, Whiteshell Laboratories, Canada.

Vesterbacka P, 2005. ^{238}U-series radionuclides in Finnish groundwater-based drinking water and effective doses. PhD thesis. Department of Chemistry, University of Helsinki.

Videnská K, Palágyi Š, Štamberg K, Vodičková H, Havlová V, 2013. Effect of grain size on the sorption and desorption of SeO_4^{2-} and SeO_3^{2-} in columns of crushed granite and fracture infill from granitic water under dynamic conditions. Journal of Radioanalytical and Nuclear Chemistry 298, 547–554.

Wadsak W, Hrnecek E, Irlweck K, 2000. Formation of americium(III) complexes with aqueous silicic acid. Radiochimica Acta 88, 61–64.

Wang Z, Felmy A R, Xia Y X, Qafoku O, Yantassee W, Cho H, 2005. Complexation of Cm(III)/Eu(III) with silicates in basic solutions. Radiochimica Acta 93, 741–748.

Unpublished documents

SKBdoc id, version	Title	Issuer, year
1261302 ver 3.0	Thermodynamic database: SKB-09	SKB, 2009

Appendix A

Sorption of inorganic radiocarbon (^{14}C) in fracture calcite

Estimation of the isotope exchange partitioning coefficient

If retardation of inorganic ^{14}C on fracture mineral coatings is modelled as an equilibrium process, the retarded travel time is given by the expression:

$$t_a = R_f t_w \tag{A-1}$$

Where, t_w is the water residence time (also referred to as the advective travel time), and the retardation factor, R_f is defined as:

$$R_f = 1 + 2K_a / \delta_t \tag{A-2}$$

Here, K_a (m) is the fracture surface area normalised sorption coefficient for the mineral coating, and δ_t (m) is the transport aperture of the fracture. If calcite is the dominant sink for sorption of inorganic ^{14}C, the recommended K_a (m) value is given by the expression:

$$K_a = f_{eq} K_d^{eq} m_s \tag{A-3}$$

Where f_{eq} is the fraction of mineral mass that is equilibrated on the timescale of transport, K_d^{eq} (m^3/kg) is the equilibrium sorption partitioning coefficient, and m_s (kg/m^2) is the specific mass of calcite per unit area of fracture surface (note: fracture polygon surface area rather than flow-wetted surface area). When applied to isotope exchange on calcite, f_{eq} is also referred to as the *exchangeable fraction* of calcite. An effective K_d value that incorporates the realisable equilibration fraction can be defined as:

$$K_d = f_{eq} K_d^{eq} \tag{A-4}$$

Given the known proportion, f_k of fractures mapped as not containing calcite, the specific mass per unit area of fracture area is:

$$m_s = (1 - f_k)\, \overline{\delta}_m\, (1 - \theta_k)\, \rho_k \tag{A-5}$$

Where, θ_k (m^3/m^3) is the average porosity of the fracture calcite, ρ_k (kg/m^3) is its crystallographic density, and $\overline{\delta}_{m(k)}$ (m) is the equivalent mean thickness of the mineral coating (i.e. for mineral k which, in this case, represents calcite). Quantitative data for the equivalent mean thickness of individual fracture minerals are compiled in Löfgren and Sidborn (2010) and are averaged over the fracture area implicitly considering surface coverage. Based on the data given in Löfgren and Sidborn (2010), the average calcite specific mass should be roughly 96 g/m^2, although it could range from as little as 57 g/m^2 to as much as 130 g/m^2 depending on the assumed porosity of the mineral coating (this has not been measured so is arbitrarily assumed to lie in the range 0.3–0.7 for the sake of scoping calculations).

The exchange reaction for replacement of non-active carbonate (predominantly ^{12}C) with ^{14}C labelled carbonate is:

$$Ca^{12}CO_{3\,(s)} + H^{14}CO_3^- \Leftrightarrow Ca^{14}CO_{3\,(s)} + H^{12}CO_3^- \tag{A-6}$$

The isotopic fractionation factor, $\alpha_{calcite}^{14C}$ for partitioning of ^{14}C and ^{12}C between aqueous and solid (calcite) phases is given by:

$$\frac{c_{14}}{c_{12}} \Big/ \frac{x}{1-x} = \alpha_{calcite}^{14C} \tag{A-7}$$

Where x is the mole fraction of ^{14}C in the calcite, c_{14} is the free concentration of $H^{14}CO_3^-$, and c_{12} is the free concentration of non-active $H^{12}CO_3^-$ in the aqueous phase. If additional fractionation effects involving aqueous phase reactions are neglected, the ratio of free carbonate to total carbonate concentration can be assumed to be the same for both ^{12}C and ^{14}C since they are otherwise chemically identical:

$$\frac{c_{14}}{c_{14(T)}} \approx \frac{c_{12}}{c_{12(T)}} \tag{A-8}$$

Assuming the validity of Raoult's law for the concentration of non-active free carbonate in equilibrium with calcite, we can also write:

$$c_{12} = (1-x)\,c_{12}^{0} \tag{A-9}$$

Where c^0_{12} is the free concentration of $H^{12}CO_3^-$ in equilibrium with pure ^{12}C calcite. If fractionation effects in the calcite isotope exchange reaction are neglected and only simple isotope exchange is considered, this implies $\alpha_{calcite}^{14C} \approx 1$ giving:

$$\frac{c_{14}}{(1-x)\,c_{12}^{0}} \Big/ \frac{x}{1-x} \approx 1 \tag{A-10}$$

Equation A-10 can be rearranged to give x explicitly:

$$x \approx \frac{c_{14}}{c_{12}^{0}} = \frac{c_{14(T)}}{c_{12(T)}^{0}} \tag{A-11}$$

Essentially, Equation A-11 is simply a formal way of stating that, at equilibrium, the ratio of radiocarbon to non-active carbon should be roughly the same in the solid and aqueous phases. From the mole fraction x of ^{14}C in the calcite, the K_d for equilibrium sorption can then be shown to be approximately equal to:

$$K_d^{eq} = \left(\frac{x}{M_w^{calcite}}\right) \cdot \frac{1}{c_{14(T)}} \approx \frac{1}{c_{12(T)}^{0} M_w^{calcite}} \tag{A-12}$$

If the units of mass concentration are estimated in mol/L (≈ mol/kg_w) and calcite molecular weight is specified as 100.09 g/mol, the K_d value is obtained with units of L/g (equivalent to m^3/kg), i.e:

$$K_d^{eq} = x \left[\frac{\text{mol } ^{14}\text{C}}{\text{mol calcite}}\right] \cdot \frac{1}{M_w^{calcite}} \left[\frac{\text{mol calcite}}{\text{g calcite}}\right] \cdot \frac{1}{c_{14(T)}} \left[\frac{\text{L}}{\text{mol } ^{14}\text{C}}\right] \tag{A-13}$$

K_d values for the contemporary groundwater situation

From the measurement data reported in the Bedrock Hydrochemistry report (Nilsson et al. 2011) for the Site Descriptive Model of SFR, the K_d for sorption of inorganic ^{14}C on fracture calcite can be readily estimated using Equation A-12. In the calculation procedure, the compositional data from Sicada are firstly charge balanced by adjusting the Cl^- concentration and then equilibrated with calcite. The calculations were made using PhreeqC (Parkhurst and Appelo 1999) using the most recent version (SKB-TDB-09) of the SKB thermodynamic database (Duro et al. 2006). Groundwater temperature was assumed to be 15°C since the available data set did not contain details of in situ sampling temperature. The extent to which the estimated K_d for ^{14}C sorption may be affected by the temperature assumption is complicated by the fact that the solubility of calcite decreases with increasing temperature. Running the same calculations at 25°C, however, does not seem to have a noticeable impact on the distribution of calculated K_d values (differing on average by only about 3% from the values calculated at 15°C).

In the raw data set there are 58 measurements, from the KFR borehole series at SFR where pH was not measured although the major ion compositions of the groundwater samples (including carbonate) are given. For these samples, the charge balance was initially achieved by adjusting the pH. The distribution of theoretically derived K_d values thus obtained is shown in Figure A-1 plotted versus pH and in Figure A-2 plotted versus sampling elevation (metres above sea level, masl). The data are plotted separately with regard to whether the charge balance was calculated by adjusting Cl^- concentrations (circular markers) or the initial pH (triangular markers).

The impact of OPC leachate on the equilibrium K_d for inorganic radiocarbon sorption on calcite has also been calculated for several of the most relevant groundwater types used to describe the evolution of groundwater chemistry surrounding the SFR repository. The results of these calculations are also shown in Figure A-1 (solid curves) plotted as a function of groundwater pH. Based on the compositions described in Auqué et al. (2013) the trajectory of K_d variation can be plotted assuming a simple hydrodynamic mixing model for neutralisation. The OPC leachate is simulated in a simplified fashion by assuming Portlandite equilibrium. This is the same mixing model used previously in support of the K_d recommendations for the geosphere rock matrix. Under such conditions, the equilibrium K_d value can exceed 100 m^3/kg (and possibly as much as 1,000 m^3/kg) for some distance until the pH is lowered by the aqueous phase buffering reactions.

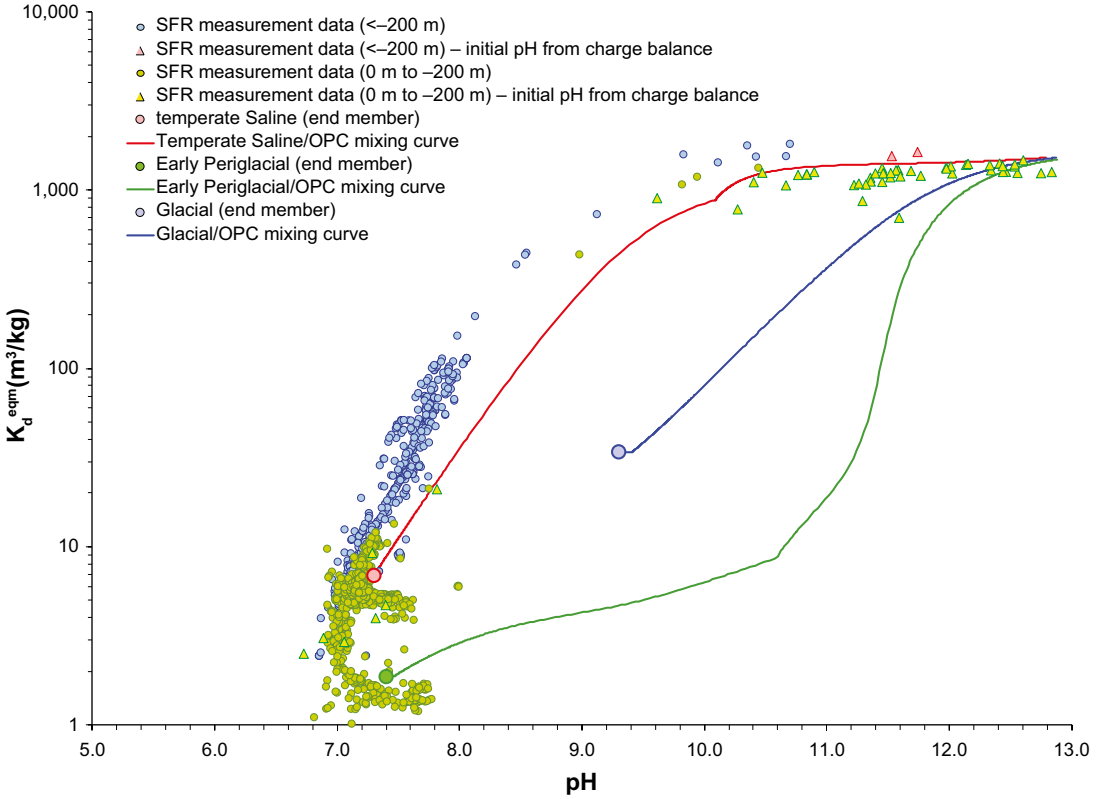

Figure A-1. *Theoretical K_d^{eq} values estimated for inorganic ^{14}C sorption on fracture calcite at Forsmark based on reported measurement data in the Site Descriptive Model (Nilsson et al. 2011) at an assumed in situ temperature of 15°C. The data are plotted vs. pH and consider full equilibration of calcite crystals. To obtain an effective K_d value for use in transport calculations, the K_d^{eq} values must be multiplied by an equilibration factor reflecting the exchangeable fraction on the timescale of transport. Also shown are trajectories for a hypothetical pH buffering process related to hydrodynamic mixing of OPC leachate and the particular "type" groundwaters considered in this work.*

The calculations strongly indicate that the K_d for inorganic radiocarbon sorption on calcite should be significantly higher in zones featuring elevated pH levels due to mixing with OPC leachate from SFR, although the extent and persistence of these zones along potential migration paths is largely unknown. For the purpose of making scoping calculations, a K_d^{eq} value of 10 m^3/kg is assumed in following discussions as being approximately representative of the contemporary groundwater situation at shallow depth. For the SFR safety assessment calculations, however, it might be advisable to adopt a lower K_d^{eq} value of perhaps 1–2 m^3/kg to ensure conservatism in the calculation of radiological risk in the geosphere.

As can be seen from both Figure A-1 and Figure A-2, there is a trend to increasing K_d with increasing depth (decreasing elevation) owing to the inverse correlation with total carbonate content of the groundwater which decreases with depth. Since the estimated K_d values are very closely tied to the equilibrium status of calcite, additional calculations have been made to assess whether the initial groundwater compositions (as reported) are not in equilibrium with respect to calcite, and furthermore what the implication is for K_d when equilibrium is assumed.

The rationale for this is twofold. Firstly, at the surface of calcite crystals where the uptake of ^{14}C actually takes place, local equilibrium will exist even if the bulk groundwater composition exhibits disequilibrium with regard to calcite. Any K_d value used to represent the sorption on fracture calcites must therefore reflect the local equilibrium at the crystal surface rather than the bulk groundwater. Secondly, if the bulk groundwater is indeed undersaturated with respect to calcite (negative saturation index, SI < 0) while local equilibrium conditions exist at the crystal surface, this would imply net ongoing dissolution of the calcite. If the bulk groundwater is oversaturated (SI > 0), on the other hand, this would imply a net precipitation.

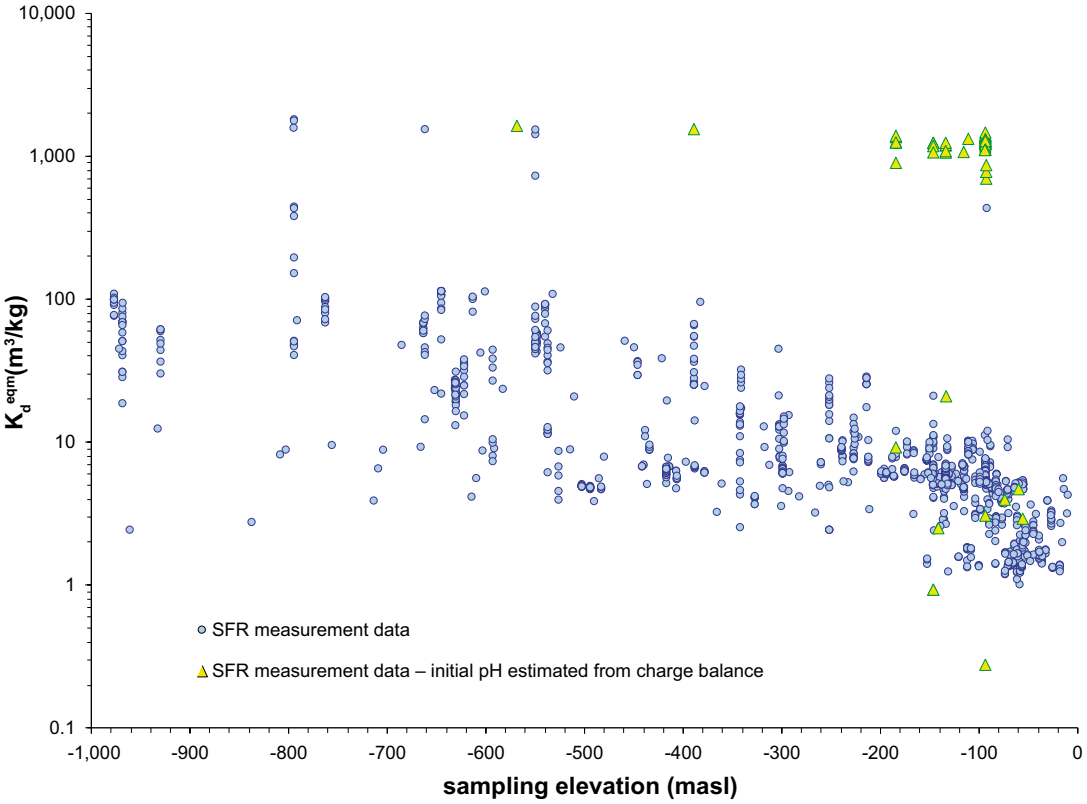

Figure A-2. *Theoretical K_d^{eq} values estimated for inorganic ^{14}C sorption on fracture calcite at Forsmark based on reported measurement data in the Site Descriptive Model (Nilsson et al. 2011) at an assumed in situ temperature of 15°C. The data are plotted. vs. sampling elevation (metres above sea level) and consider full equilibration of calcite crystals. To obtain an effective K_d value for use in transport calculations, the K_d^{eq} values must be multiplied by an equilibration factor reflecting the exchangeable fraction on the timescale of transport.*

Mechanistically, isotope exchange should occur regardless of whether calcite crystals are undergoing net precipitation or dissolution if there is equilibrium at the surface of the mineral grain. The extent to which exchange occurs, however, depends on the dynamics of isotope uptake relative to the precipitation or dissolution which is difficult to predict a priori. Temporal fluctuations in calcite saturation may also be a driving force which, if recurring, might possibly lead to a greater exchangeable fraction (i.e. effective penetration depth in calcite crystals) than if the groundwater were always assumed to be in constant equilibrium. It is not clear, however, whether the apparent fluctuations in saturation index are legitimate or artefactual (perhaps relating to difficulties involved in obtaining representative samples).

Figure A-3 shows the variation of apparent calcite saturation index plotted versus sampling elevation. The saturation indices of the measurement data are very scattered with many samples clearly taken from the same borehole and sampling elevation displaying considerable temporal fluctuation in apparent saturation index. The data set as a whole has a slight mean tendency to oversaturation which becomes more prominent in the near surface. It is noted that the trend may, at least in part, be related to the constant temperature profile assumed in the PhreeqC calculations and may be considered an artefact.

The impact of calcite over- or undersaturation on K_d is complicated since when the groundwater solutions are equilibrated with calcite, a shift in both pH and carbonate speciation takes place. Figure A-4 shows a cross-plot of K_d calculated with forced calcite equilibrium versus the K_d calculated for the reported groundwater compositions (speciated and charge-balanced only). The calculations suggest that, with some exceptions, the calcite-equilibrated K_d values are approximately the same as those obtained using the initial groundwater measurement data without consideration of calcite equilibrium.

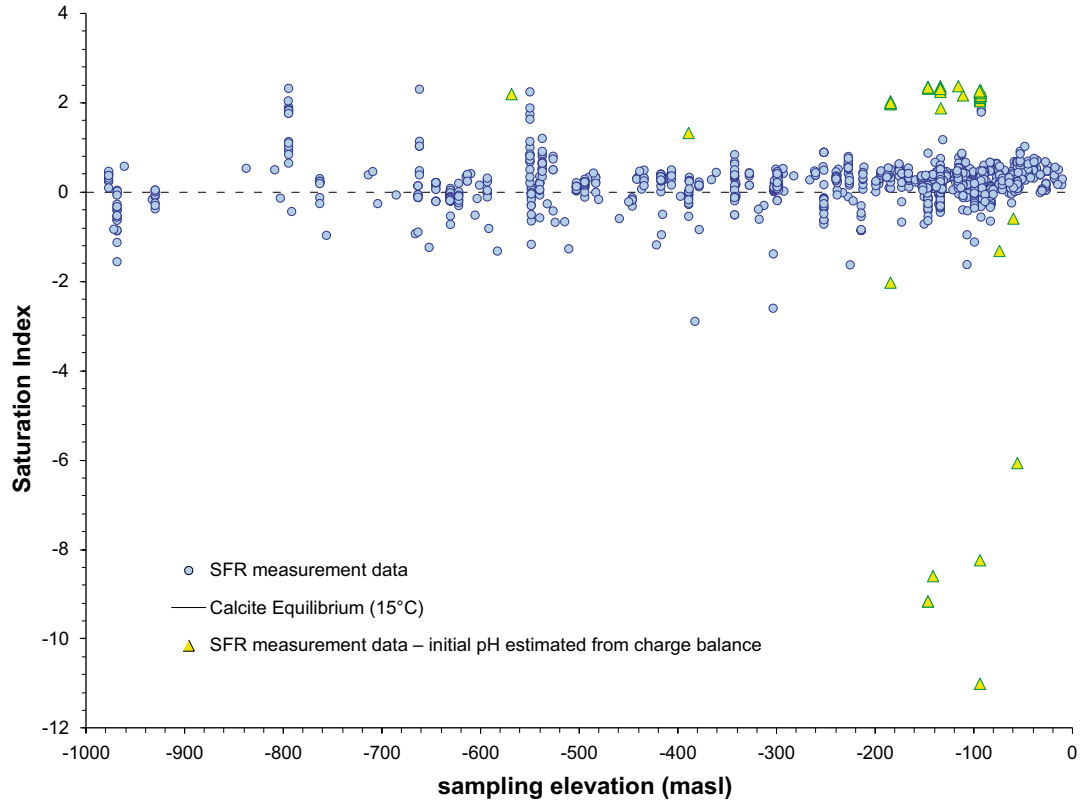

Figure A-3. *Calcite saturation index of reported measurement data (calculated with PHREEQC and an assumed average in situ temperature of 15°C) plotted vs. sampling elevation (metres above sea level).*

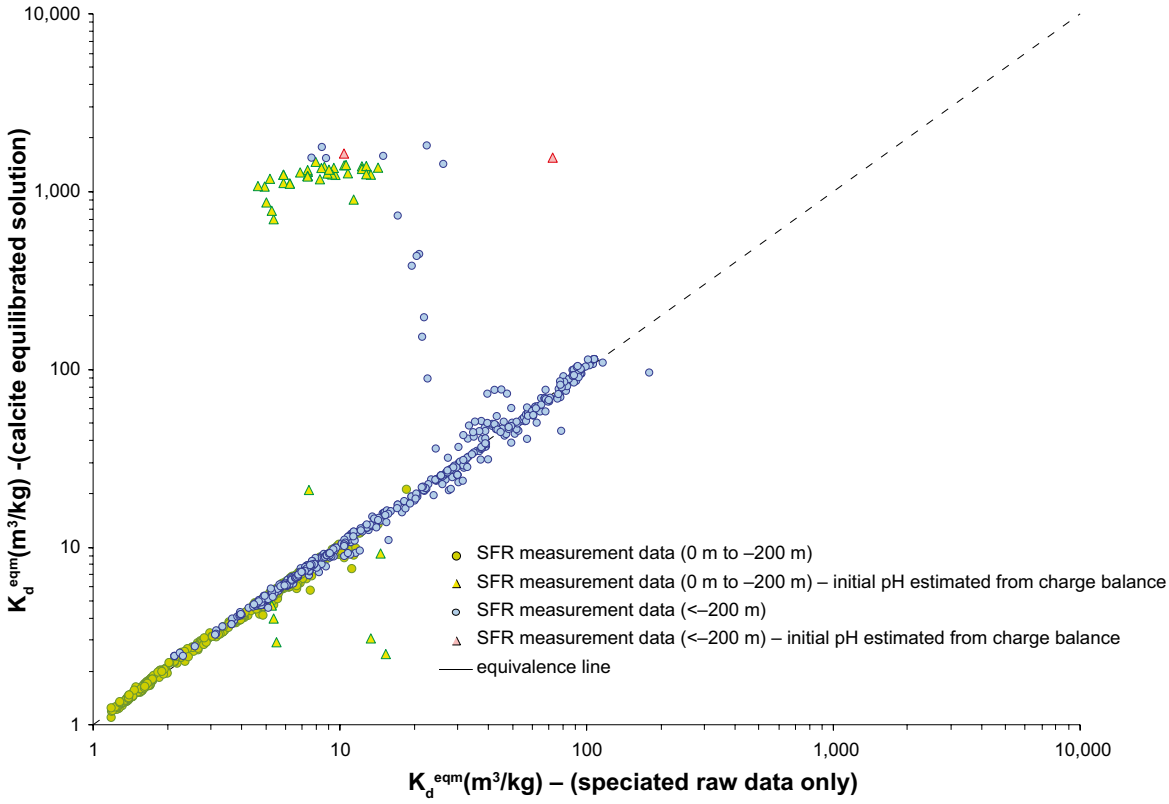

Figure A-4. *K_d values for groundwater with forced calcite equilibrium (calculated with PHREEQC) vs. K_d values estimated for original non-calcite equilibrated compositions, speciated and charge-balanced only.*

The exceptions, however, appear to be predominantly high pH samples where the measured carbonate concentrations are much higher than that predicted by the equilibrium calculations. It is not clear why this is the case, although it may be related to how reported carbonate concentrations were estimated in the high pH samples. Also, it is not clear whether the charge-balance estimated pH for the KFR borehole samples are unbiased. The high pH estimates for these samples could therefore be due to suspect analytical data. Although it seems feasible that these data do reflect an OPC leachate influence, this cannot be certain and is why the pH charge-balanced data are plotted separately in the figures presented in this section.

It is speculated that the lower limit of K_d values at around 1–2 m^3/kg in the shallow groundwater may be related to the relatively high CO_2 partial pressure in altered meteoric water infiltrating from the biosphere. The small cluster of K_d values at the high end of the scale (~1,000 m^3/kg) could be affected by alkaline effluent from SFR as inferred from their relatively high pH. Mixing of groundwater with a significant amount of OPC leachate raises the pH and reduces the equilibrium carbonate concentration when calcite equilibrium is imposed. This can imply high K_d values in zones where there is significant OPC alkalinity present which may then dominate the transport retardation of inorganic ^{14}C (see mixing trajectories in Figure A-1).

Estimation of the equilibration fraction, f_{eq}

The fraction of calcite that can be equilibrated on the timescale of transport depends on the specific surface area of the fracture calcite and the depth in the calcite crystals to which isotope exchange can be reasonably expected to occur. For a 1-dimensional uptake process, the equilibration fraction is defined as:

$$f_{eq} = \frac{\eta}{\eta_{\max}} \qquad \text{(A-14)}$$

Where, η is the average depth of isotope exchange and $\eta_{\max}$ is the maximum penetration depth in the mineral crystal. The maximum penetration depth for isotope exchange averaged over a heterogeneous sample can be estimated by simple volumetric balancing, i.e:

$$\eta_{\max} = \frac{1}{A_s \rho_s} \qquad \text{(A-15)}$$

Where, A_s (m^2/kg) is the specific surface area of calcite and ρ_s (kg/m^3) is its crystallographic density (2,710 kg/m^3). A BET surface area of 2.2 m^2/g is reported by Byegård et al. (2008) for calcite dominated fracture types at the Forsmark site. If it is assumed that this is approximately representative of the calcite mineral grains comprising the fracture coating, this implies a maximum penetration depth on the order of ~0.17 μm (1.7×10^{-7} m). In Bradbury et al. (2010) it was speculated that approximately the first 30 or so, monolayers (~10^{-8} m) at the calcite surface should be readily accessible over safety assessment timescales. This estimate was based upon earlier work by Stipp et al. (1994, 1996) relating to the observed uptake of Cd^{2+} and Zn^{2+} into pristine Iceland spar calcite samples. For the Forsmark site-specific fracture calcite, a penetration depth of 10^{-8} m would imply an equilibration fraction of about ~6%.

In most studies reported in the literature, the focus is typically upon fractionation of oxygen isotopes in actively precipitating calcite owing to its relevance for paleoclimate reconstruction using speleothems (i.e. stalactites, flowstones, and similar cave drip formations). There appear to be very few, or no studies that specifically assess dynamics of low temperature isotope fractionation for natural calcites exposed to groundwater under nominally equilibrium conditions and the studies that do exist may be affected by initial conditions leading to re-crystallisation of the calcite being studied. An estimate of ~8×10^{-24} m^2/s was given by Lahav and Bolt (1964) for self diffusion of ^{45}Ca in a commercial grade calcite in contact with a solution equilibrated with the same material.

It is noted that the persistence of isotopic zoning in environmental speleothems would tend to suggest extremely low solid state diffusivities, certainly not higher than the estimate given by Lahav and Bolt (1964). Extrapolation of high temperature (400°C–800°C) solid state diffusivities reported in the literature (e.g. Cherniak 2010) through use of the Arrhenius equation also typically implies ambient temperature diffusivities less than 10^{-35} m^2/s and in some cases as little as 10^{-50} m^2/s in the case of the data reported by Fisler and Cygan (1999).

The average penetration depth for a diffusing solute is given by Neretnieks (1980) as:

$$\eta \approx 2\sqrt{\frac{D_c t}{\pi}} \tag{A-16}$$

Given the diffusivity reported by Lahav and Bolt (1964) and assuming a contact time of around 6 months, one would obtain a penetration depth of roughly the same magnitude as that speculated by Bradbury et al. (2010). As discussed in Crawford (2006) the appropriate contact time for transport retardation is given by the fracture mineral retention time of the solute, which when used together with Equation A-16 gives an effective depth of penetration associated with the transport retardation. The travel time is equal to the sum of advective travel time (t_w), fracture mineral retention time (t_a), and rock matrix retention time (t_m):

$$t_R = t_w + t_a + t_m \tag{A-17}$$

The fracture mineral retention time is given by:

$$\overline{t_a} = \frac{F}{2} f_{eq} K_{ds} m_s \tag{A-18}$$

Combining Equation A-18 with Equation A-14 and A-16 and solving for f_{eq} gives:

$$f_{eq} \approx \frac{2F D_c K_{ds} m_s}{\pi \eta_{\max}^2} \tag{A-19}$$

Based on the solid state diffusivity reported by Lahav and Bolt (1964), one would expect full equilibration ($f_{eq} \approx 1$) to be attained in Forsmark fracture calcites for F-factors greater than 200 y/m. This, however, assumes that the process of isotope exchange actually occurs by way of a diffusive mechanism which is not corroborated and may not be correct. It is conceivable that the isotope exchange is an entropy driven mixing process that appears similar to diffusion over short timescales, although is mechanistically limited to some depth in the calcite crystal (e.g. surface renewal). The assumption of a solid state diffusion mechanism therefore would be non-conservative for radiological risk estimates since the diffusion depth is only limited by the effective crystal radius.

Most fracture calcites at Forsmark appear to be very old, as far as can be determined using various geochronological and radiometric dating methods (Sandström et al. 2008). The reported data for site specific calcites also generally exhibit differences in $^{87}Sr/^{86}Sr$ and Ca/Sr ratios that would seem to indicate isotope and trace element disequilibrium with groundwater. As noted in Appendix B of the transport modelling report for SR-Site (SKB 2010), measured $^{234}U/^{238}U$ and $^{230}Th/^{234}U$ isotope ratios in bulk fracture minerals also appear to be in disequilibrium with the corresponding values for groundwater and, presumably also matrix porewater.

These observations, if deemed representative for fracture calcites, could be taken to indicate low range equilibration fractions since one would not expect to see substantial isotopic disequilibrium if the equilibration fraction was high. Regrettably, many of the calcites that have been characterised are sampled from annealed fractures and thus may not be representative of calcites in flow-bearing fractures. It is also important to remember that a number of different processes involving deposition and leaching of uranium over geological time can give rise to similar patterns of $^{234}U/^{238}U$ and $^{230}Th/^{234}U$ disequilibrium so interpretation is difficult.

Radiocarbon measurements on old fracture calcites sampled from near-surface flow-bearing fractures might be able to give a definitive answer concerning appropriate equilibration fractions for inorganic ^{14}C on the relevant transport timescale of up to a few thousand years, although such data does not exist at the present time. On the other hand, if it is not possible to measure radiocarbon activity in calcites hosted in flow bearing fractures although the contacting groundwater does have a measurable radiocarbon age, this would also imply a very low equilibration fraction. Owing to the lack of data constraining the equilibration depth for calcite, we assume the value of 10^{-8} m given by Bradbury et al. (2010), thereby giving an effective K_d value of 0.06 m^3/kg (i.e. corresponding to an equilibrium K_d value of 1 m^3/kg and assuming $f_{eq} \approx 6\%$).

Comparison with literature K_d data

In the data compilation by Bradbury et al. (2010) for generic Swiss argillaceous rock, the exchangeable fraction of calcite is estimated to be 0.27% based on a penetration depth of 10^{-8} m and a BET surface area for calcite of ~0.1 m^2/g. The lower equilibration fraction estimated by these authors is due to the significantly lower BET surface area specified for the calcite which implies larger calcite crystal sizes. Based on the porewater compositions (50–4,800 mg/L HCO_3^-) estimated for generic argillaceous rock and the equilibration fraction of 0.27%, K_d estimates in the range 3.4×10^{-4} m^3/kg to 3.4×10^{-2} m^3/kg are obtained for the calcite mineral fraction.

A K_d value of 2.94×10^{-2} m^3/kg is reported by Hershey et al. (2003) in laboratory batch experiments for inorganic radiocarbon sorption on calcite with a BET surface area of 2.5 m^2/g and a contact time of 210 days. From the reported concentrations of dissolved carbonate in the batch experiments (~120 mg/L), a theoretical equilibrium K_d value of ~5 m^3/kg is estimated using Equation A-12 thus implying an equilibration faction of 0.6%. From the BET surface area of the crushed materials used in the batch experiments, a penetration depth on the order of 9×10^{-10} m is estimated. This is significantly less than the value of 10^{-8} m cited previously and only slightly more than a single monolayer thickness of $CaCO_3$ based on the crystallographic unit cell volume of calcite.

A K_d value of 8.3×10^{-2} m^3/kg is reported by Andersson et al. (1983) in batch experiments using crushed calcite (0.045–0.125 mm sieve size), a contact time of 6 months, and a dissolved carbonate concentration of 123 mg/L. This implies an equilibration fraction on the order of 1.7% for the calcite studied. Sheppard et al. (1998) report radiocarbon K_d values in the range 8×10^{-3}–5×10^{-2} m^3/kg for a number of crushed natural calcite samples (0.038–0.85 mm) and a contact time of 24 months. For the equilibrated carbonate concentration of 16.8 mg/L reported by the authors, this implies equilibration fractions in the range 0.02–0.14%. Neither the Andersson et al. (1983) nor Sheppard et al. (1998) data sets include BET surface areas, however, so an equivalent penetration depth cannot be estimated.

As can be seen from these discussions, uncertainty concerning the appropriate penetration depth for isotope exchange and the BET surface area of the calcite mineral grains can have some significance for estimated equilibration fraction and the magnitude of the effective K_d for transport retardation. Based on the penetration depth of 10^{-8} m estimated by Bradbury et al. (2010) and BET surface areas of site specific fracture calcites characterised in the site investigations, an equilibration fraction of 6% appears reasonable. At the other extreme, if only the first monolayer at the calcite surface is considered exchangeable (7×10^{-10} m), an equilibration fraction on the order of 0.4% is estimated for the site specific materials. K_d values reported in experiments discussed above by other authors, however, appear to suggest even lower equilibration fractions, although this may be at least partly due to larger calcite crystal sizes used in experiments.

Potential retardation of inorganic ^{14}C transport at SFR by sorption on fracture calcite

The average retarded travel time, t_R for transported inorganic radiocarbon can be readily calculated using Equation A-18 if the contribution of advective travel time and matrix retention time are neglected. The impact of transport retardation for a constant source activity of inorganic ^{14}C can be assessed by examining the ratio of travel time to radiocarbon half-life ($t_{½}$ = 5,700 y). The results of this screening calculation are shown in Figure A-5. In general, transport retardation in the geosphere will only have a appreciable impact on biosphere fluxes if the $t_R/t_{½}$ ratio significantly exceeds unity. A travel time equivalent to 5 half-lives of ^{14}C, for example, corresponds to a reduction in transported activity by a factor of 32 relative to the source.

As can be seen from Figure A-5, an F-factor in excess of 2×10^5 is required for the retarded transport time to reach parity with the ^{14}C half-life. Since the travel time is roughly proportional to the F-factor and K_d value (i.e. by way of Equation A-18), if high pH conditions can be shown to persist for a few tens of metres along potential migration paths downstream from the SFR repository, this could result in significant reductions in transported radiocarbon activity relative to that obtained in the parts of the geosphere not affected by OPC leachate. Assumption of a conservative equilibrium K_d value of 1–2 m^3/kg based on the lowest reported carbonate concentrations, however, can be shown to give a negligible retardation effect for all conceivable hydrodynamic conditions for migration from the SFR repository.

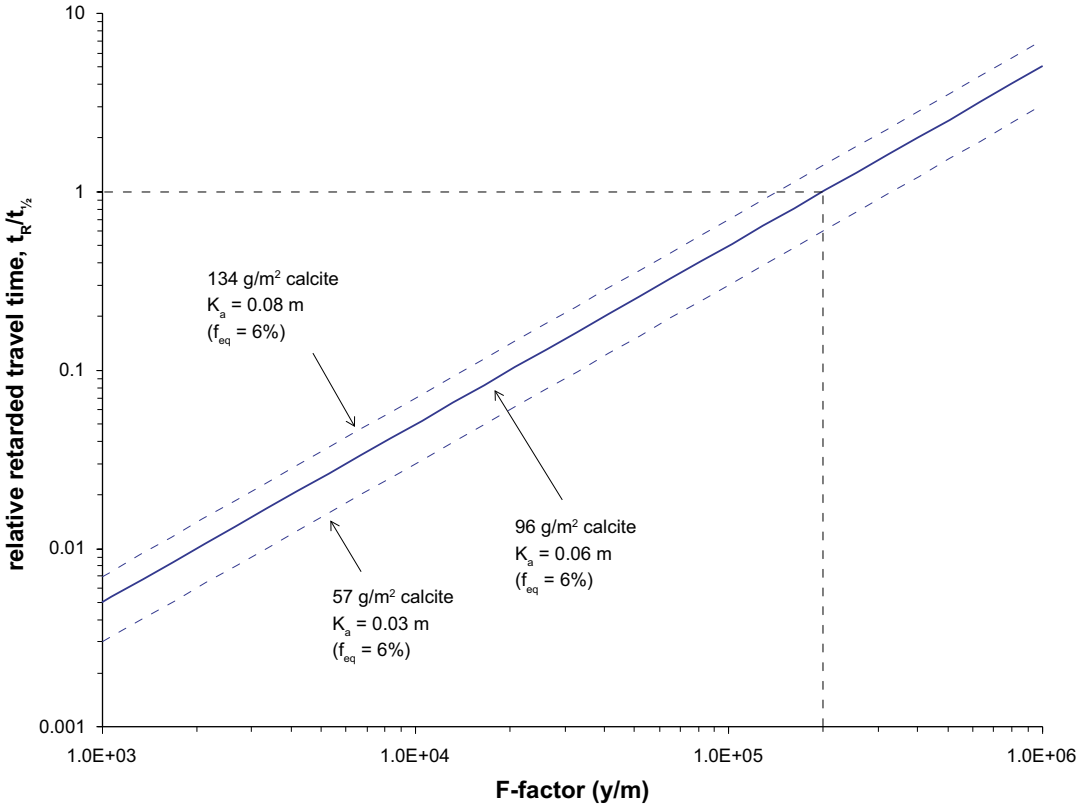

Figure A-5. *Impact of radiocarbon retention on fracture calcite as given by the $t_R/t_{½}$ ratio plotted as a function of F-factor for potential migration paths through the geosphere. The calculations assume negligible advective travel time and matrix retention time and an equilibrium K_d of 10 m^3/kg which is deemed approximately representative of the contemporary (non OPC-affected) near surface groundwater.*

The OPC affected groundwater samples (and hypothetical mixing curves) shown in Figure A-1 suggest that equilibrium K_d values of up to ~1,000 m^3/kg might be possible in the near field with pH levels in the range 10–11 (or higher). If the calcite abundance in the near-field is of similar magnitude as that assessed for the geosphere, very significant retarded travel times equivalent to several half-lives of ^{14}C may be achievable over relatively short distances even for very low F-factors as shown in Figure A-6.

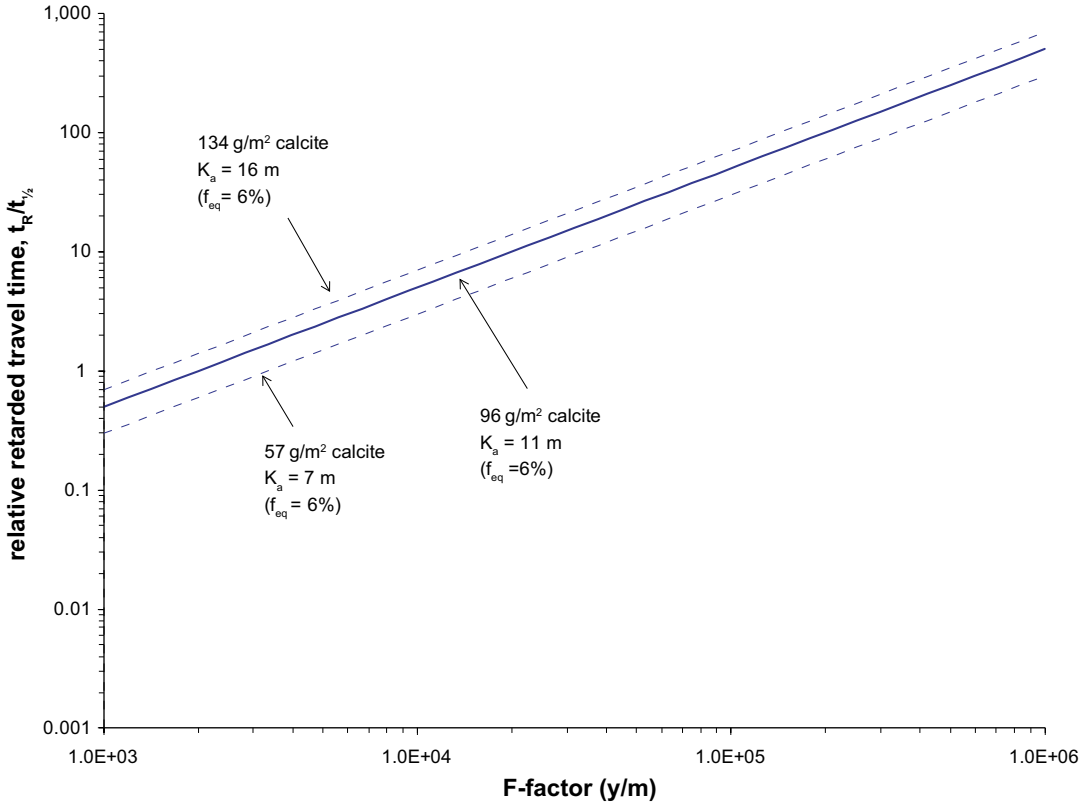

Figure A-6. *Impact of radiocarbon retention on fracture calcite as given by the $t_R/t_{½}$ ratio plotted as a function of F-factor for potential migration paths close to the SFR near-field zone. The calculations assume negligible advective travel time and matrix retention time and an equilibrium K_d of 1,000 m^3/kg which is deemed approximately representative of high pH groundwater strongly affected by OPC-leachate.*

Appendix B

Sorptive transport retardation of nuclides on gravel backfill

If the advective transport of dissolved radionuclides in contact with gravel in a hydraulic cage surrounding the repository is modelled as an equilibrium retardation process, the retarded travel time is given by the expression:

$$t_a = R_f t_w \tag{B-1}$$

Where, t_w is the water residence time (or advective travel time), and the retardation factor, R_f is defined as:

$$R_f = 1 + f_{eq} \mathrm{K_d^*} \rho_b \left(\frac{1 - e_f}{e_f} \right) \tag{B-2}$$

Here, $\mathrm{K_d^*}$ (kg/m^3) is the bulk sorption coefficient for the gravel, ρ_b (kg/m^3) is the bulk density of the gravel matrix material, e_f is the flow porosity of the gravel bed (also referred to as fractional voidage), and f_{eq} is the fraction of the gravel mass that can be considered to be equilibrated on the time scale of transport. The bulk sorption coefficient of the gravel including its free storage porosity, θ_m is customarily defined as:

$$K_d^* = \frac{\theta_m}{\rho_b} + K_d \tag{B-3}$$

Where $\mathrm{K_d}$ (m^3/kg) is the ordinary sorption coefficient for the rock matrix. Provided that the gravel is a crushed form of the site specific rock for which recommended $\mathrm{K_d}$ values are derived, the same data recommended for use in SR-PSU transport calculations can be used.

If the gravel particles are sufficiently large and the water residence time in the gravel bed is sufficiently short that the gravel particles are not diffusively equilibrated on the timescale of transport, uptake of radionuclides to the gravel may be approximated as a matrix diffusion problem assuming an effectively unbounded rock matrix. If this condition can be reasonably fulfilled, the average penetration depth to which a solute will diffuse in a semi-infinite medium is given by Neretnieks (1980) as:

$$\overline{\eta} = 2\sqrt{\frac{D_a t_c}{\pi}} = 2\sqrt{\frac{D_e t_c}{\mathrm{K_d^*} \rho_b \pi}} \tag{B-4}$$

Where the apparent diffusivity, $\mathrm{D_a}$ (m^2/y) is defined in terms of the effective diffusivity, $\mathrm{D_e}$ (m^2/y) as:

$$D_a = \frac{D_e}{\mathrm{K_d^*} \rho_b} \tag{B-5}$$

The contact time, t_c (y) for the diffusive uptake which characterises the retention process is the rock matrix retention time of the radionuclide in the gravel bed. For a matrix diffusion process, the median rock matrix retention time of the radionuclide is:

$$t_c = \frac{D_e \mathrm{K_d^*} \rho_b}{4\left(erfc^{-1}\left(0.5\right)\right)^2} F^2 \tag{B-6}$$

Where the parameter F (y/m) is the hydrodynamic transport resistance, otherwise referred to as the F-factor.

Substituting this expression into Equation B-4 gives:

$$\overline{\eta} \approx \frac{D_e F}{\sqrt{\pi} \cdot erfc^{-1}\left(0.5\right)} = 1.1829 \times D_e F \tag{B-7}$$

It should be noted that the effective penetration depth associated with transport retardation is the same regardless of the sorption $\mathrm{K_d}$ since the sorption terms in Equation B-4 and B-6 mutually cancel, thereby giving only a dependency on the effective diffusivity and the F-factor (Crawford 2006,

Löfgren et al. 2007, Moreno and Crawford 2009). The equivalent F-factor for a bed of pseudo-spherical gravel particles is equal to the ratio of the external surface area of gravel particles and flow rate. This can be shown to be equivalent to:

$$F = \frac{6\lambda}{d_p}\left(1 - e_f\right)t_w \qquad \text{(B-8)}$$

Where, λ is a surface roughness/sphericity correction factor (λ=1 for a sphere), and d_p (m) is the average gravel particle diameter. The average penetration depth can then be shown to be:

$$\bar{\eta} \approx \frac{D_e}{\sqrt{\pi}\cdot erfc^{-1}\left(0.5\right)}\cdot\frac{6\lambda}{d_p}\left(1 - e_f\right)t_w \qquad \text{(B-9)}$$

The equilibration fraction for a gravel particle is then given by the volume ratio of the equilibrated outer shell of the particle (with thickness equal to the diffusive penetration depth) and the total volume of the particle:

$$f_{eq} \approx 1 - \left(\frac{d_p - 2\bar{\eta}}{d_p}\right)^3 \qquad \left(\text{for } \bar{\eta} \le d_p/2\right) \qquad \text{(B-10)}$$

It should be noted that the equilibration fraction calculated by Equation B-10 is only approximate since it does not properly consider saturation effects related to the physically limited diffusion depth in the gravel particle. The value of f_{eq} therefore becomes less accurate as the particle reaches diffusive equilibrium. For the purposes of radionuclide transport calculations in SR-PSU, it is likely that the approximation afforded by Equation B-10 is reasonable given other underlying data uncertainties, particularly if the effective penetration depth is only a fraction of the characteristic particle diameter.

Figure B-1 shows a comparison between the saturation curve (diffusive uptake) obtained using an exact model of spherical diffusion (Crank 1975) and that obtained using the simplified penetration depth approach. The comparison suggests that the approximate method should give no more than a 5% deviation relative to the exact model of spherical diffusion. A more accurate estimate of the equilibration fraction is only possible by modelling the radionuclide transport as a coupled advective flow and matrix diffusion problem in a bed of spherical particles with a fixed maximum diffusion depth equal to the particle radius.

Using the simplified Equation B-9 for the effective penetration depth associated with retardation together with Equation B-10 allows one to calculate the equilibration fraction f_{eq} very simply for a given particle diameter, effective diffusivity of gravel particles, fractional voidage, and water residence time in the gravel bed. For the purposes of these calculations, a typical rock matrix effective diffusivity of 10^{-14} m^2/s (3.16×10^{-7} m^2/y) is reasonable to assume, although the mechanical damage incurred by the material during crushing may increase the effective diffusivity by as much as a factor of 10 or more. For the following calculations, a gravel bed fractional voidage of 0.3 is also assumed, although values in the range of 0.3–0.5 are not unusual for beds of regular spherical or prismatic solids of relatively constant particle size (Coulson et al. 1991).

Figure B-2 and Figure B-3 show the calculated results for f_{eq} given for a range of particle sizes and several different water residence times. The f_{eq} calculated in this fashion for a given particle size and specific water residence time can then be inserted directly in Equation B-2 to obtain the relevant retardation factor for sorptive retention in the gravel bed. For a gravel particle size of 10 mm and a water residence time of 1 y (which can be obtained from particle tracking calculations), a fractional equilibration of 50% is estimated. This implies, in this particular example, that the retardation effect is half that which would be calculated for a fully equilibrated gravel material using Equation B-2. For a 25 mm particle and water residence time of 1 y, the f_{eq} would be on the order of about 20%.

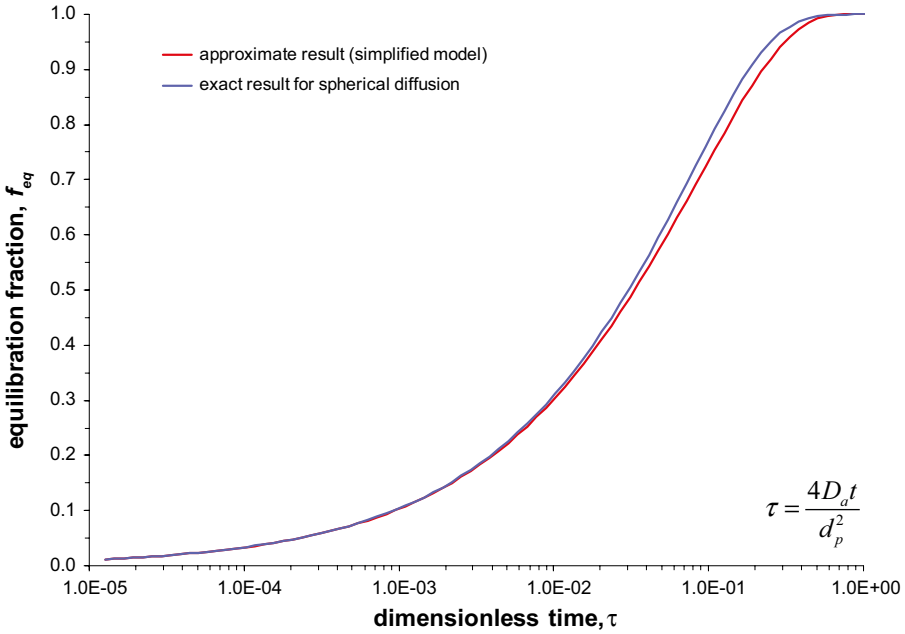

Figure B-1. *Comparison of the particle equilibration fraction calculated using an exact model for spherical diffusion (Crank 1975) and that obtained using a simplified penetration depth representation. Data are plotted as a function of dimensionless contact time for a constant concentration boundary condition. The maximum deviation of the approximate model is less than 5% relative to the exact calculation.*

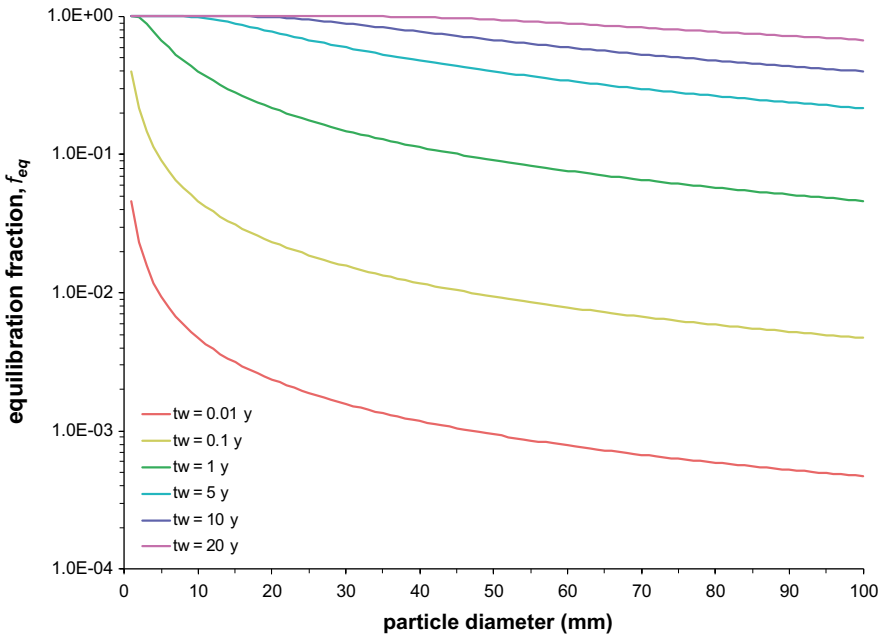

Figure B-2. *Fractional equilibration, f_{eq} of gravel particles plotted as a function of particle diameter for various water residence times in the gravel bed. Calculations assume spherical gravel particles (λ=1), as well as typical values for the effective diffusivity (10^{-14} m^2/s) and gravel bed voidage fraction (0.3).*

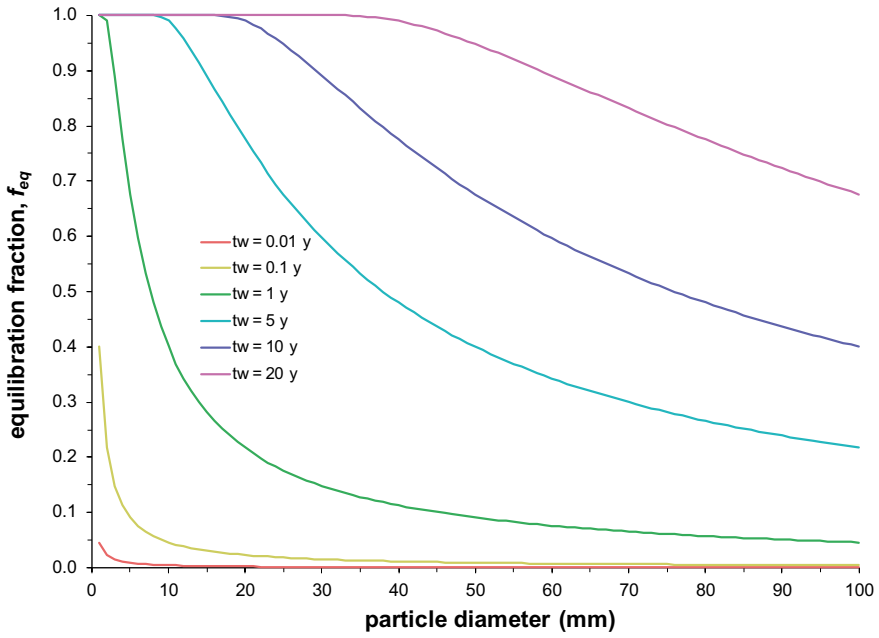

Figure B-3. *Same as previous figure although with f_{eq} plotted on a linear axis to enhance detail at high equilibration fractions.*

Appendix C

On the sorption mechanisms of Selenium and Polonium within the rock matrix

In this report, the sorption of Selenium (^{79}Se) is considered to be sufficiently low that a K_d of zero is recommended as being conservative for radionuclide transport calculations since predominance of the more strongly sorbing Se(IV) state cannot be guaranteed for the specified groundwater redox conditions. At the same time, the recommended K_d for Polonium (^{210}Po) is assessed as possibly being of non-zero magnitude, with sorptivity based on geochemical analogy with Se(IV). Although this might seem to be an inconsistent use of data for different nuclides, the choice may be defensible in the case if any or all of the following conditions can be fulfilled:

1) A state of redox equilibrium exists for the Po system resulting in a relative predominance of Po(IV) which differs from that predicted for Se.
2) Near surface groundwaters characteristic of migration paths leading to the biosphere are less strongly reducing (more oxidising) than the Eh ranges specified by Auqué et al. (2013) thus permitting Po(IV) redox speciation near flowpath exits to the biosphere.
3) The geochemical analogy with Se is overconservative and significantly underpredicts the sorption of migrating Po.

In this appendix, the geochemistry of elements in the same group of the periodic table (i.e. Se, Te, and Po) are considered in detail to assist in the K_d recommendation.

Geochemical and sorptive characteristics of Selenium

Selenium is redox sensitive and is known to exist in Se(-II), Se(0), Se(IV), and Se(VI) redox states. The relative predominance of the different species and redox states are shown in Figure C-1.

In its most reduced form, the selenide ion Se(-II)/Se^{2-} has very low solubility and is typically limited by mineral phases such as $FeSe_{(s)}$ and $FeSe_{2(s)}$ in groundwater containing dissolved ferrous iron (e.g. Kang et al. 2013). It may also form solid solutions with mackinawite (FeS) or pyrite (FeS_2) where Se(-II) substitutes for S(-II) and S(-I), respectively (e.g. Finck et al. 2012). In the aqueous phase, selenide is mostly present as HSe^- at circumneutral to alkaline pH levels when Se(-II) is predominant. At lower pH levels the H_2Se species may form preferentially which, similarly to its sulphur analogue, is volatile.

Pure phase, elemental Se is the only solid known in the zero-valent state and it has low solubility ($< 10^{-9}$ M) in equilibrium with variable proportions of Se(IV) and Se(-II) species in solution (see overlapping predominance fields in Figure C-1). Studies of Se migration under relatively strongly reducing conditions (i.e. presence of pyrite) in boom clay indicate that elemental Se(0) is formed preferentially rather than the Se(-II) containing ferrous minerals discussed above (Beauwens et al. 2005, Breynaert et al. 2010). Recent work by Kang et al. (2013) suggests that the low solubility of Se(0) coupled with the fast kinetics of $FeSe/FeSe_2$ oxidation by selenite, Se(IV)/SeO_3^{2-} favours the formation of elemental Se(0) and may be a reason for the redox disequilibrium of the selenium system frequently observed in natural reducing environments.

Under redox transitional conditions, the selenite ion (SeO_3^{2-}) dominates the aqueous phase speciation of Se(IV) while under oxidising conditions, selenate ion (SeO_4^{2-}) is the main aqueous species of Se(VI). While Se(-II) is considered relatively immobile due to the existence of solubility controlling mineral phases, dissolved HSe^- is not thought to sorb to any great extent and is generally assumed to be non-sorbing. The Se(IV) and Se(VI) redox states, on the other hand are typically considered important for migration processes on account of the absence of solubility limiting phases and their weak sorptivity. Being oxyanions, the sorption of Se(IV) and Se(VI) only occurs by binding reactions involving positively charged surface groups. As discussed in Crawford (2010), most data also suggest that Se(VI) sorbs less strongly than Se(IV).

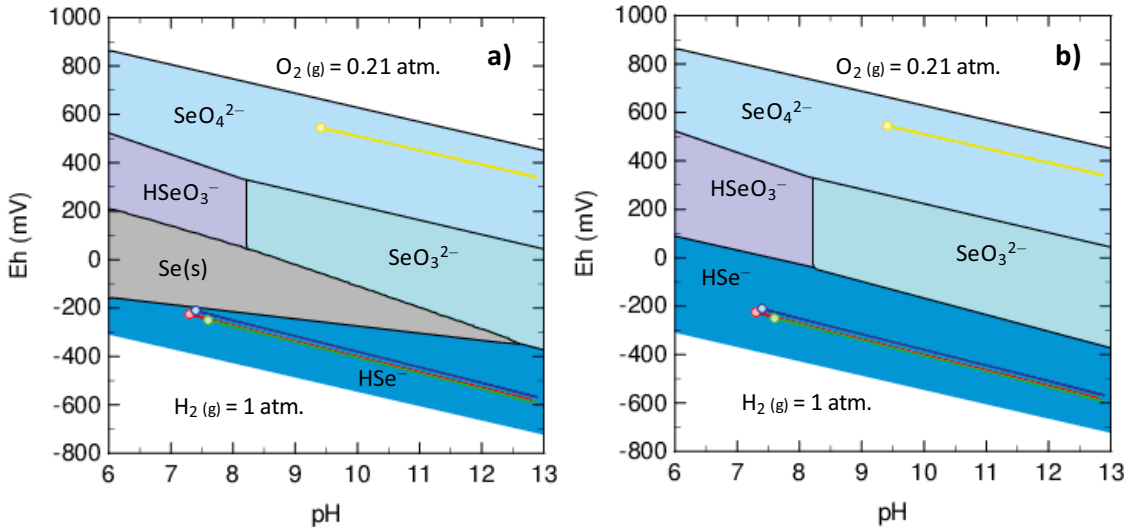

Figure C-1. *Eh-pH diagram showing predominance of Se species and redox states for the Se-O-H_2O-Na-Cl system for Σ Se = 10^{-8} M, 0.1 M NaCl, and 25°C calculated using PhreePlot (Kinniburgh and Cooper 2011). Panel a) shows the overall distribution of redox species including solid phases, whereas b) shows data for the aqueous phase only. Both panels are overlaid with the Eh-pH trend for the mixing of type groundwaters with OPC leachate. The curves show the calculated trend for Saline (red), Early Temperate (blue), Late Temperate (green), and Glacial (yellow).*

Since the net charge of most mineral surfaces is overwhelmingly negative at neutral to alkaline pH levels, the only minerals upon which these species will sorb are those with points of zero net proton charge close to the prevailing pH of the groundwater. Such minerals have non-negligible fractions of positively charged surface groups that can bind anionic sorbing solutes. In granitic rock, this tends to rule out sorption on most minerals except for the various oxide forms of iron which may be present as accessory or secondary mineral phases (i.e. ferric oxyhydroxides, goethite, hematite, or magnetite).

Sorption of Se(IV) and Se(VI) in crushed granite has been studied by Jan et al. (2007, 2008) and shown to be strongly associated with Fe-containing accessory minerals, principally goethite, $FeO(OH)_{(s)}$ as ascertained by X-ray diffraction spectroscopy (XRD). In the study by Jan et al. (2008) it was speculated that the goethite content of the granite samples was most likely related to low temperature weathering of biotite resulting from sample preparation (i.e. crushing, washing and drying of samples). The sorption of Se(VI) was found to be significantly weaker than Se(IV) and difficult to quantify. Under sufficiently oxidising conditions where Se(VI) is the dominant redox state (i.e. the glacial groundwater type), it is therefore not possible to recommend anything other than a K_d of approximately zero for describing the migration behaviour of Se in transport calculations.

Since there is clear evidence for sorption of Se(IV) in association with ferric oxides, it is reasonable to assume that the K_d is roughly proportional to the amount of Fe(III) present in various oxide forms in the rock matrix. The Se(IV) sorption experiments made by Jan et al. (2007) strongly suggest as much and they report K_d values ranging from 6.4×10^{-3} m^3/kg to 8.8×10^{-3} m^3/kg for crushed Taiwanese granite in contact with various water compositions (deionised water, aquifer groundwater, and seawater affected groundwater). By comparing the sorption of Se(IV) before and after stepwise sequential extraction of Fe containing phases, the authors concluded that about 27% of the total Fe content of the rock (1.13 wt% Fe_2O_3) could be associated with the bulk of the Se retention capacity which they interpreted as being related to amorphous and crystalline Fe-oxides.

Literature K_d data cited in Crawford (2010) for Se(IV) sorption in granite ranged from 10^{-4} m^3/kg to 0.2 m^3/kg, which after approximate correction for the increase in surface area resulting from crushing suggested a cautious best estimate of about 3×10^{-4} m^3/kg for intact metagranite/metagranodiorite characteristic of the Forsmark site. A recent work by Videnská et al. (2013) suggests K_d values on the order of 1.7×10^{-4} m^3/kg to 5×10^{-4} m^3/kg based on interpretation of breakthrough curves from

column experiments involving an unspecified crushed granite (0.63–0.8 mm and 0.8–1.25 mm size fractions). The model used in the interpretation, however, only considered equilibrium sorption and therefore may have underestimated the true sorptive uptake. The discrepancy between K_d values fitted to the leading (sorptive uptake) and trailing edges (desorption) of the breakthrough curves strongly intimates the possibility of diffusive disequilibrium.

Recent work by Missana (2013) indicate K_d values ranging from 2×10^{-3} m^3/kg (oxic conditions) to 8×10^{-3} m^3/kg (anoxic conditions) for the sorption of Se(IV) on Äspö diorite. Spectroscopic measurements made using PIXE (particle induced X-ray emission) reported by the same author also demonstrate a strong association with Fe-containing minerals. Äspö diorite, however, is known to have a significantly higher biotite and Fe content (~20 wt% biotite and ~5 wt% Fe_2O_3) than Forsmark metagranite (~5.4 wt% and ~2.7 wt% Fe_2O_3) and therefore could be expected to exhibit greater sorptive affinity for Se(IV) than Forsmark site specific rock.

Geochemical and sorptive characteristics of Polonium

The element Selenium (Se) together with Tellurium (Te), and Polonium (Po) are each members of the Chalcogen Group 16 of the periodic table also containing Oxygen (O) and Sulphur (S). Although they share many chemical characteristics, there are subtle differences related to decreasing electronegativity (or, increasing electropositivity) with increasing atomic number down the group.

The main Po isotope of interest is ^{210}Po belonging to the ^{238}U ($4n$+2) decay chain/radium series and therefore is ubiquitous in nature. The ^{218}Po and ^{214}Po isotopes are also part of the same decay chain although have very short half-lives and are usually not considered individually on account of fast secular equilibrium. The ^{210}Po isotope (t½ 138.4 days) is the main decay product of ^{210}Pb (t½ 22.3 y) and is frequently assumed to be in secular equilibrium with ^{210}Pb for dose calculation purposes. This requires firstly that transport times are sufficiently long that secular equilibrium can be assumed and secondly, that the effective sorptivity of Pb and Po are approximately the same order of magnitude during migration.

Although the broad qualitative chemical properties of Po and its various redox states have been described in detail in some early works (e.g. Bagnall 1962, Figgins 1961), thermodynamic data suitable for modelling of speciation under environmental conditions is relatively sparse. Where such data exists it is very inconsistent and frequently contradictory. This is partly related to the extreme experimental difficulties imposed when working with such an intensely radioactive, α-emitting substance. ^{210}Po is the only isotope of Po that is easily produced and isolated, and since there are no stable isotopes it must be studied at trace concentrations which largely rules out standard spectroscopic methods (Ansoborlo et al. 2012). Redox transitions are particularly difficult to study since the ^{210}Po causes radiolysis if present in sufficiently high aqueous concentrations. Of the 33 known isotopes of Po, only ^{209}Po (t½ 102 y) and ^{208}Po (t½ 2.9 y) have longer half-lives than ^{210}Po and are thus potentially amenable to experimental methods, although these are somewhat more difficult to produce and separate (e.g. Bagnall 1962, Colle et al. 1995, Neuhausen et al. 2004).

The first detailed account of Po redox chemistry can be found in the original reference work by Pourbaix (1974) which predicts a large field of Po(IV)/PoO_3^{2-} stability at circumneutral to alkaline pH levels and mildly reducing to oxidising Eh levels. Under more reducing conditions there is a field of stability for metallic Po(0) not dissimilar to that described above for Se and also a region of predominance for Po(-II) at very low Eh values.

Since thermodynamic constants derived from the electrode potentials cited by Ansoborlo et al. (2012) may be uncertain, comparison with the redox speciation of another more closely related element than Se might give clarity in the discussion. The only element which is closer to Po in terms of chemical properties is Tellurium (Te). Po is more metallic in character than Te, although the geochemical similarity is much closer than for Se. The thermodynamic properties of Te in aqueous solution are also relatively well known owing to its co-occurrence with gold (Au) in hydrothermal systems. Figure C-2 shows the relative predominance of various Te species as a function of pH and Eh using the data compiled by McPhail (1995).

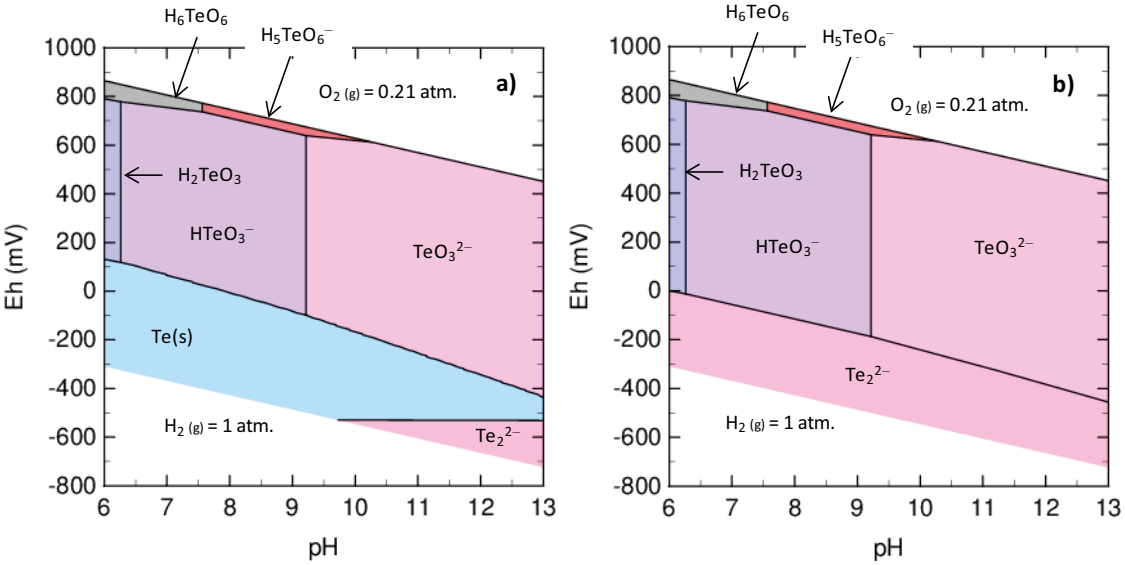

Figure C-2. *Eh-pH diagram showing predominance of Te species and redox states for the Te-O-H_2O system for Σ Te = 10^{-8} M, 0.1 M NaCl, and 25°C based on reaction data given by McPhail (1995) showing, a) overall predominance considering all dissolved and precipitated species, and b) for the aqueous phase only.*

As can be seen from Figure C-2, there is a region of relative Te(-II) predominance which is similar to that calculated for Se(-II). The existence of a corresponding region for Po(-II) predominance might imply diminished K_d values for Po sorption in the rock matrix below that deemed reasonable for Po(IV) based on the analogy with Se(IV). If one accepts the validity of the proposed geochemical analogy, it is not possible to argue for Po(IV) redox speciation at the Eh levels specified for the SR-PSU groundwaters, although it may occur in less reducing, near surface locations. It is noted here that the main uncertainty associated with predictions of Po redox speciation is the unavailability of relevant thermodynamic data which, at present, is not possible to address in an adequate manner. Furthermore, it must be remembered that the predominance diagrams shown for both Se and Te do not consider the additional impact of surface complexation reactions which may shift the relative boundaries of the redox predominance fields.

K_d recommendation for ^{210}Po sorption in the geosphere

To the extent that Po can be assumed to be predominantly speciated in tetravalent form as PoO_3^{2-}, the K_d recommended for transport calculations should be at least as high as that expected for sorption of its approximate geochemical analogue, SeO_3^{2-}. In Crawford (2010) the recommended K_d for SeO_3^{2-} in the rock matrix was set to 3×10^{-4} m^3/kg, although it may in fact exhibit greater sorptivity since the corrections for surface area increase due to crushing, being based on total BET surface area (rather than based on ferric oxide reactive surface area), might be over-conservative.

The only experimental data that has been found for Po sorption on relevant geological materials is that reported by Baston et al. (1998), where a K_d range of 0.1–0.23 m^3/kg was estimated (duplicate measurement) for crushed Japanese granodiorite in contact with a semi-synthetic groundwater (rock-equilibrated deionised water). Reducing conditions (Eh ≤ –200 mV) were initially achieved by addition of Na-dithionite, although α-radiolysis may have altered this during the four month contact time. K_d values about an order of magnitude higher than the range cited above were obtained when phase separation was performed by filtration (< 0.45 µm and < 10,000 MWCO, respectively) rather than centrifugation which suggests possible colloid formation. No information was given concerning the particle size of the crushed rock. It is noted that the reported K_d was roughly the same as that estimated for Am(III) in the same study suggesting relatively strong sorption. The more metallic character of Po together with its well observed tendency to form colloids and strongly interact with glassware surfaces in laboratory settings (e.g. Ansoborlo et al. 2012 and references therein) suggests that the geochemical analogy with Se may be less than ideal and possibly over-conservative.

A further consideration that is highly relevant to this discussion is the fact that the exceptionally short half-life of ^{210}Po means that probably only the first few tenths of a mm of the rock matrix adjacent to fracture surfaces is relevant for migration processes involving this nuclide. The greater degree of weathering oxidation of the rock in the immediate vicinity of the fracture surfaces as well as the nearly ubiquitous presence of ferric oxides in fracture mineral coatings themselves suggests that the effective K_d for ^{210}Po(IV) sorptive retardation is unlikely to be less than 10^{-3} m^3/kg and most likely, higher. In addition to this, the very short half-life of ^{210}Po relative to the ^{210}Pb parent means that only the last few metres to perhaps a few tens of meters of a migration path probably need to be considered for the K_d data selection since any ^{210}Po generated closer to source would decay long before reaching the biosphere. If the groundwater redox conditions in these parts of the migration flowpath differ significantly to the specified SR-PSU type groundwaters (i.e. are less strongly reducing), sorption of Po(IV) might occur.

Supporting data from natural analogue studies

There are a number of studies where statistics of naturally occurring ^{238}U series radionuclide activities have been examined in groundwater wells of various kinds (e.g. Seiler 2011, Vesterbacka 2005). Most studies, however, focus upon ^{238}U, ^{226}Ra, and ^{222}Rn and very few specifically address ^{210}Pb and ^{210}Po activities. Statistics compiled by Vesterbacka (2005) appear to suggest median ^{210}Po/^{210}Pb activity ratios slightly higher than 1 in drilled groundwater wells and slightly less than 1 for shallow excavated wells. This may reflect the more reducing nature of drilled wells versus excavated wells. Distributions are skewed, however, and it is difficult to properly compare ^{210}Po/^{210}Pb activity ratios for pooled data sets, since the results depend upon how the underlying data are binned or otherwise categorised. For ^{210}Po/^{210}Pb activity ratios equal to or less than unity, the assumption of secular equilibrium with ^{210}Pb would be conservative in radiological risk assessment. For ^{210}Po/^{210}Pb activity ratios greater than unity, however, this would be a non-conservative assumption.

In a study by Seiler (2011), ^{210}Po activities up to 100 times the detection limit of ^{210}Pb were reported for drinking water wells in a naturally uranium rich area of northern Nevada. In a follow up study by Seiler et al. (2011) it is speculated that ^{210}Po may have been mobilised in the aquifer in question by microbial sulphur cycling involving sulphate reduction followed by abiotic reduction of MnO_2 by H_2S, and microbial disproportionation of elemental S. In this mechanism, the mobilised ^{210}Po is primarily associated with Mn oxides rather than Fe oxides. This appears to be supported by previous studies linking elevated ^{210}Po levels and MnO_2 reduction in lacustrine environments (Balistrieri et al. 1995, Benoit and Hemond 1990) and anoxic ponds (Kim et al. 2005). These authors speculate that the redox potential for Po(IV)/Po(-II) is close to the corresponding redox transition for the Mn(IV)/Mn(II) system and thus reduction of MnO_2 may also result in ^{210}Po mobilisation. In the work by Seiler et al. (2011), however, it is not clear whether the authors consider the possibility that high ^{210}Po/^{210}Pb activity ratios might also be partly related to strongly decreased mobility of Pb in sulphidic environments due to solubility control by PbS.

The available data for ^{210}Po and ^{210}Pb activities in the literature sources that could be found in this study are shown in Figure C-3. In general, the data indicate ^{210}Po/^{210}Pb activity ratios less than unity, although there are exceptions for individual groundwater wells. Based upon this limited statistical sample of data sets (not all of which are possibly relevant for Swedish conditions), the assumption of secular equilibrium would appear to be a conservative assumption suggesting that the transport of ^{210}Po might not need to be specifically modelled. As noted previously for the data reported by Vesterbacka (2005), however, the actual activity ratio likely to be encountered in any particular drinking water well is very strongly dependent on the redox environment of the immediate surroundings and it is not possible to say with certainty that secular equilibrium is always a good assumption as the data reported by Seiler (2011) seem to indicate.

Statistical data for ^{210}Po/^{210}Pb activity ratios in Swedish groundwater do not appear to exist in the open literature as far as can be ascertained by the present author. Data for ^{210}Po and other α-emitters in the ^{238}U decay chain, however, are reported by Isam Salih et al. (2002) for bedrock wells at 328 sites in the Östergötland and Kalmar municipalities in South-Eastern Sweden (^{210}Pb is a β-emitter and therefore not included in the analysis). The measured ^{210}Po activities were found to vary from 8.45 to 947 mBq/L with a median of 63.3 mBq/L, although from this data it is not possible to say anything about ^{210}Po/^{210}Pb disequilibrium. More detailed statistical data for these naturally occurring radionuclides in drinking water wells is obviously needed for site specific conditions in Sweden in order to bring clarity to this issue.

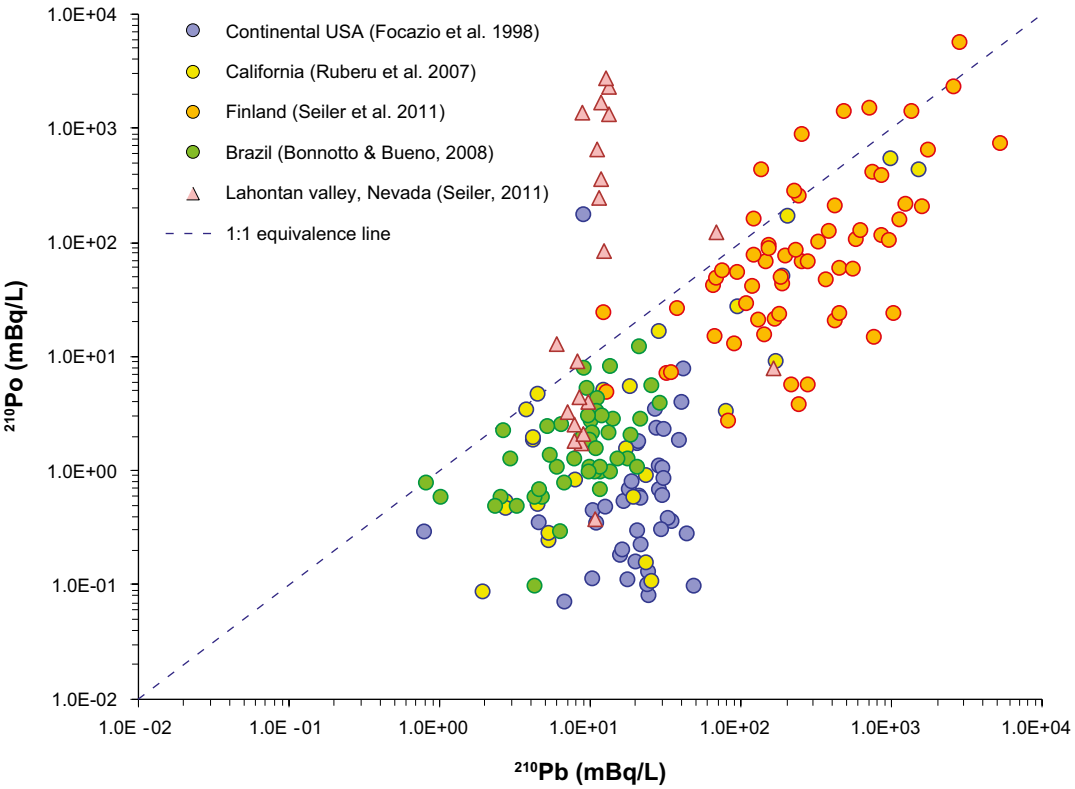

Figure C-3. *Cross plot of groundwater well ^{210}Po and ^{210}Pb activities reported by various authors in the open literature for geographically dispersed sites in the continental USA (Focazio et al. 1998); California (Ruberu et al. 2007); Finland (Seiler et al. 2011); Guarani aquifer, Brazil (Bonotto and Bueno 2008); and Lahontan Valley, Nevada (Seiler 2011). All but three of the data points for ^{210}Pb in Seiler (2011) were non-detects and therefore reported at the sample specific detection limit. The data due to Seiler (2011) and Seiler et al. (2011) were digitised from Figures in the cited papers since numerical values were not reported.*